NRC·CNRC

NRC Publications Archive
Archives des publications du CNRC

# Fire Performance of Houses. Phase I. Study of Unprotected Floor Assemblies in Basement Fire Scenarios. Part 5 - Results of Tests UF-06, UF-06R and UF-06RR (Wood I-Joists B)

Bénichou, N.; Su, J. Z.; Bwalya, A. C.; Lougheed, G. D.; Taber, B. C.; Leroux, P.; Thomas, J. R.

For the publisher's version, please access the DOI link below./ Pour consulter la version de l'éditeur, utilisez le lien DOI ci-dessous.

**Publisher's version / Version de l'éditeur:**
https://doi.org/10.4224/20377158
*Research Report (National Research Council of Canada. Institute for Research in Construction), 2009-03-31*

**NRC Publications Archive Record / Notice des Archives des publications du CNRC :**
https://nrc-publications.canada.ca/eng/view/object/?id=8f07dbef-7b79-4f84-9125-f9acd4fd4b73
https://publications-cnrc.canada.ca/fra/voir/objet/?id=8f07dbef-7b79-4f84-9125-f9acd4fd4b73

Access and use of this website and the material on it are subject to the Terms and Conditions set forth at
https://nrc-publications.canada.ca/eng/copyright
READ THESE TERMS AND CONDITIONS CAREFULLY BEFORE USING THIS WEBSITE.

L'accès à ce site Web et l'utilisation de son contenu sont assujettis aux conditions présentées dans le site
https://publications-cnrc.canada.ca/fra/droits
LISEZ CES CONDITIONS ATTENTIVEMENT AVANT D'UTILISER CE SITE WEB.

**Questions?** Contact the NRC Publications Archive team at PublicationsArchive-ArchivesPublications@nrc-cnrc.gc.ca. If you wish to email the authors directly, please see the first page of the publication for their contact information.

**Vous avez des questions?** Nous pouvons vous aider. Pour communiquer directement avec un auteur, consultez la première page de la revue dans laquelle son article a été publié afin de trouver ses coordonnées. Si vous n'arrivez pas à les repérer, communiquez avec nous à PublicationsArchive-ArchivesPublications@nrc-cnrc.gc.ca.

National Research Council Canada | Conseil national de recherches Canada

Canada

National Research Council Canada | Conseil national de recherches Canada

NRC · CNRC

# Fire Performance of Houses

# Phase I

# Study of Unprotected Floor Assemblies in Basement Fire Scenarios

# Part 5 – Results of Tests UF-06, UF-06R and UF-06RR (Wood I-Joists B)

Research Report: IRC-RR-250

Date: March 31, 2009

Authors: N. Bénichou, J.Z. Su, A.C. Bwalya, G.D. Lougheed, B.C. Taber, P. Leroux, J.R. Thomas

INSTITUTE FOR RESEARCH IN CONSTRUCTION
Fire Research Program

## TABLE OF CONTENTS

## LIST OF FIGURES

## LIST OF TABLES

## ABSTRACT

This report documents part of the research project involving a series of full-scale fire experiments in a test facility that simulated a two-storey single-family house with a severe, fast growing fire originating in an unfinished basement to study the fire performance of the floor/ceiling assembly constructed over the basement. The report presents the results and analysis of Tests UF-06, UF-06R and UF-06RR carried out in the test house with unprotected wood I-joist B floor/ceiling assemblies above the basement with an open basement doorway (no door in the doorway leading from the first storey to the basement). A number of measurements were taken at various locations during the tests such as temperatures, smoke alarm activation times, smoke optical density, floor deflection and concentrations of CO, $CO_2$ and $O_2$. For these three tests, untenable conditions on the upper storeys were reached before structural failure of the test floor assemblies. The test results show good repeatability.

**FIRE PERFORMANCE OF HOUSES**

**PHASE I**

# STUDY OF UNPROTECTED FLOOR ASSEMBLIES IN BASEMENT FIRE SCENARIOS

**Part 5 – Results of Tests UF-06, UF-06R and UF-06RR (Wood I-Joists B)**

N. Bénichou, J.Z. Su, A.C. Bwalya, G.D. Lougheed, B.C. Taber, P. Leroux and J.R. Thomas

## 1 INTRODUCTION

### 1.1 Background

Risk of fires in buildings and concerns about their potential consequences are always present. Canada's fire death rate has continuously declined for the last three decades; much of this decline is attributed to the introduction of residential smoke alarms (this is also the case in the United States). With the advent of new materials and innovative products for use in construction of single-family houses, there is a need to understand what impacts these materials and products will have on occupant life safety under fire conditions and a need to develop a technical basis for the evaluation of their fire performance.

The National Building Code of Canada (NBCC) [1] generally intends that major structural load-bearing elements (floors, walls and roofs) have sufficient fire resistance to limit the probability of premature failure or collapse during the time required for occupants to evacuate safely [2]. Historically, the NBCC has not specified a minimum level of fire performance (fire resistance) of these structural elements in single-family houses.

In Canada, the Canadian Construction Materials Centre (CCMC) is called upon to evaluate the use of new materials and innovative construction products for compliance with the NBCC. Some of the more recent innovative structural products, seeking recognition for use in housing, are made of new composite and non-traditional materials that may have unknown fire behaviour. When evaluating new structural products, part of the CCMC challenge is related to the fact that no guidance or criteria are provided in the NBCC regarding the fire performance of structural systems used in single-family houses.

The Canadian Commission on Construction Materials Evaluation (CCCME) guides the operation of CCMC. Through the CCCME, CCMC sought the views of the Canadian Commission on Building and Fire Codes (CCBFC), which guides the development of the NBCC. After review and discussion, both the CCBFC and CCCME agreed that a study on the factors that affect the life safety of occupants of single-family houses should be conducted.

## 1.2 Goals of the Research

The National Research Council of Canada Institute for Research in Construction (NRC-IRC) undertook research into fires in single-family houses to understand the impact of residential construction products and systems on occupant life safety.

This research project sought to achieve the following goals:

1. To determine the significance of the fire performance of structural materials used in houses to the life safety of occupants.
2. To identify methods of measuring the fire performance of unprotected structural elements used in houses.
3. To measure and establish the fire performance of traditional house construction to facilitate the evaluation of the fire performance of innovative construction products and systems.

## 1.3 General Research Approach

Figure 1 shows a possible chronological sequence of relevant critical events that might occur in a fire scenario. It is acknowledged that the chronology of the occurrence of events may differ, and in some cases can shift in ordering.

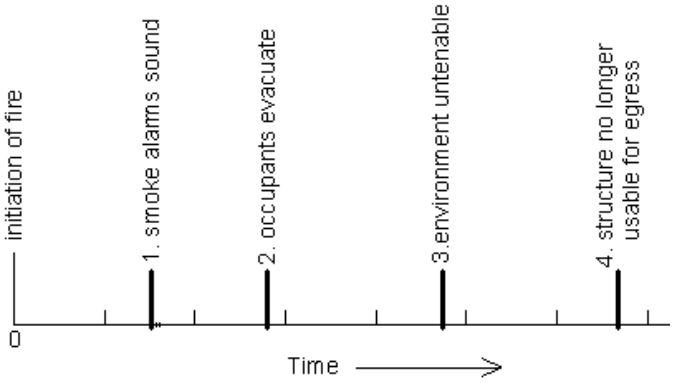


**Figure 1. Possible chronological sequence of events affecting the life safety of occupants in a fire situation**

The research sought to establish, through experimental studies and using specific fire test scenarios, the typical sequence of the following events (measured from initiation of a fire), using a test facility intended to represent a typical code-compliant single-family house:

1. Sounding of smoke alarms (Event 1 as shown in Figure 1).
2. Loss of tenability within the environment of the first, second or subsequent storey(s) (Event 3).
3. Loss of integrity of the floor assembly and/or loss of its function as a viable egress route on the first or second storey(s)[1] (Event 4).

[1] The state of the egress route(s) on the first storey is relevant to the evaluation of the performance of the basement foundation walls and floor structure constructed over the basement;

The research also sought to establish a basis for prediction or estimation of the required safe egress times expected for ambulatory occupants assuming a tenable indoor environment and a structurally sound evacuation route. A review of the literature on the waking effectiveness of occupants to smoke alarms, the delay time to start evacuation and the timing of escape in single-family houses was conducted. The objective of the review was to identify a range of estimated times families would take to awake, prepare and move out of their home after perceiving the sound of a smoke alarm during the night in winter conditions (Event 2 shown in Figure 1). This literature review was a separate but parallel study to the experimental studies. The results of the literature review are provided in Reference [3].

### 1.4 Scope of the Research Projects

The overall research consisted of a number of phases of experimental studies with each phase investigating a specified structural element based on specified fire scenarios.

Phase 1 (2004 to 2007) of the experimental study focused on basement fires and their impacts on the structural integrity of unprotected floor assemblies above a basement and the tenability conditions in a full-scale test facility. It is acknowledged that, a basement is not the most frequent site of household fires but it is the fire location that is most likely to create the greatest challenge to the structural integrity of the 1$^{st}$ storey structure, which typically provides the main egress routes. The study of fires originating in basements also provides a good model for the migration of combustion products throughout the house and its egress paths. The data collected during this phase of the project provided important indicators for identifying and evaluating the sequence for the occurrence of critical events shown in Figure 1.

This research focused on the life safety of occupants in single-family houses. The safety of emergency responders in a fire originating in single-family houses was not within the scope of this research project. Technical data collected during this research could aid in clarifying the potential risks associated with firefighting activities.

### 1.5 Content of this Document

This report documents the results of the initial phase of work involving an experimental study of the structural fire performance of the floor/ceiling assembly (1st floor) constructed over the basement level of a test house. Specifically, this report contains the data and analysis of Tests UF-06, UF-06R and UF-06RR of the Phase I study carried out in the test house with an unprotected wood I-joist B floor/ceiling assembly. This includes results on the fire scenarios, tenability, structural integrity, and the sequence of Events 1, 3 and 4, as illustrated in Figure 1.

---

the state of the egress route on the second storey is relevant to the evaluation of the performance of the above-grade wall structures and floor structure over the first storey.

## 2 EXPERIMENTAL STUDY

To undertake this research, NRC-IRC constructed a three-level experimental facility, representing a typical two-storey detached single-family house with a basement. The facility allows the study of structural fire performance, as well as smoke movement and tenability under fire conditions for single-family houses. The facility has a total floor area of approximately 95 $m^2$ per storey and is shown in Figure 2.


**Figure 2. Three-storey facility**

### 2.1 Geometry - Compartments in the Facility

#### 2.1.1 Fire Compartment in Basement

The layout of the basement is shown in Figure 3. The basement was partitioned to create a fire room representing a 27.6 m2 basement living area, or about 1/4 of the total basement area. This compartment size was chosen based on a survey carried out by NRC [4]. The area of the basement that was not used for the fire compartment was blocked off during the fire tests. The height of the basement was 2.44 m. The ceiling clear height depended on the depth of the floor assembly being tested. A rectangular exterior opening measuring 2.0 m wide by 0.5 m high and located 1.8 m above the floor was provided in the south wall of the fire room. The size of the opening was chosen based on the results of the survey carried out by NRC [4]. A 0.91 m wide by 2.05 m high doorway opening located on the north wall of the fire room led into an empty stairwell enclosure (without a staircase). At the top of this stairwell, a 0.81 m wide by 2.05 m high doorway led into the first storey, as shown in Figure 4. This doorway either had no door (open basement doorway) or had a door in the closed position (closed basement doorway), depending on the scenario being studied. There is no requirement for a basement door in the NBCC. Section on “Openings and their States” provides more details.

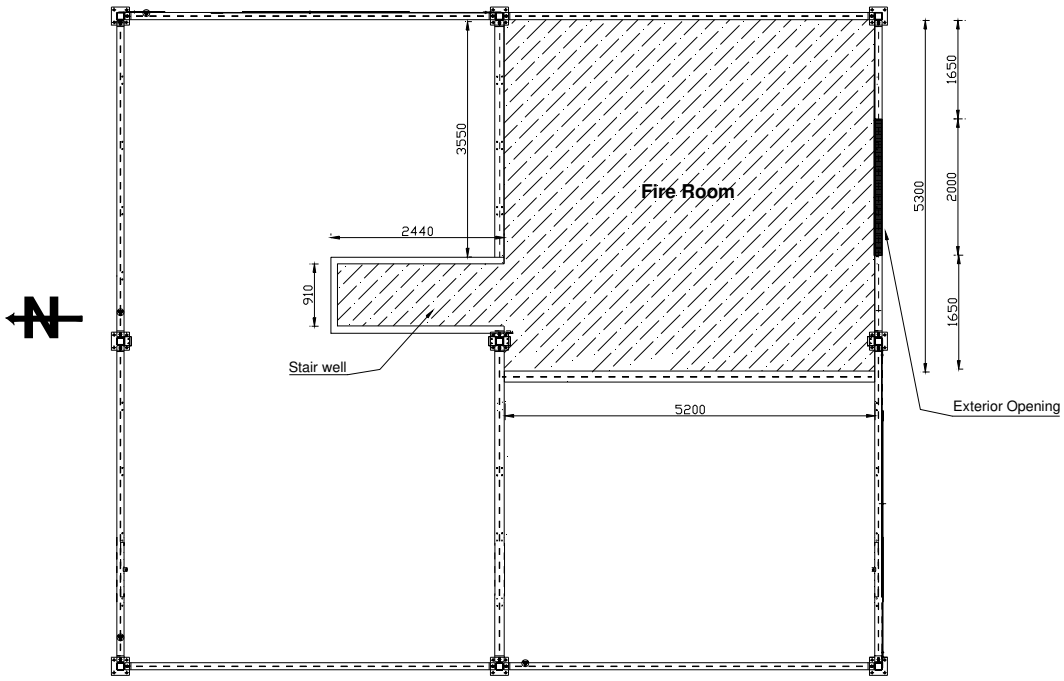


**Figure 3. Basement level layout** (dimensions in mm)

### 2.1.2 First Storey

The first storey had an open-plan layout with no partitions, as shown in Figure 4. A test floor assembly was constructed on the first storey directly above the fire room for each experiment. The remainder of the floor on the first storey was constructed out of non-combustible materials. The height of the storey was about 2.44 m. As shown in Figure 4, this storey had 2 door openings: a door opening to the outside (dimensions of 0.89 m by 2.07 m) and a door opening that connected the basement to the first storey (dimensions of 0.81 m by 2.05 m). This storey also connected to the 2nd storey by a staircase in the middle of the storey area. This staircase to the second storey was not enclosed. The floor being tested was positioned in the southeast quarter of the first storey, on top of the fire compartment.

### 2.1.3 Second Storey

The layout of the second storey is shown in Figure 5. This storey was partitioned to contain two identical bedrooms with dimensions of 3.75 m by 4.47 m connected by a corridor with dimensions of 1.1 m x 4.45 m. The height of the storey was 2.44 m. In all tests, the door of the southeast bedroom remained closed whereas the door on the southwest bedroom was kept open. The size of the door openings was 0.81 m by 2.05 m. The remaining area of the second storey that was not used was blocked off during the fire tests.

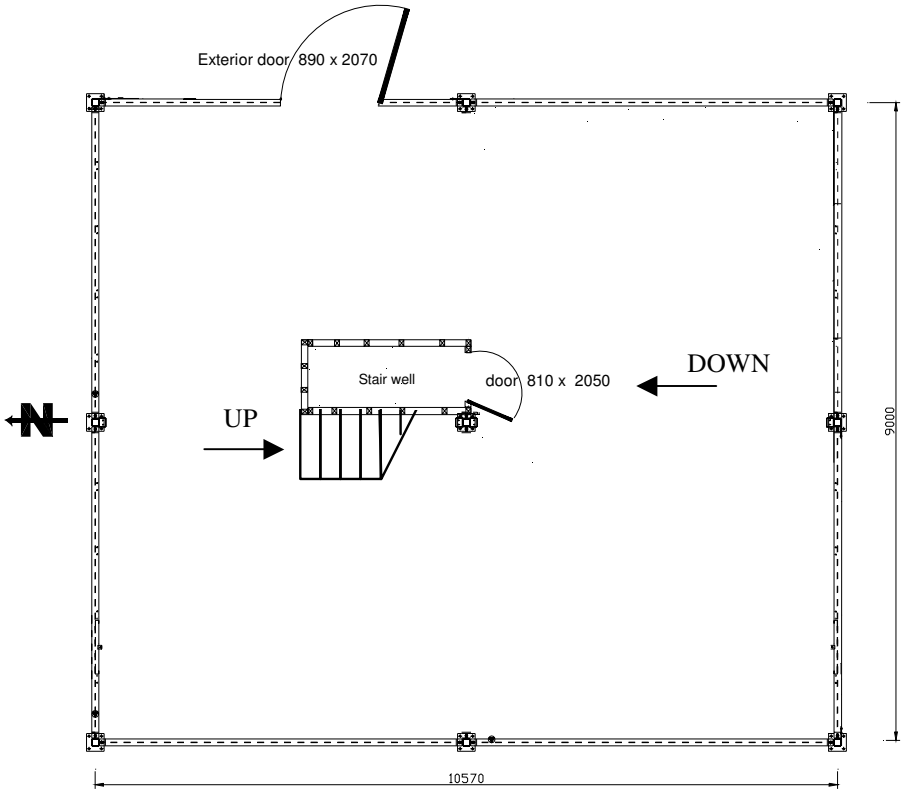


**Figure 4. First storey layout** (dimensions in mm)

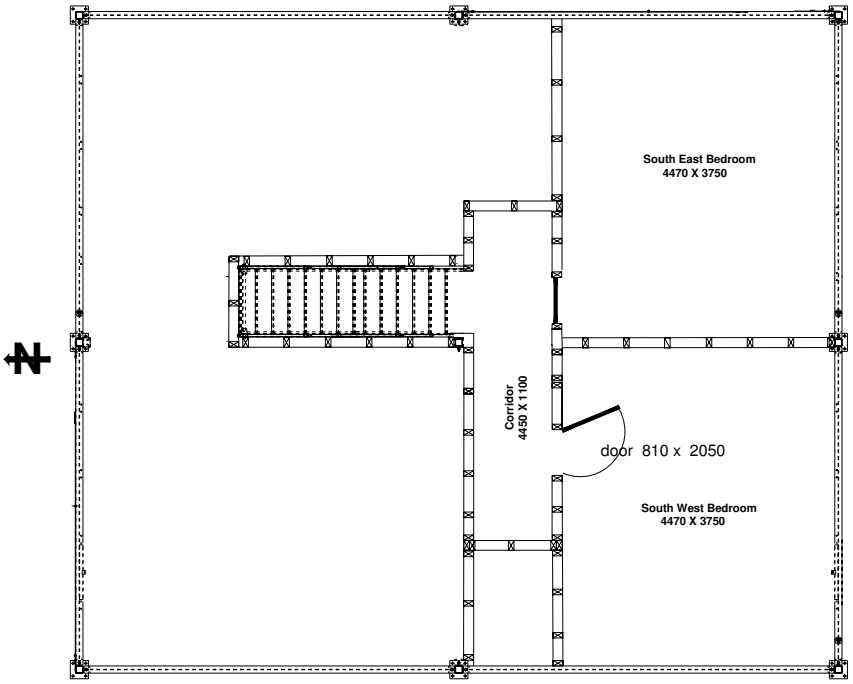


**Figure 5. Second storey layout** (dimensions in mm)

## 2.2 Lining Materials in Compartments

The compartments were lined with different materials. For the basement level, the walls of the fire compartment were lined with 12.7 mm thick regular gypsum board. There was no ceiling finish in the fire compartment, so the floor assembly, including both the framing supports (I-joists) and the underside of the subfloor (oriented strand board, OSB), was unprotected and exposed. For the first and second storeys, cement board covered the walls, and the ceilings were covered with 12.7-mm thick regular gypsum board. There was no finished floor in the 1st storey, so the upper surface of the OSB subfloor used on the floor assembly being tested was exposed. In the remainder of the compartment on the first storey, the floor was noncombustible. The OSB that was used for the subfloor was chosen on the basis of a study on the performance of different OSBs when exposed to fire [5].

## 2.3 Openings and their States

The openings included: on the basement level, a rough window opening; on the first storey, a door opening to the outside and a door opening at the top of the empty stairwell enclosure (contained no stairs) leading from the basement level; on the second storey, a door opening in the corridor at the top of the stairs leading from the first storey and door openings from the corridor leading to each of the two bedrooms. The size of all the doorways were typical of those used in housing. The single window opening in the basement (2.0 m x 0.5 m) represents an area equal to the size of two typical basement windows.

The doors on the door openings were inexpensive moulded-fibreboard hollow-core interior doors with minimum size styles and rails or solid-core exterior wood doors. The rough window opening in the basement level was covered with a noncombustible panel that could open at the appropriate time in each fire test.

At the start of a test, the rough window opening in the basement and the exterior door on the first storey leading to the outside were closed. Both were opened at critical times during a test (see Section 2.6 Testing Procedure). The doorway on the first storey leading to the basement had no door (open basement doorway) in the three tests. On the second storey, during the test, the door to the southwest bedroom was open, and the door to the southeast bedroom was closed.

There was no heating, ventilating and air-conditioning or plumbing system installed in the test house, i.e., no associated mechanical openings in the floor.

## 2.4 Fuel Load in the Fire Compartment

The selection of the fuel load and its arrangement in the fire compartment was a critical element in this experimental work. A study was conducted to select the fire scenario and fuel package, which was used in this phase of the project [6]. This fuel package consisted of a mock-up sofa constructed with 9 kg of exposed polyurethane foam (PUF), the dominant combustible constituent of upholstered furniture, and 190 kg of wood cribs beside and underneath the mock-up sofa. A photograph of the fuel package is shown in

Figure 6. The mock-up sofa was constructed with 6 blocks of flexible polyurethane foam (with a density of 32.8 kg/m$^3$) placed on a metal frame. Each block was 610 mm long by 610 mm wide and 100 mm or 150 mm thick. The 150-mm thick foam blocks were used for the backrest and the 100 mm thick foam blocks for the seat cushion. The PUF foam was used without any upholstery fabric that is used in typical upholstered furniture. The wood cribs were made with spruce lumber pieces, each piece measuring 38 mm x 89 mm x 800 mm. For the small cribs located under the mock-up sofa, four layers with six pieces per layer were used. The other two cribs used eight layers.

The placement of the fuel package in the basement fire compartment is illustrated in Figure 7. The mock-up sofa was located at the center of the floor area. The mock-up sofa was ignited in accordance with the ASTM 1537 test protocol [7] and the wood cribs provided the remaining fire load to sustain the fire for the desired period of time.

**Figure 6**. Fuel package

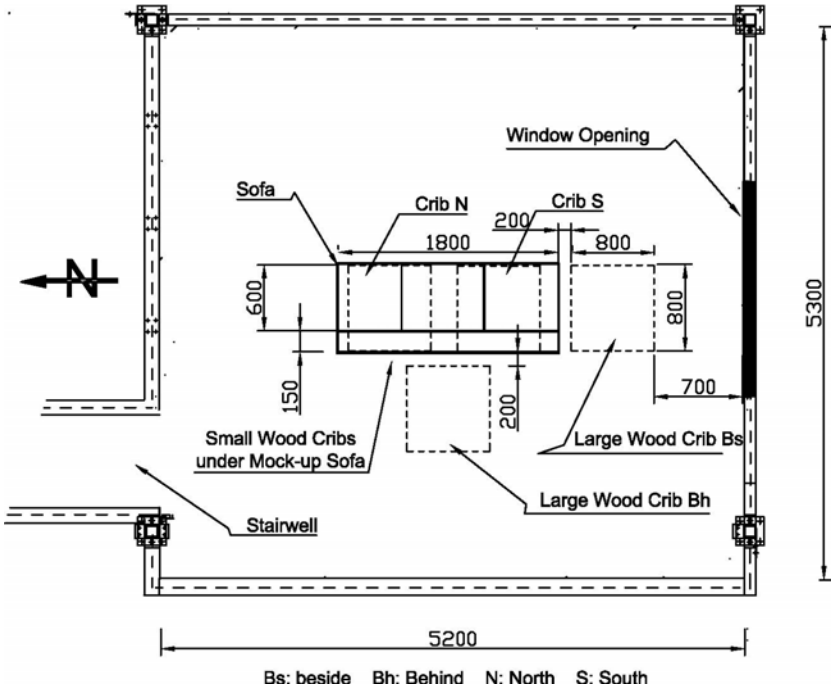


**Figure 7. Arrangement of the fuel package in the fire compartment**

(dimensions in mm)

## 2.5 Instrumentation in the Different Compartments and Exterior

The following is a summary of the instrumentation installed inside and around the exterior of the test facility.

### 2.5.1 Fire Compartment in Basement

The instrumentation in the basement fire room included the following:

- Four vertical arrays of thermocouples located at the quarter points of the fire room to measure temperatures at heights of 0.4, 0.9, 1.4, 1.9 and 2.4 m above the floor level.
- Thermocouples located at the basement exterior opening (window) to measure the temperature at the simulated window and the temperature of the gas plume after the mock-window was opened.
- Residential photoelectric smoke alarms located near the stairwell.
- Air velocity measurements at the basement exterior opening (window).
- Differential pressure measurement between the fire compartment and the exterior of the test facility, located 2.0 m above the floor.
- Video recording of the burning fuel package.
- Thermocouples measuring temperatures in the wood cribs.

The positioning of the instrumentation in the fire compartment on the basement is shown in Figure 8.

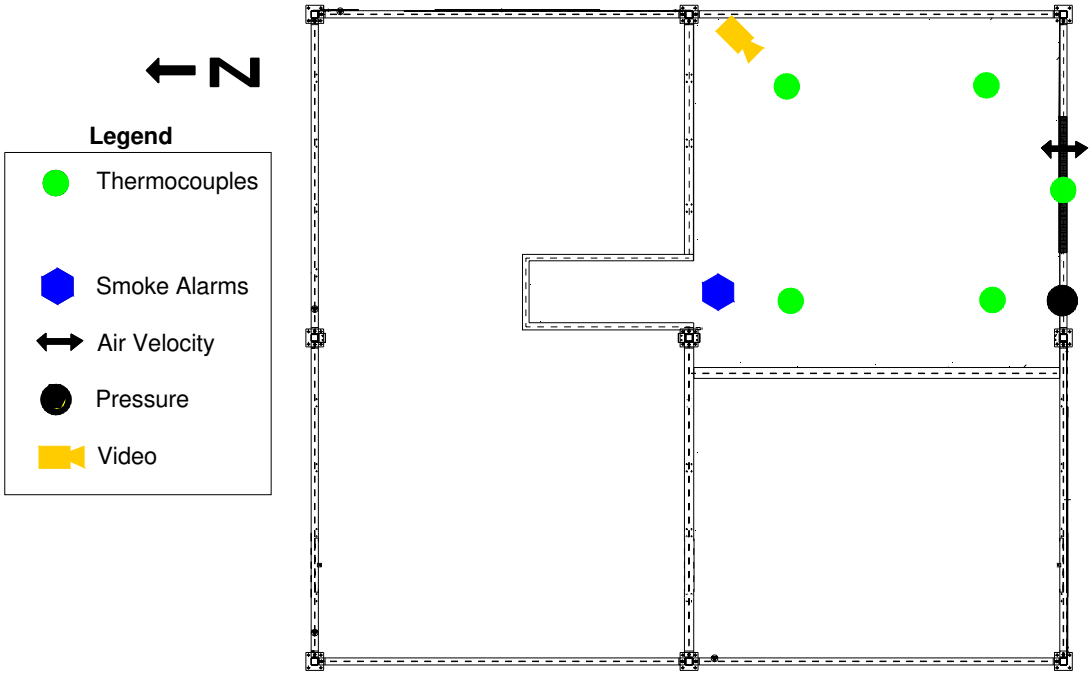


**Figure 8. Fire Compartment instrumentation**

### 2.5.2 First Storey

The instrumentation on the first storey included the following:

- Four vertical thermocouple arrays at the quarter points of the whole floor area.
- One vertical thermocouple array located at the door opening of the stairwell from the basement level.
- Gas sampling ports at the southwest quarter point, including:
  - $CO/CO_2/O_2$ at 0.9 m and 1.5 m above the floor.
  - Fourier Transform Infrared Spectroscopy (FTIR) at 1.5 m above the floor.
- Smoke density measurements at the southwest quarter point at 0.9 m and 1.5 m above the floor.
- Residential ionization and photoelectric smoke alarms located on the ceiling near the doorway to the basement.
- Air velocity measurements located at top of the basement stairwell at ceiling height and at 1.5 m above the floor.
- Differential pressure measurement between the fire compartment in the basement level and the first storey.
- Video recording from two locations.

The positioning of the instrumentation on the first storey is shown in Figure 9.

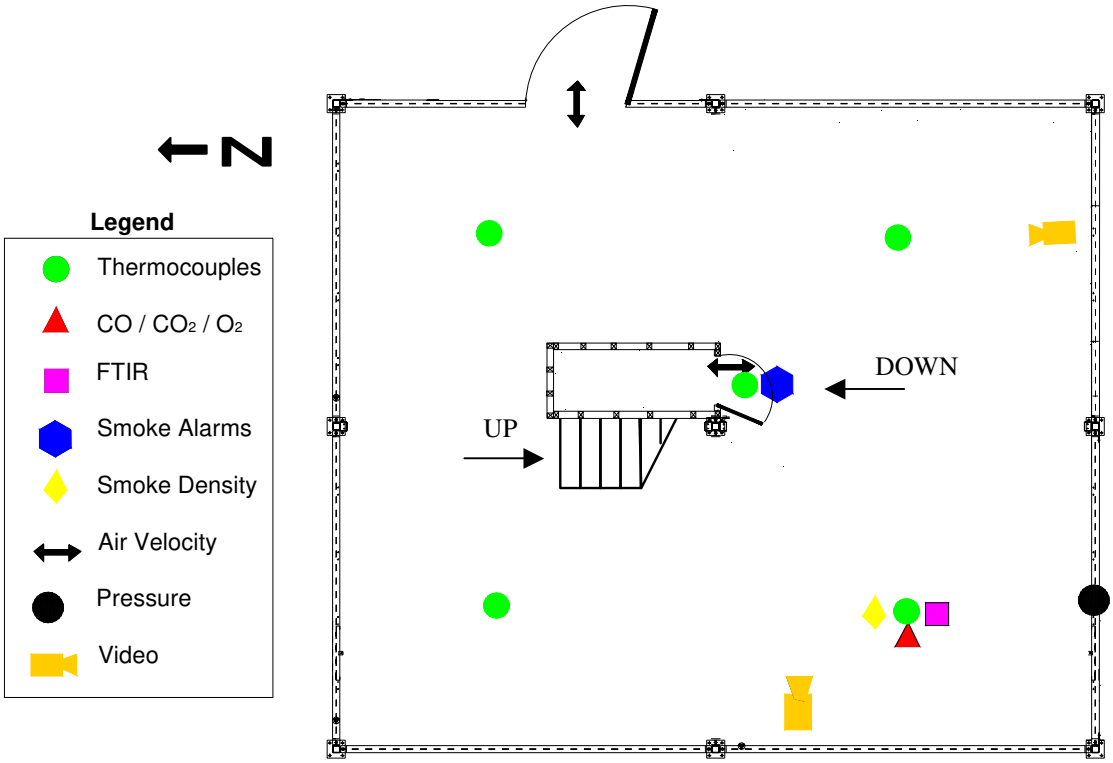


**Figure 9. First storey instrumentation**

### 2.5.3 Second Storey

The instrumentation on the second storey included the following:

- One vertical thermocouple array in the corridor at the top of the stairs.
- One vertical thermocouple array in the center of each bedroom.
- Residential ionization and photoelectric smoke alarms located on the ceiling in the corridor at the top of the stairs.
- Residential ionization and photoelectric smoke alarms located on the ceiling at the centre of each bedroom.
- Gas analysis ($CO/CO_2/O_2$) in the corridor at the top of the stairs at 0.9 m and 1.5 m above the floor.
- Smoke density measurements in the corridor at the top of the stairs at 0.9 m and 1.5 m above the floor.
- Air velocity measurements located at the top of the stairs at ceiling height and at 1.5 m above the floor.
- Video recording in the corridor.

The positioning of the instrumentation on the second storey is shown in Figure 10.

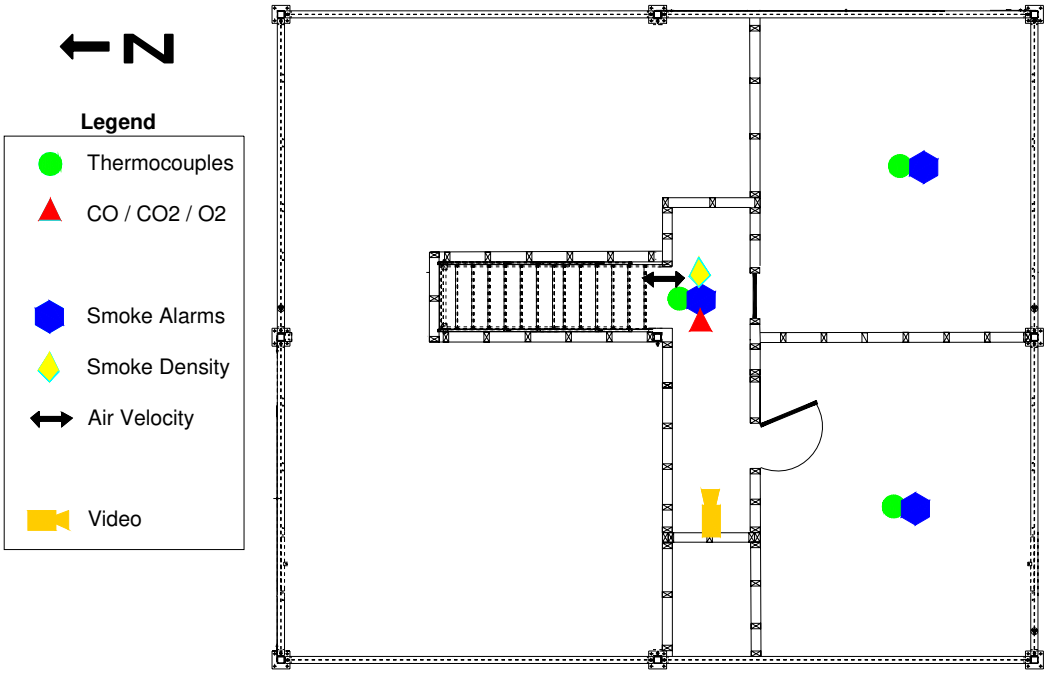


**Figure 10. Second storey instrumentation**

### 2.5.4 Exterior

Instrumentation of the facility exterior included the following:

- Air velocity measurements located at the basement window opening.
- Air velocity measurements located at the exterior door opening on the first storey.
- Video recording of the exterior window opening in the fire compartment on the basement level and the exterior door opening on the first storey.

## 2.6 Testing Procedure

The mock-up sofa was ignited in accordance with the ASTM 1537 test protocol [7] and data was collected at 5 s intervals throughout each test.

The non-combustible panel that covered the fire room's exterior rough window opening during the initial stage of each test was manually removed when the temperature measured at the top-center of the opening reached 300°C. The removal of the panel was to provide ventilation air necessary for combustion.

The exterior door on the first storey was opened at 180 s after ignition and left open, simulating a situation where some occupants, who would have been in the test house, escaped leaving the exterior door open while other occupants may still have been inside the house.

The tests were terminated by extinguishing the fires using a manually operated sprinkler system when one of the following occurred (singly or in combination):

- Excessive flame penetration through the floor assembly;
- Structure failure of any part of the floor assembly;
- Compromise of safety of the test facility.

## 2.7 Construction Details of the Floor Assemblies

Eleven full-scale floor assemblies were tested in this first phase of the project. In each test, the floor assembly was installed in the three-storey test facility to create the ceiling portion over the fire compartment in the basement level. The floor assemblies had no ceiling sheathing attached on the underside, leaving the framing members and the subfloor exposed and unprotected from exposure to the fire from the burning fuel package.

For each type of floor assembly tested, the floor joist/truss spans were either chosen from the appendices of the NBCC or calculated based on the ultimate and serviceability limit states. Therefore, the floor joists/trusses could either span the entire length of the fire compartment space or require an intermediate beam support for shorter spans. When designing the assemblies, various aspects were considered including what is typically used for framing and subfloor materials in housing today, consideration of serviceability limit states, typical spacing, typical spans, typical depths, etc. As well, the assemblies were loaded at 50% of the specified load in the NBCC (see Section 2.9).

Details on the tested assembly (wood I-joists B) are provided below[2].

### 2.7.1 Floor Assemblies with Wood I-Joists B

The three tests, documented in this report, were conducted using wood frame floor assemblies constructed using wood I-joists B and an OSB subfloor. The overall dimensions of the wood I-joist assemblies were 5250 mm by 5150 mm. Specific dimensions of the various components of the assemblies are provided in Figure 11 to Figure 14.

The wood I-joists B were 302 mm deep, with an OSB web of 9.5 mm thick and finger-joint lumber flanges (38 mm by 64 mm). The I-joists were spaced at 400 mm on centre (see Figure 11). Based on calculations of maximum strength and deflection, the I-joist span length chosen was 4.813 m (see Figure 11). This span allowed the wood I-joists B to extend across the entire length of the fire compartment (with no need for an intermediate support). Figure 12 shows the supporting beams.

[2] Another report (Part 2) also provides information on testing of an unprotected wood I-joist A floor/ceiling assembly.

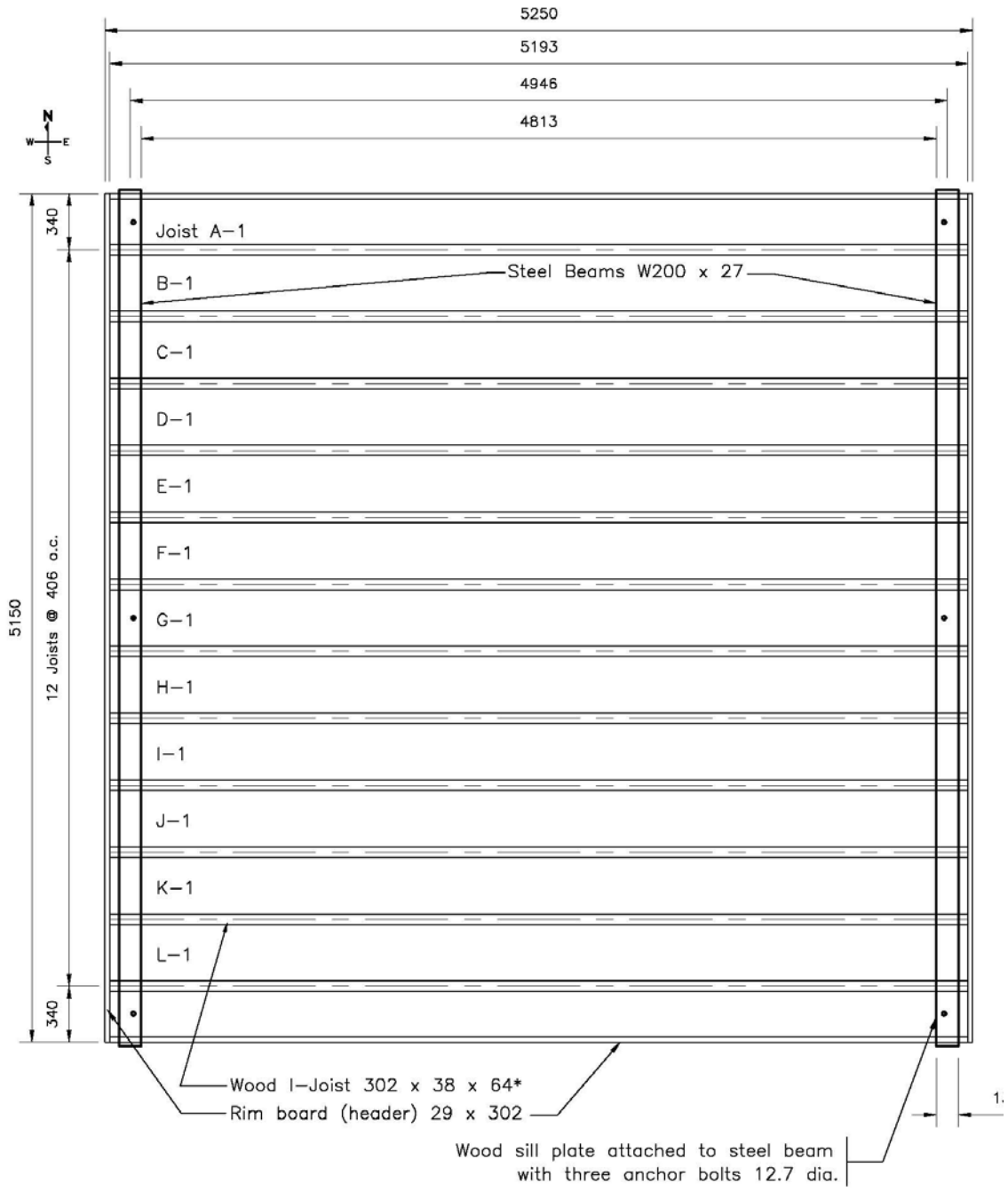


**Figure 11. Wood I-joist B layout details** (all dimensions in mm)

Each wood I-joist B floor assembly was supported by two horizontal beams, each of which was supported by two columns (a total of four columns for each assembly) as illustrated in Figure 12. The beams were bolted to the columns, which were stiffened by bars and rested stably on the floor under the weight of the assembly and beams.

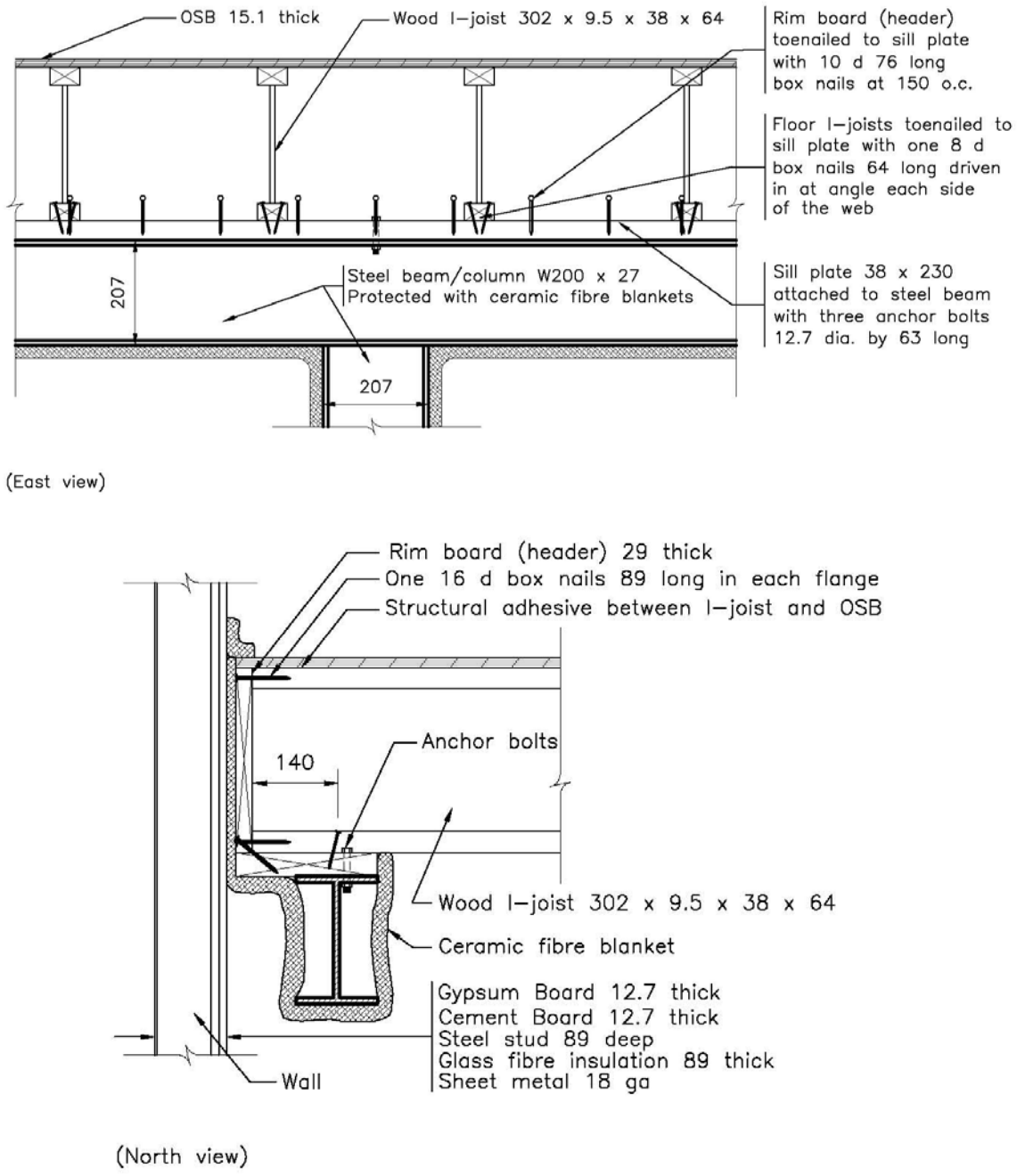


**Figure 12. End connection details and supports** (all dimensions in mm)

Figure 12 also shows the details of the end connection. Ceramic fibre blankets were used to fill any gaps between the assembly and the end walls. Ceramic fibre blankets were also used to protect the steel beams and columns so that they were not subjected to fire and would not fail during the tests.

In the wood I-joist B test assemblies (UF-06, UF-06R and UF-06RR), OSB rim boards (headers) 29 mm thick x 302 mm deep, were placed around the perimeter of the assemblies as shown in Figure 11. The OSB rim boards on the North and South ends of

the assemblies (parallel to the joists) were reinforced with laminated strand lumber (LSL) rim boards (32 mm thick, 3.66 m long, grade 1.3E).

OSB was used as the subfloor material in the floor assemblies. The specific OSB material used was selected based on a separate study documented in reference [5]. The subfloor panels were 15.1 mm thick in all assemblies, with a full panel size being 1.2 x 2.4 m. The longer panel edges had a tongue and groove profile while the short panel edges were square-butt ends. Figure 13 shows the layout of the subfloor. The nailing pattern and description of nails used to attach the OSB panels to the wood I-joists and rim board (header) are shown in Figure 14.

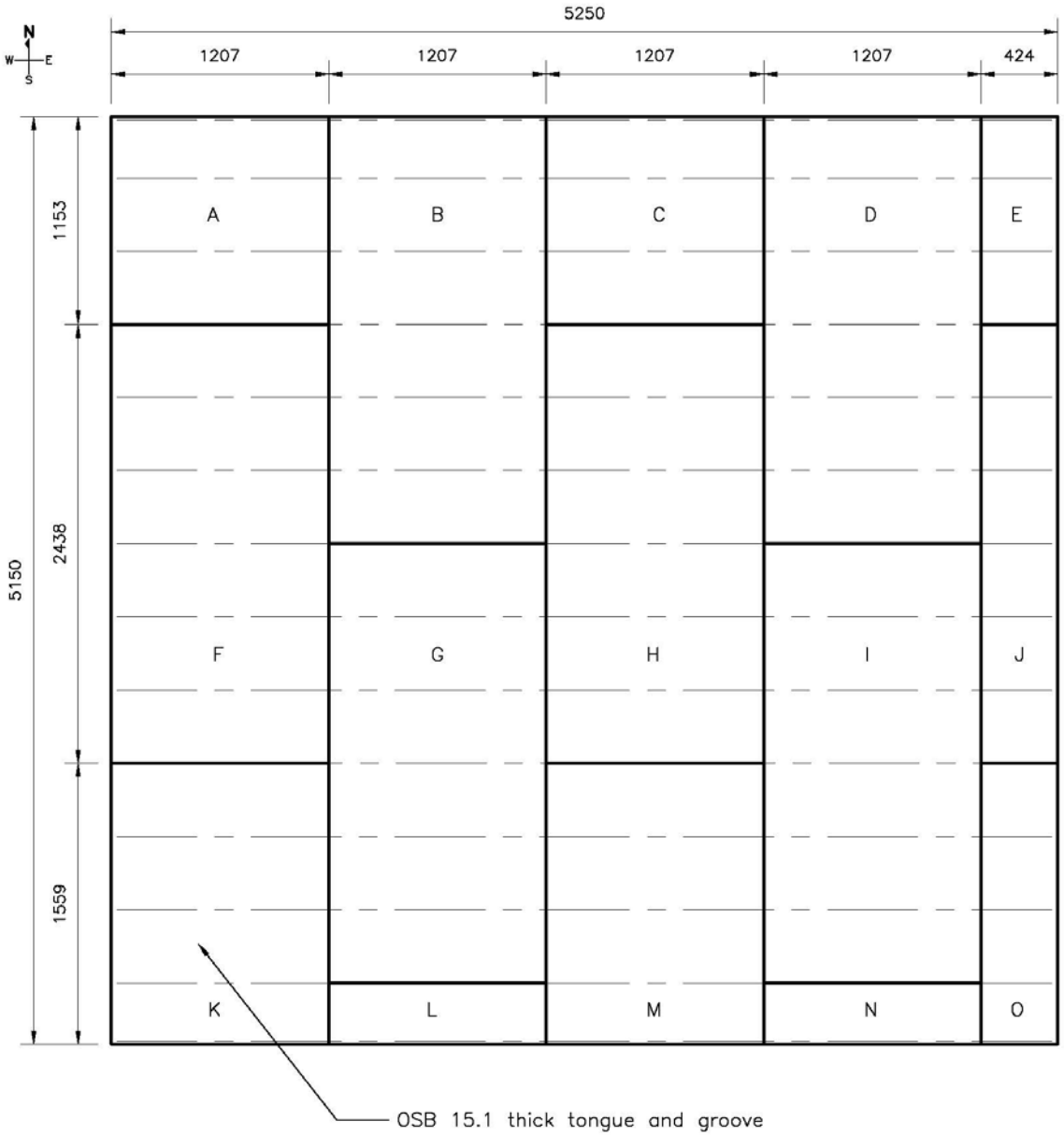


**Figure 13. Subfloor layout** (all dimensions in mm)

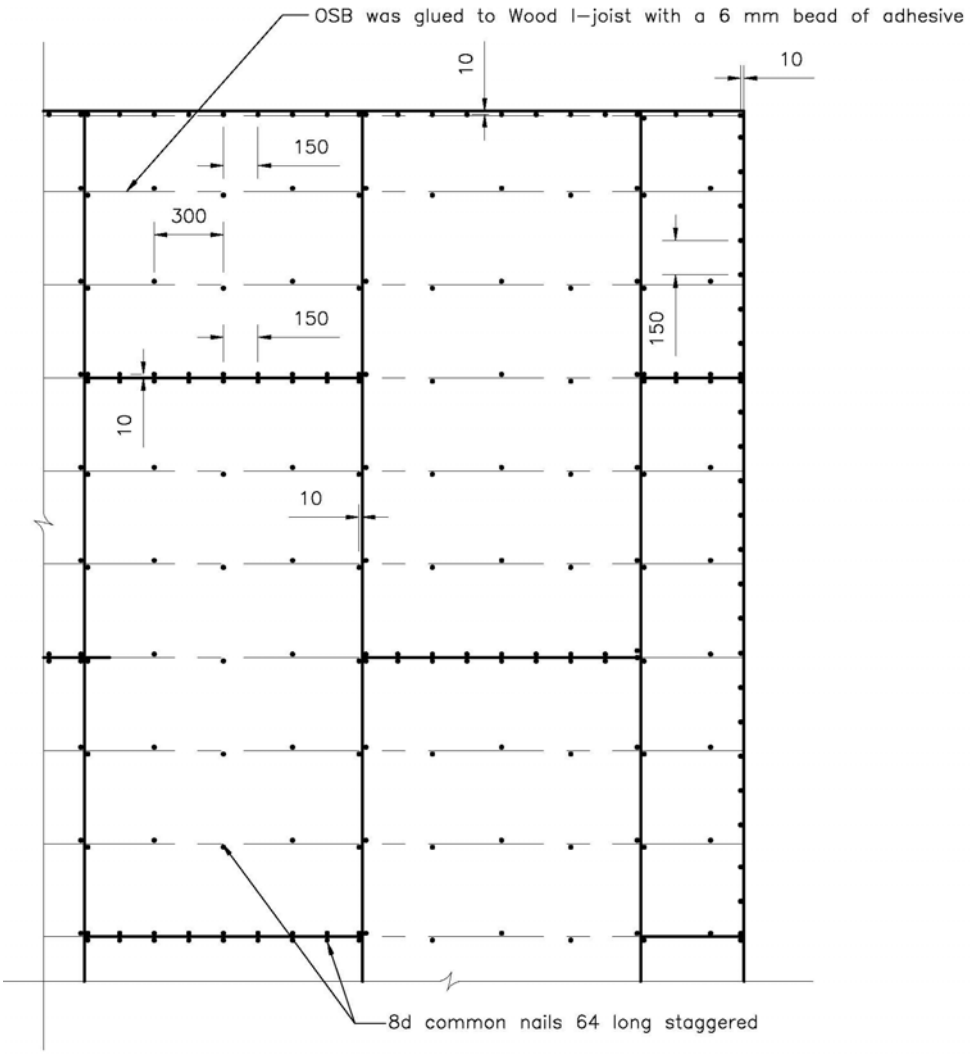


**Figure 14. Subfloor nail pattern and nail description** (all dimensions in mm)

The experimental setup and floor assemblies were exactly the same for Tests UF-06, UF-06R and UF-06RR. The only differences between the tests were the support brackets for the columns in the fire room. In Test UF-06, the support brackets for the columns were sloped and anchored to the floor. Tests UF-06R and UF-06RR used horizontal lateral support brackets for the columns (same as those used in all other tests in Phase 1). These repeat tests were conducted to determine whether the support brackets had any effect on structural response of the floor assembly in the fire tests, and to address, to a certain degree, the variability and repeatability of the tests.

## 2.8 Instrumentation of the Floor Assemblies

### 2.8.1 Temperatures in the Floor Assemblies

Ninety-four Type K (20 gauge) chromel-alumel thermocouples, with a thickness of 0.91 mm, were used for measuring temperatures at a number of locations throughout each assembly. The thermocouple locations on the unexposed and exposed sides of the assemblies are shown in Figure 15 and Figure 16. These locations were chosen to monitor the conditions of the assembly at critical locations during the fire tests.

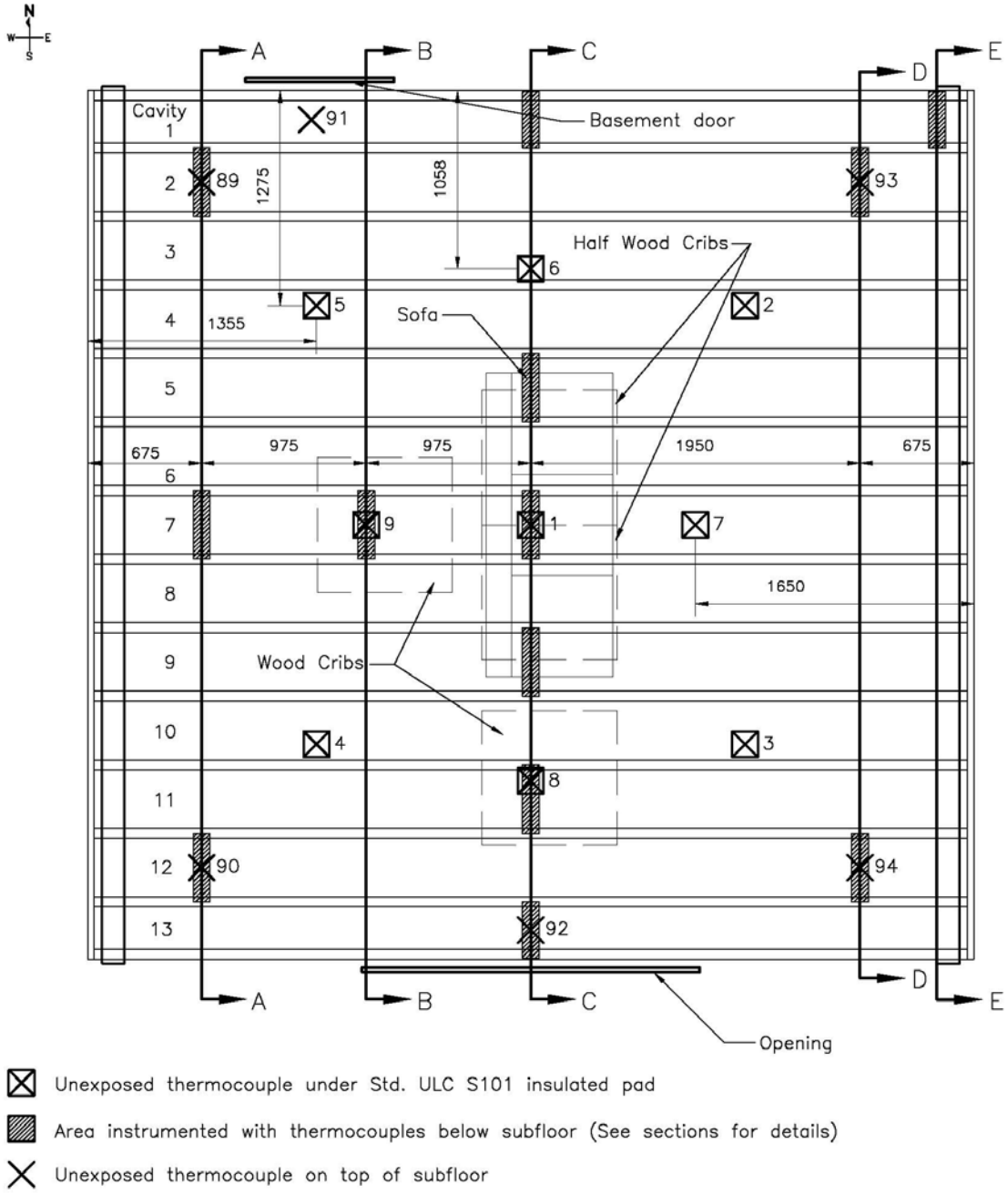


**Figure 15. Thermocouples locations** (all dimensions in mm)

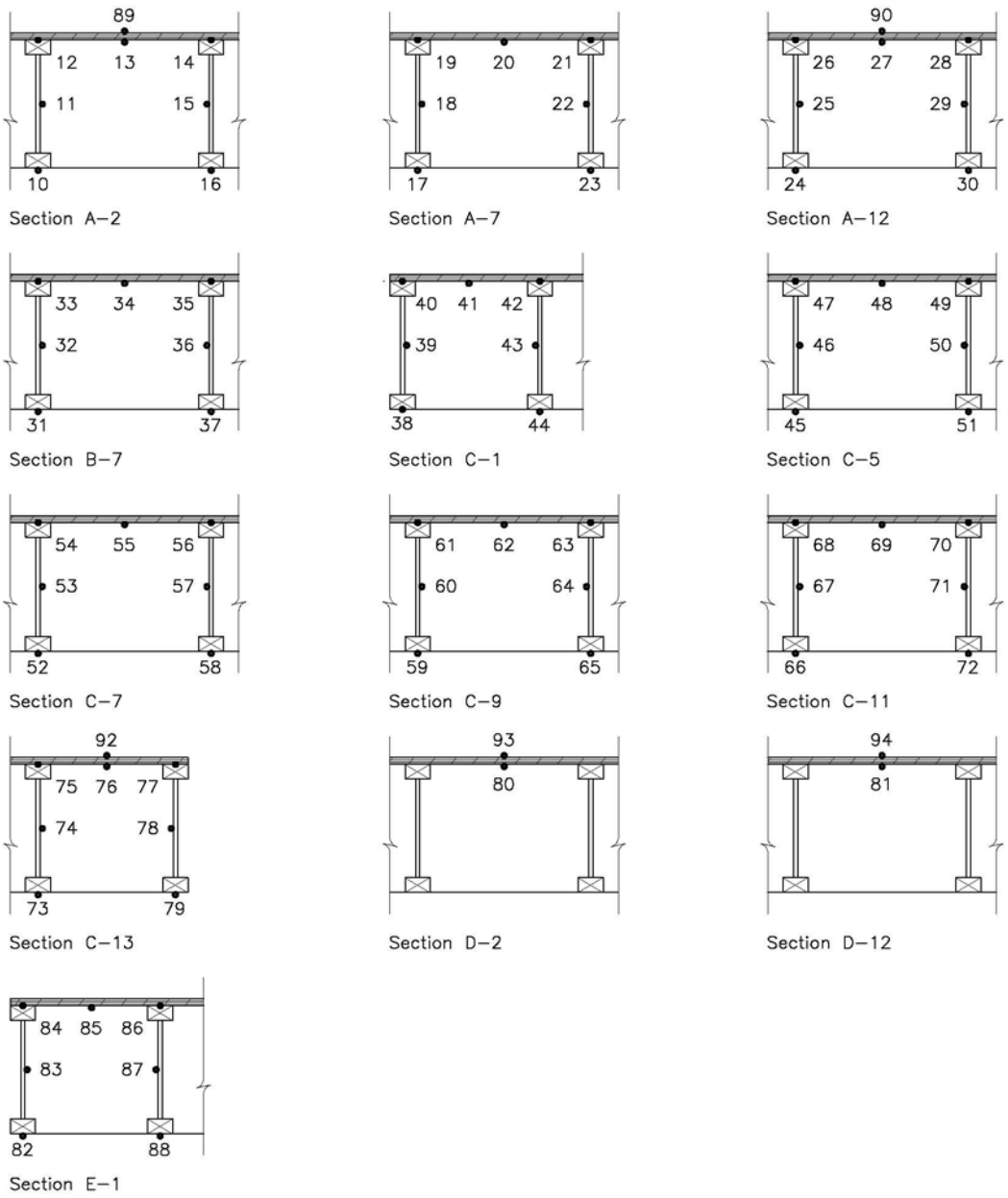


**Figure 16. Thermocouples locations reflecting the different sections shown in Figure 15**

### 2.8.2 Flame Penetration of the Floor Assembly

Flame penetration through the floor assembly is considered to be an initial indicator of the impending failure of the assembly. A device was developed and used for the tests to better determine the time for flames to penetrate the floor. The special device consisted of a wire mesh placed at 3 locations on the unexposed surface of the floor assembly, specifically at three of the tongue and groove joints, as shown in Figure 17. A detailed description of the device is provided in reference [8].

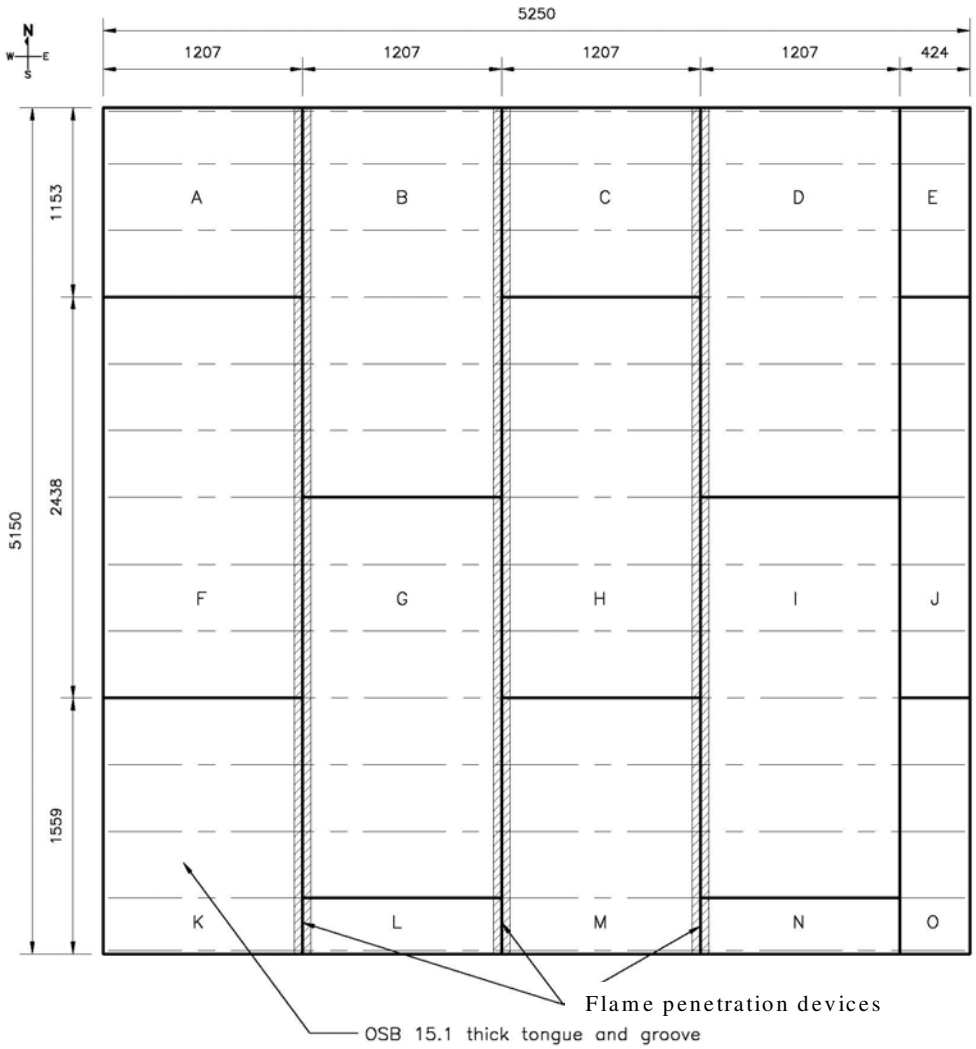


**Figure 17. Wire mesh device to detect flame penetration** (all dimensions in mm)

### 2.8.3 Deflection of the Floor Assemblies

The floor deflection was measured at 9 points. The measurement technique utilized 9 rods that were touching the tops of 9 concrete blocks placed on the unexposed surface of the floor assembly at the locations shown in Figure 18. This ensured that the downward movement of the subfloor was monitored during the fire exposure. The deflections were recorded using the electro-mechanical method described in reference [9].

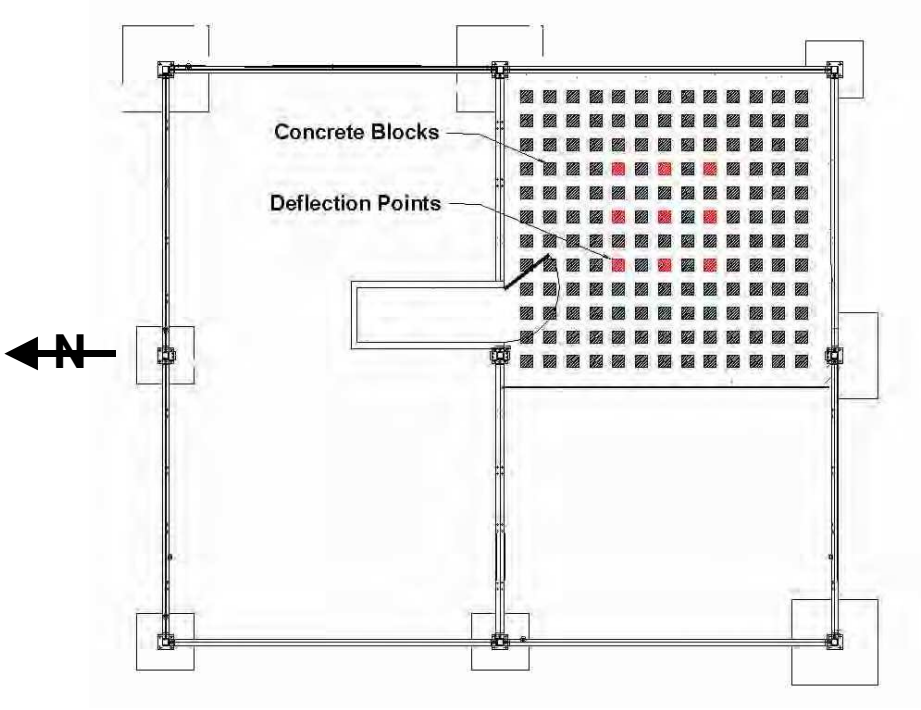


**Figure 18. Loading blocks and locations of the deflection measurement points on the unexposed side of the floor**

## 2.9 Loading of the Floor Assembly

The load applied on the floor assemblies was equal to the self-weight (dead load) of the assembly plus an imposed load (live load) of 0.95 kPa (i.e., half of that prescribed by the NBCC [1] for residential occupancies, i.e., half of 1.90 kPa). The rationale to use this combination was based on the fact that in a fire situation, only part of the prescribed load is available. In fact, a number of international standards (Eurocode [10], New Zealand and Australian standards [11 and 12], and ASCE 13]) use a load combination similar to the one used in this study for fire design purposes. The total imposed load applied to the floor was equal to 0.95 kPa multiplied by the floor area; this is equivalent to approximately 25 kN.

The loading method consisted of 144 concrete blocks (totalling 2490 kg) distributed uniformly on the floor as shown in Figure 18. The blocks were 190 x 190 x 390 mm (nominal 8" x 8" x 16") and weighed 17.3 kg each. To prevent the blocks from falling into the basement and causing any damage, a restraining system was designed using a series of pipes attached to beams on both ends, which were secured to the steel frame of the 3-storey house, as shown in Figure 19. The pipes were inserted through the hollow cores of the concrete blocks prior to the fire tests. The weight of the pipes was included in the total imposed load.

**Figure 19. Device to hold the loading blocks**

Calculations of the maximum imposed loads (live load) that the floors were capable of supporting (based on the span used and production of maximum allowable bending stress/deflection, whichever applies, calculated in accordance with CAN/ULC-S101 standard [14]) indicate that these floors had a large strength reserve. The calculated reserves in %, based on comparison of the loading requirement with maximum imposed loads, which govern in this case, are shown in Table 1.

**Table 1. Reserve Live Load Capacity**

| Test Number | Imposed load (kPa) | Maximum imposed load (kPa) | | Reserve of live load capacity (governed by strength) (%) | Reserve of live load capacity (governed by deflection) (%) |
|---|---|---|---|---|---|
| | | Strength | Deflection | | |
| UF-06<br>UF-06R<br>UF-06RR | 0.95 | 5.70 | 4.56 | 83% | 79% |

# 3 RESULTS OF THE TESTS

## 3.1 Recording of Results

Compartments and floor assemblies were instrumented with smoke alarms, thermocouples, gas analyzers (CO, $CO_2$ and $O_2$), smoke density instruments, pressure measurement instruments, and video cameras. The measurements of temperatures, gas concentrations, smoke density, and pressure were recorded at 5-second intervals using a Solotron data acquisition system.

In the following sections, discussions of the different recorded results are carried out. Figures showing various quantities have been organized as follows:

- Figure 20 to Figure 26 show the test results for temperatures vs. time in the compartments, and at different openings (basement window opening, door opening to the basement, door opening to the outside), and at the top of the stairs (between the basement and first storey, and between the first and second storeys).
- Figure 27 shows the test the test results for temperatures vs. time on the unexposed side of the floor assemblies.
- Figure 28 shows the test results for temperatures vs. time on the exposed side of the floor assemblies.
- Figure 30 shows the test results for deflection vs. time on the unexposed side of the floor assemblies.
- Figure 31 shows the results from the flame-sensing devices.
- Figure 32 to Figure 46 show the smoke and gas measurement results (CO, $CO_2$, $O_2$ and optical density) and tenability conditions vs. time in the compartments.
- Figure 47 to Figure 49 show the test results for the sequence of fire events in Tests UF-06, UF-06R and UF-06RR.

Although velocity measurements were recorded at various openings during the experiments, they are not discussed in this report. However, these results may be useful for fire modeling purposes in the future.

## 3.2 Observations and Recordings

Table A 1, Table A 2 and Table A 3 show the test summary for Tests UF-06, UF-06R and UF-06RR, respectively. This includes a short description of the tests, the times for various events, and the detection times for all smoke alarms that operated. The tests were stopped after indications of either the structural or load-bearing failure of the floors.

## 3.3 Time-temperature Curves at Different Locations

### 3.3.1 Temperatures in the Compartments

In the following sections, the temperatures in the basement, first storey, and second storey are discussed. All thermocouple trees provided measurements at 0.4, 0.9, 1.4, 1.9 and 2.4 m above the floor level. Figure 20 to Figure 22 show these temperatures.

#### 3.3.1.1 Basement

Figure 20 (a to d), Figure 20 (R-a to R-d) and Figure 20 (RR-a to RR-d) show the temperatures in the basement fire compartment at the 4 room quarter points, southeast (SE), southwest (SW), northeast (NE) and northwest (NW), respectively for Tests UF-06, UF-06R and UF-06RR.

In almost all the cases the temperatures rose to a maximum of 700 to 800ºC in the first 100 to 140 s due to the high rate of heat release from the mock-up sofa near its peak burning rate. As shown in the figures, the initial temperature rise was faster at the 2.4 m height than the other heights because the hot smoke layer formed first at the ceiling and flames also impinged on the ceiling.

Just after the peak temperatures, there was a decrease in temperatures likely due to the combined effect of opening the basement window and the fact that a significant portion of the polyurethane foam component of the fuel package had been consumed. The temperature decrease could also be due to the opening of the exterior door on the first storey, which created a movement of air and smoke between the basement and first storey. The fresh air coming from the basement window also increased combustion of the wood cribs and the exposed floor assembly, which caused the temperatures to begin increasing steadily again, reaching a maximum temperature of about 800ºC in most cases.

After the floor failure, the fire was extinguished using sprinklers. The temperatures decreased after that. It should be noted that the temperatures (due to the mock-up sofa burning) were lower in the case of the NE thermocouple tree. This may be partially attributed to the fact that the NE corner was less impacted by the fire, as it was farthest away from the fire source and that most of the hot gases were moving to the upper storeys through the SE to NW path.

For the three tests, combustion was dominated by the mock-up sofa in the first 120 to 180 s, while the wood cribs and floor assembly, including the subfloor, provided the fuel for combustion after this period. The sudden peaks in the time-temperature curves may be due to the ignition of combustible (wood) at different locations of the floor during the fire.

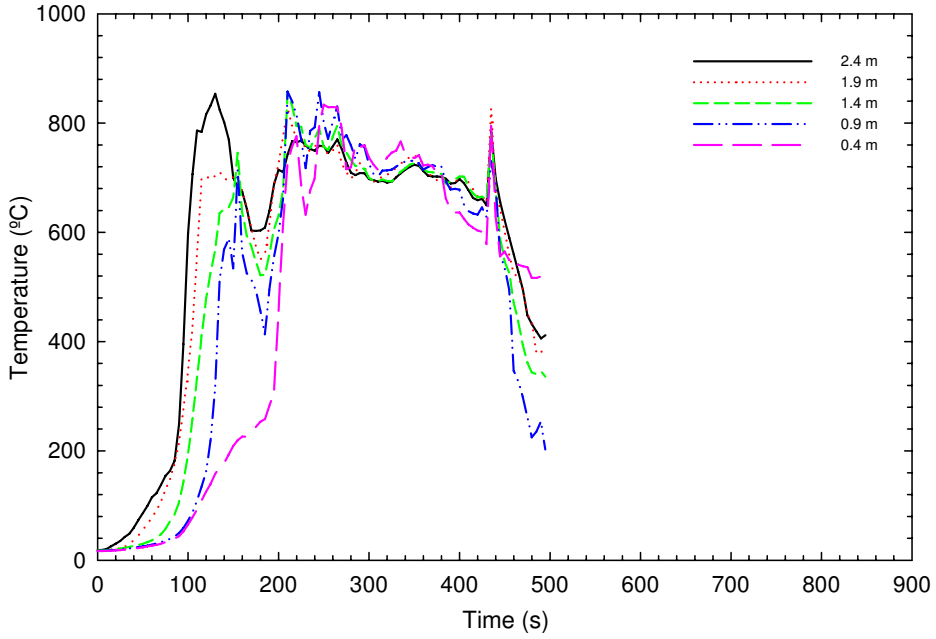


a) Basement SE quadrant

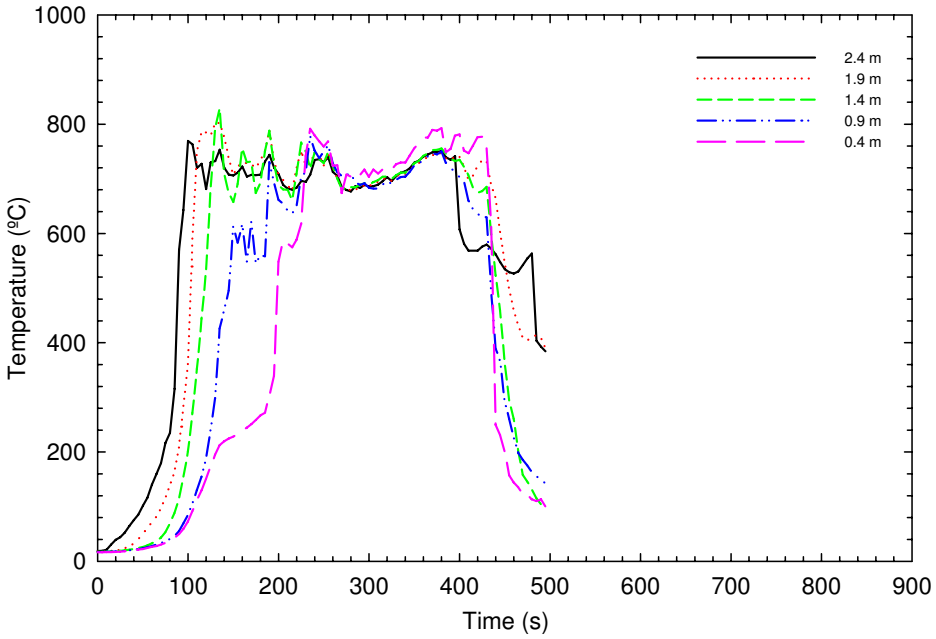


b) Basement SW quadrant

**Figure 20 (a and b). TC Trees in the basement – Test UF-06 at SE and SW quadrants**

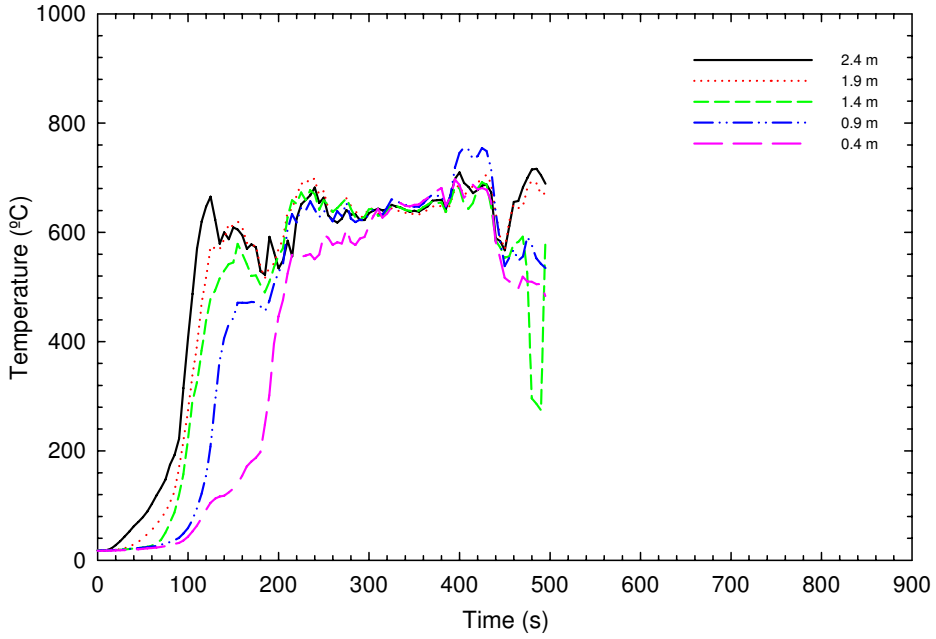


c) Basement NE quadrant

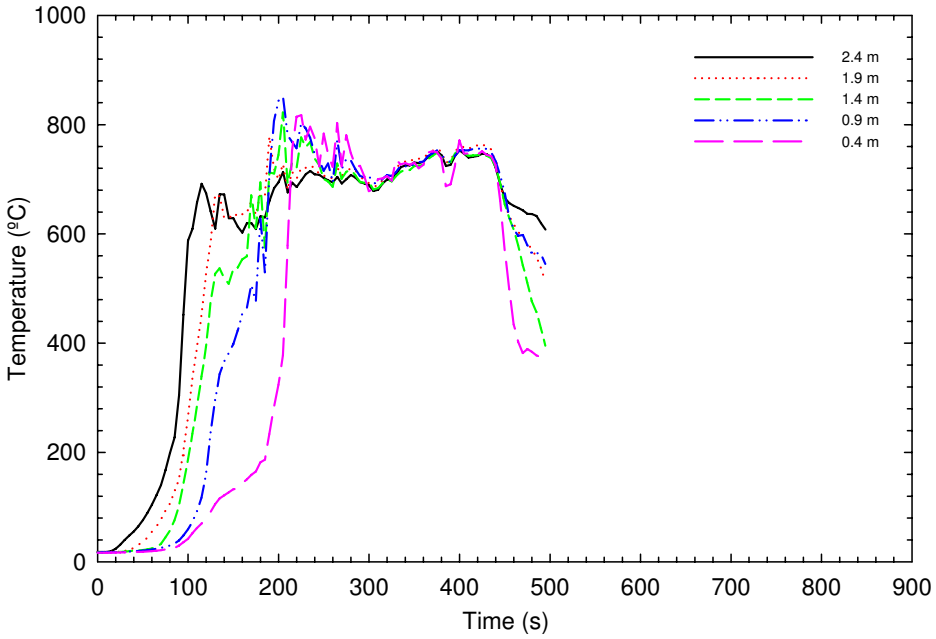


d) Basement NW quadrant

**Figure 20 (c and d). TC Trees in the basement – Test UF-06 at NE and NW quadrants**

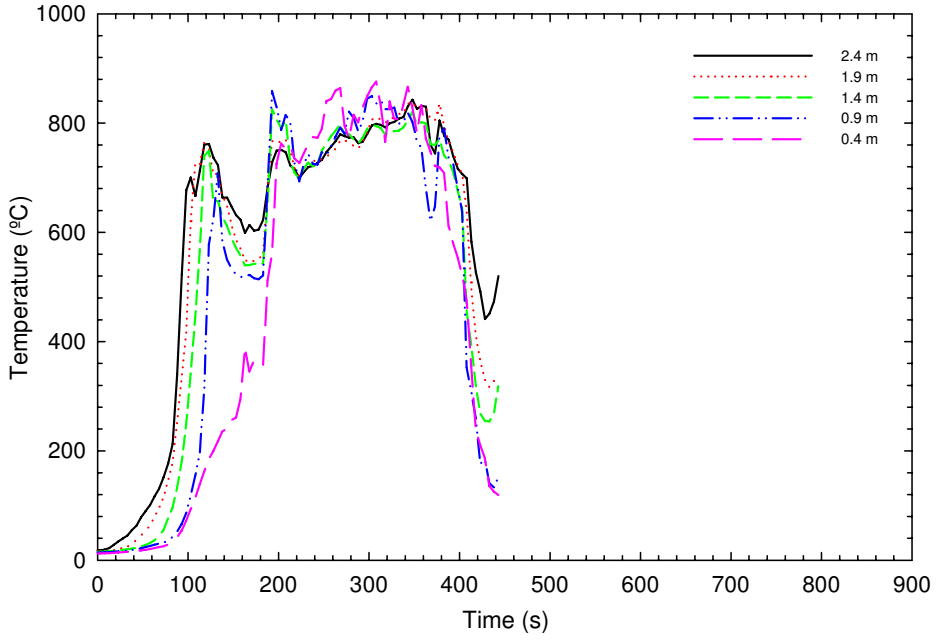


a) Basement SE quadrant

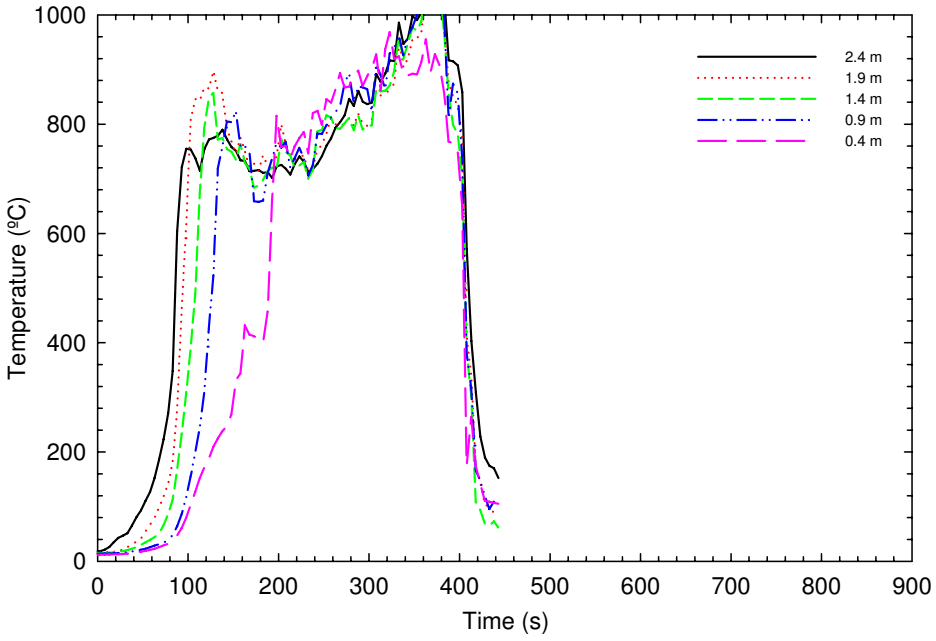


b) Basement SW quadrant

**Figure 20 (R-a and R-b). TC Trees in the basement – Test UF-06R at SE and SW quadrants**

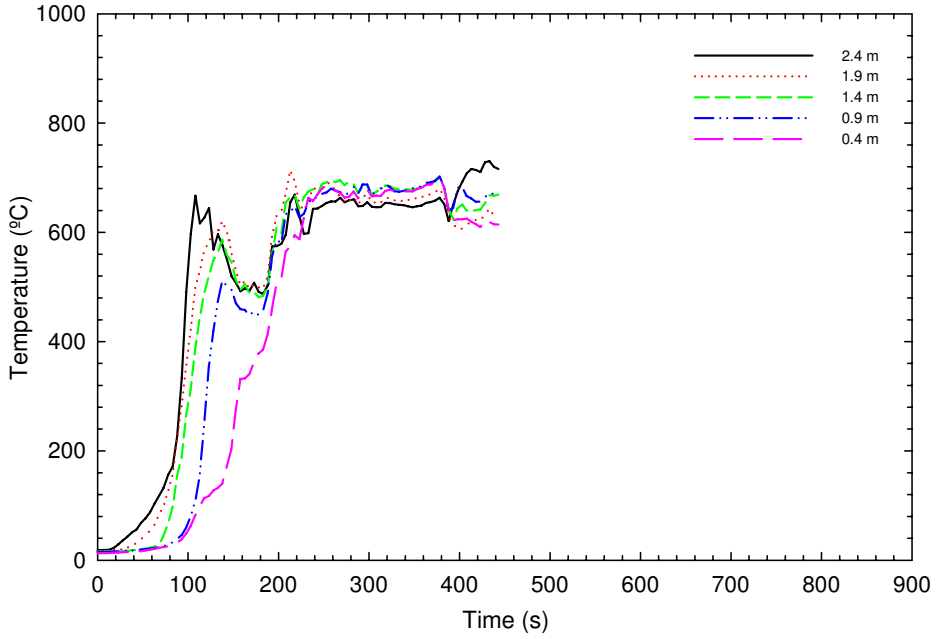


c) Basement NE quadrant

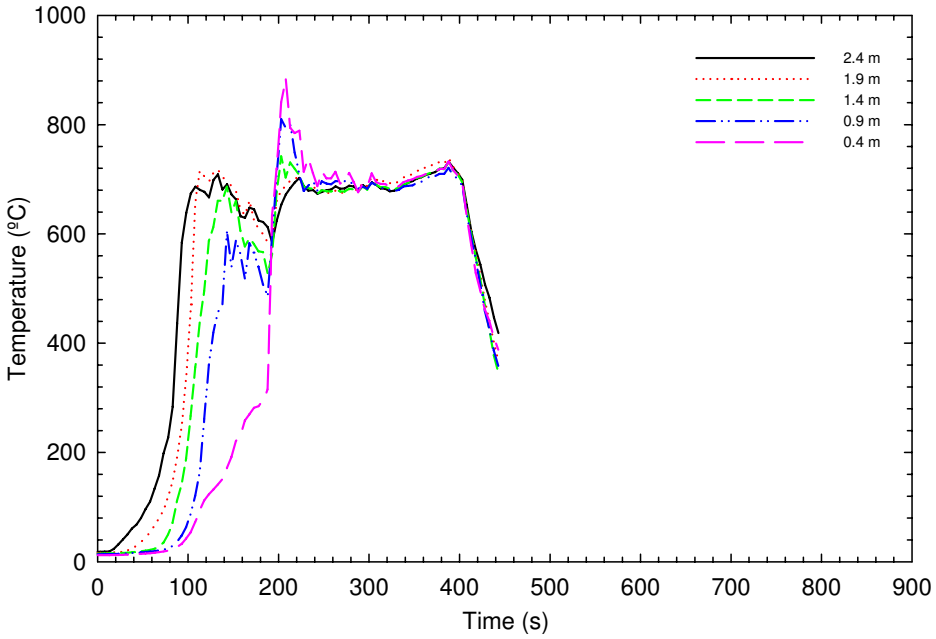


d) Basement NW quadrant

**Figure 20 (R-c and R-d). TC Trees in the basement – Test UF-06R at NE and NW quadrants**

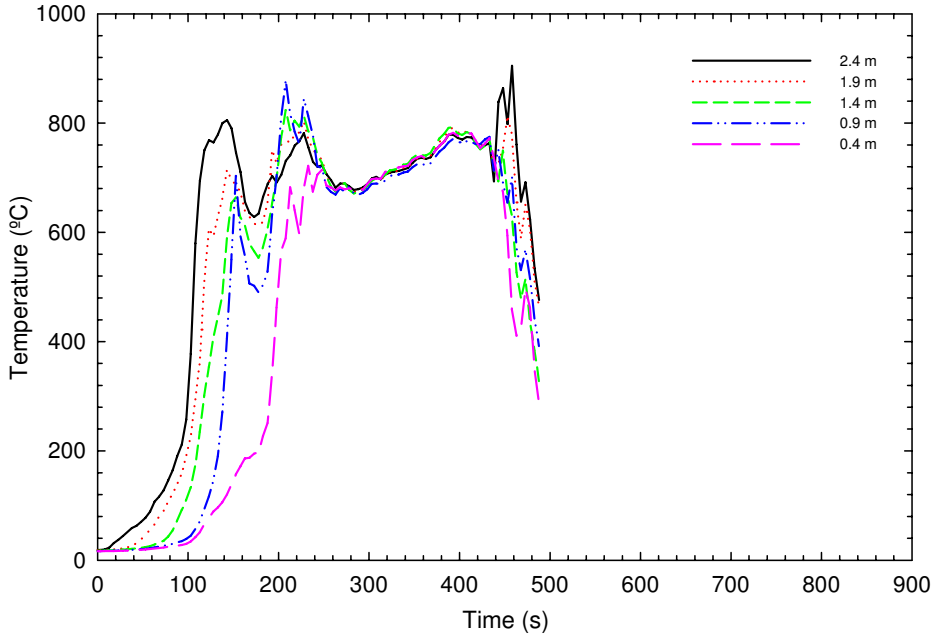


a) Basement SE quadrant

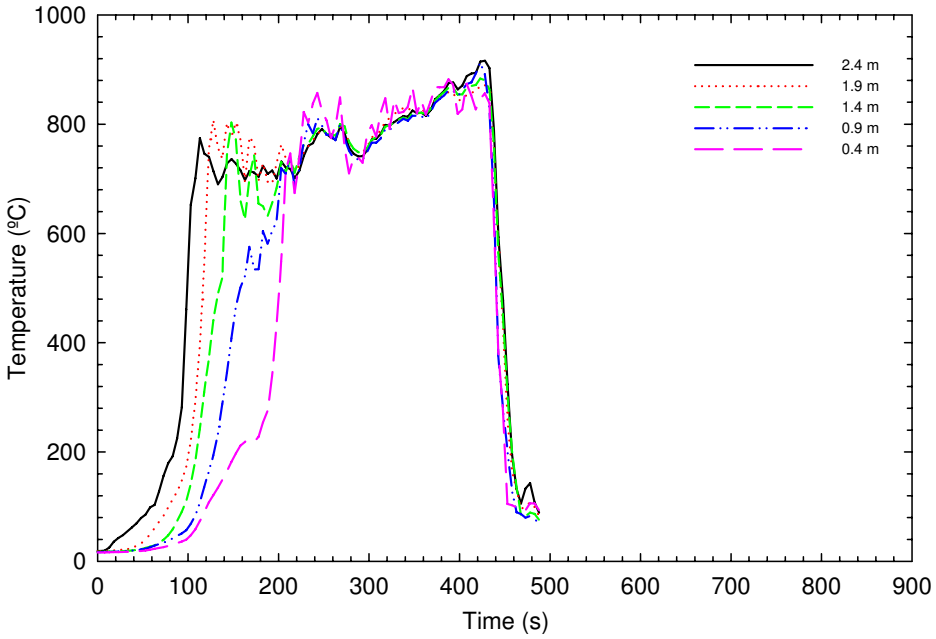


b) Basement SW quadrant

**Figure 20 (RR-a and RR-b). TC Trees in the basement – Test UF-06RR at SE and SW quadrants**

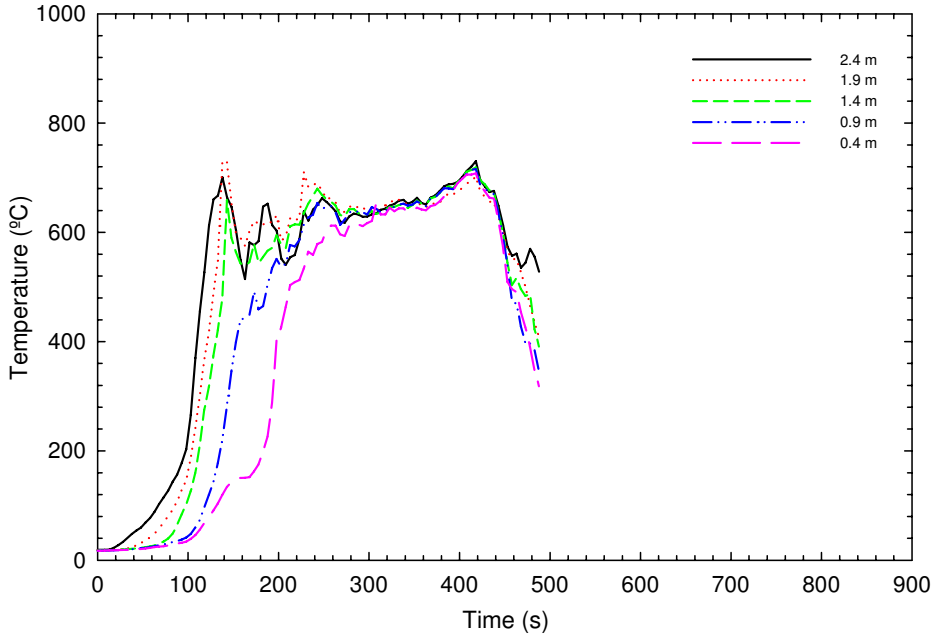


c) Basement NE quadrant

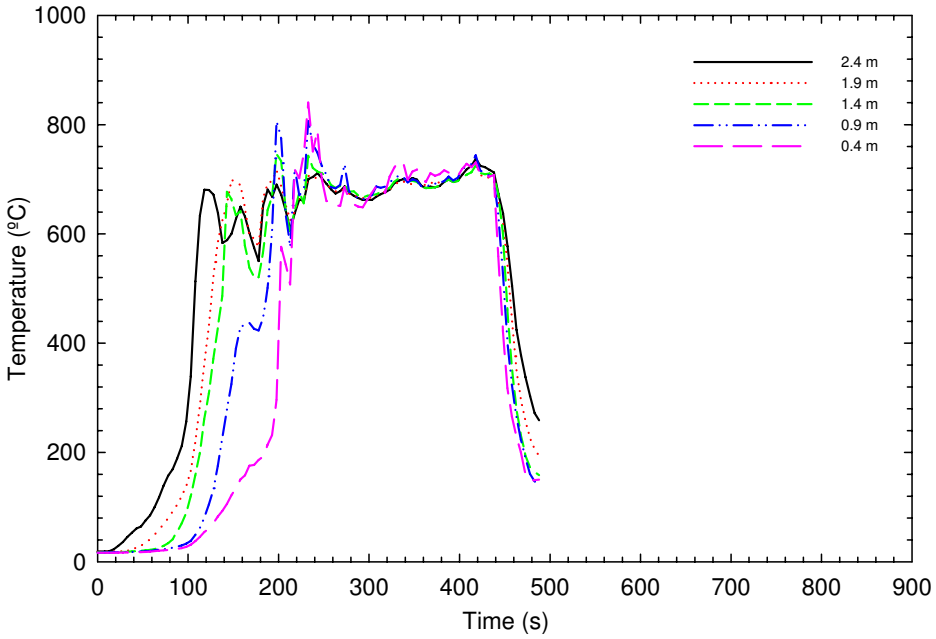


d) Basement NW quadrant

**Figure 20 (RR-c and RR-d). TC Trees in the basement – Test UF-06RR at NE and NW quadrants**

3.3.1.2 First storey

Figure 21 (a to d), Figure 21 (R-a to R-d) and Figure 21 (RR-a to RR-d) show the temperatures on the first storey at the SE, SW, NE and NW quarters, respectively, for Tests UF-06, UF-06R and UF-06RR.

In all cases, the temperatures increased due to the heating of the floor from below and the hot gases and smoke migrating from the basement. The temperatures peaked at about 220 s and decreased probably due to the opening of the exterior door on the first storey and fresh air coming into the first storey. The highest temperatures were recorded at the SE thermocouple tree because the fire in the basement fire compartment was just underneath this tree.

Close to the end of the tests, there was a sharp increase in temperatures at the four room quarter points, which may be an indication that flame had penetrated through the floor. Finally, the temperatures decayed because of the extinguishment of the fire.

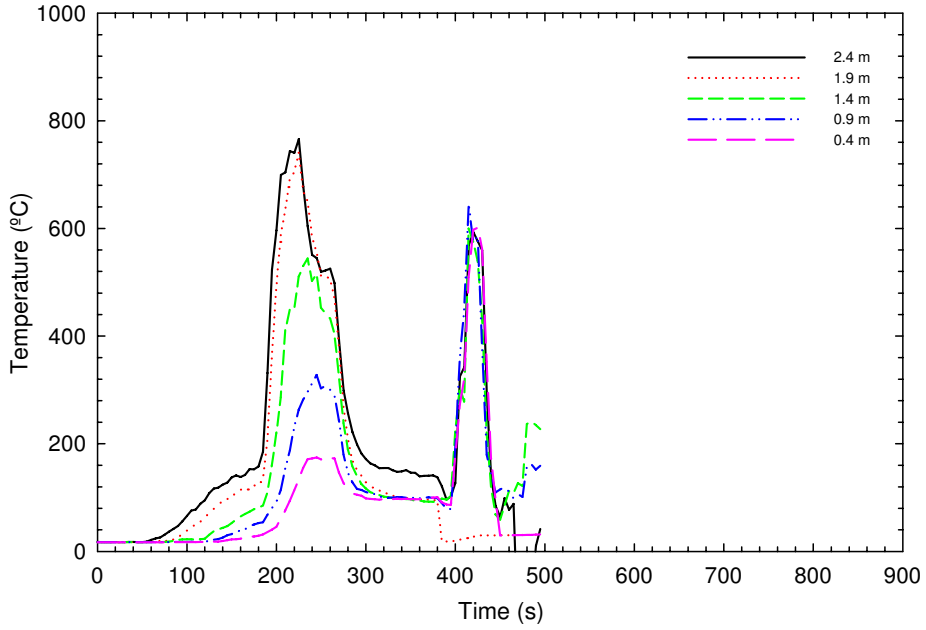


a) 1st Storey SE quadrant

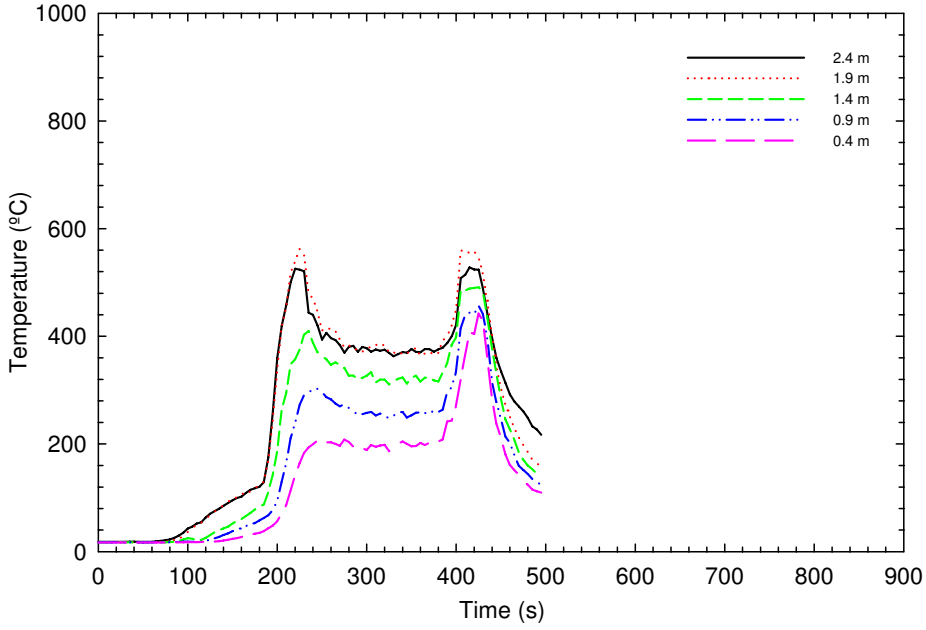


b) 1st Storey SW quadrant

**Figure 21 (a and b). TC trees on the first storey – Test UF-06 at SE and SW quadrants**

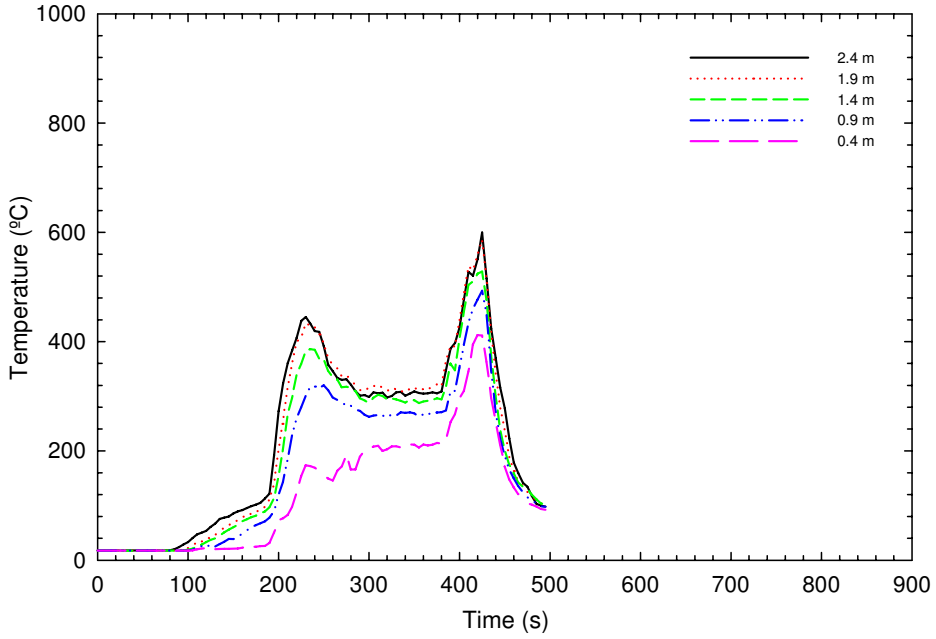


c) 1st Storey NE quadrant

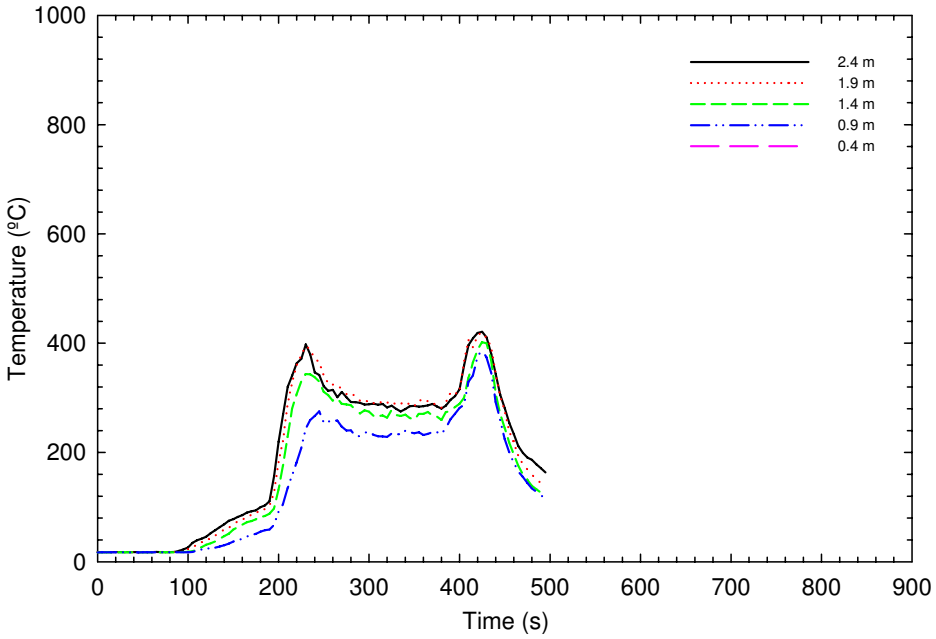


d) 1st Storey NW quadrant

**Figure 21 (c and d). TC trees on the first storey – Test UF-06 at NE and NW quadrants**

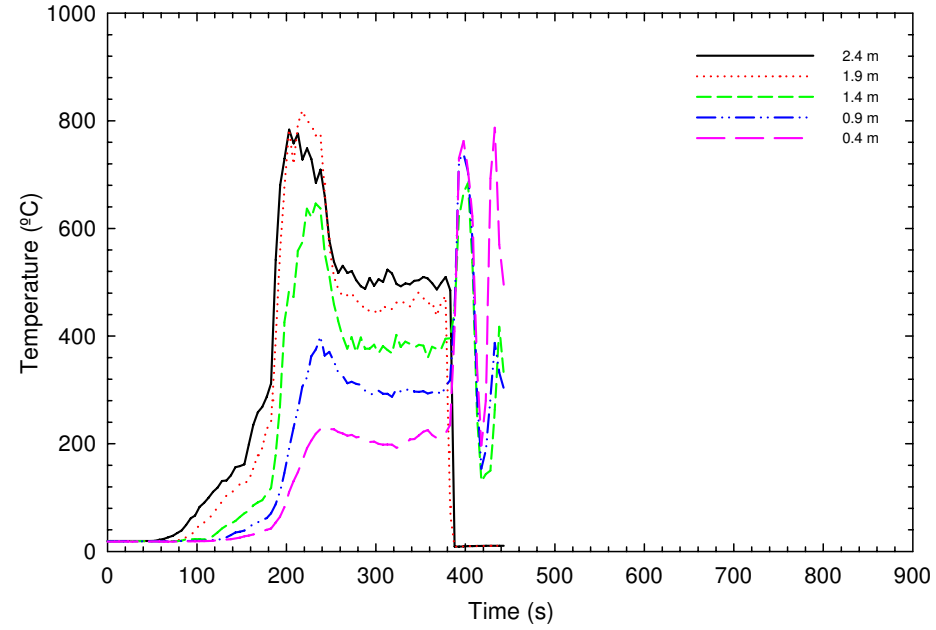


a) 1st Storey SE quadrant

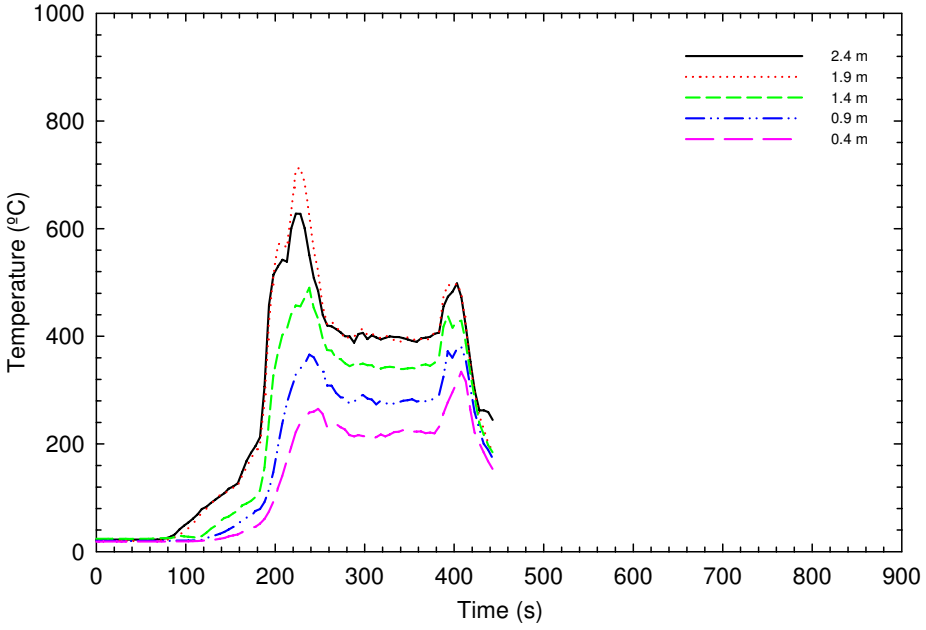


b) 1st Storey SW quadrant

**Figure 21 (R-a and R-b). TC trees on the first storey – Test UF-06R at SE and SW quadrants**

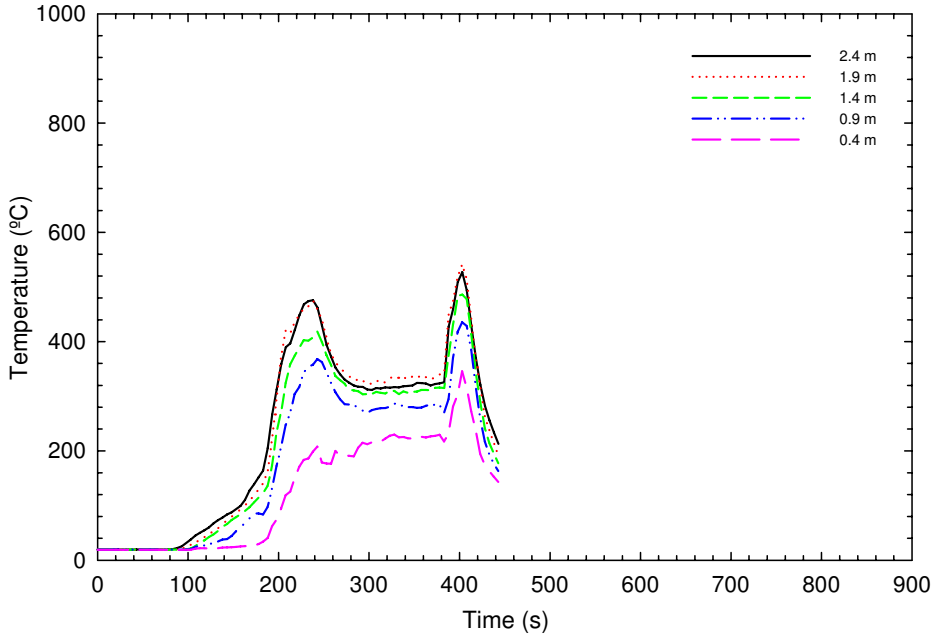


c) 1st Storey NE quadrant

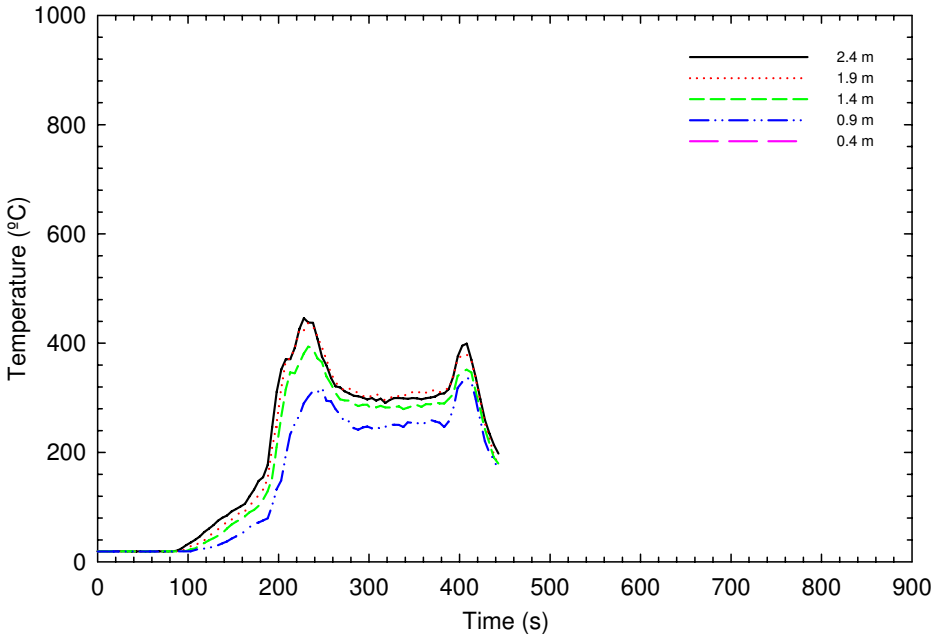


d) 1st Storey NW quadrant

**Figure 21 (R-c and R-d). TC trees on the first storey – Test UF-06R at NE and NW quadrants**

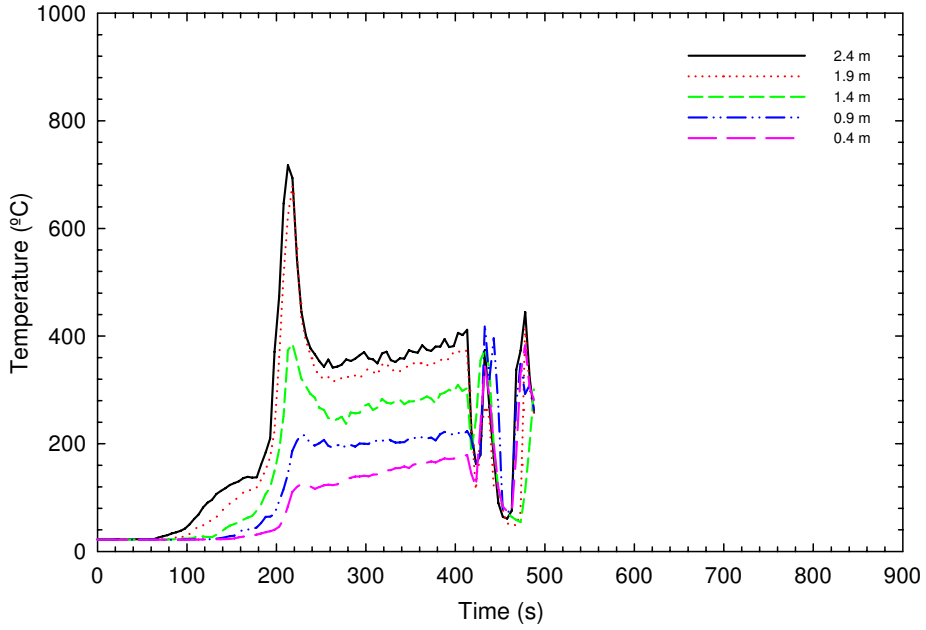


a) 1st Storey SE quadrant

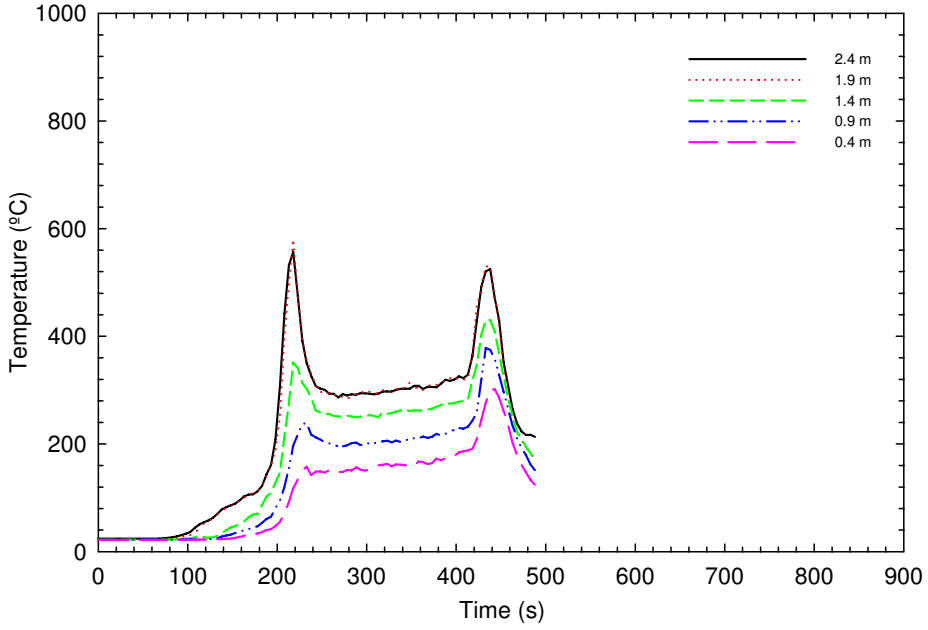


b) 1st Storey SW quadrant

**Figure 21 (RR-a and RR-b). TC trees on the first storey – Test UF-06RR at SE and SW quadrants**

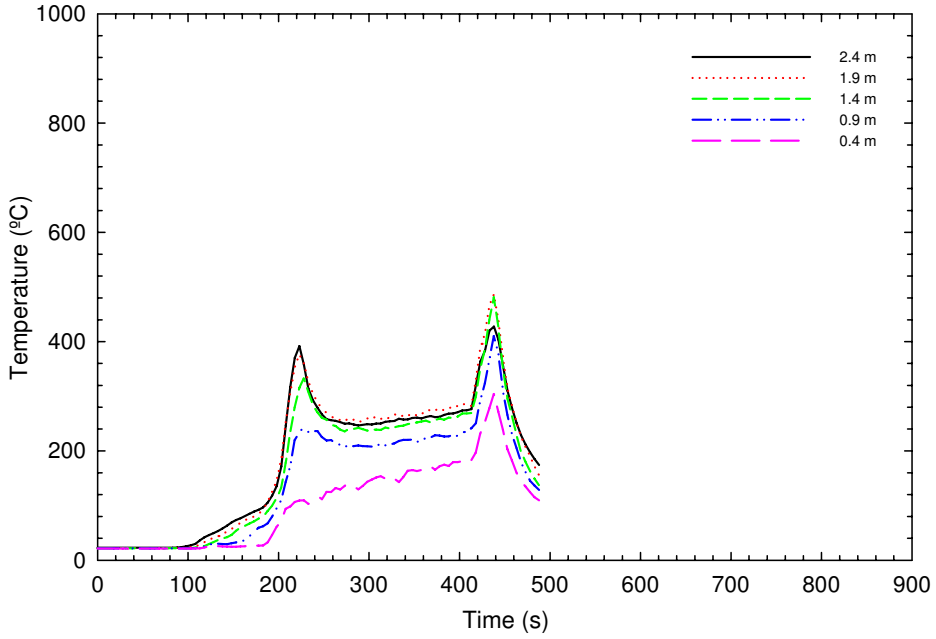


c) 1st Storey NE quadrant

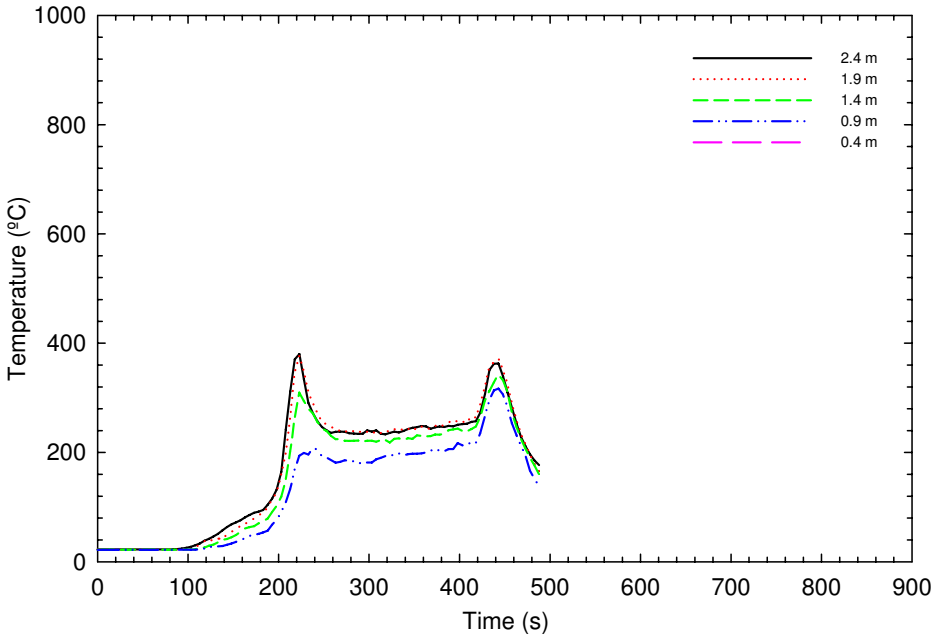


d) 1st Storey NW quadrant

**Figure 21 (RR-c and RR-d). TC trees on the first storey – Test UF-06RR at NE and NW quadrants**

#### 3.3.1.3 Second storey

Figure 22 (a and b), Figure 22 (R-a and R-b) and Figure 22 (RR-a and RR-b) show the temperatures in the SE and SW bedrooms, respectively for Tests UF-06, UF-06R and UF-06RR. The door to the SE bedroom was closed while the door to the SW bedroom was open.

Ambient temperature was measured for about the first 220 s for SE bedroom and 120 s for SW bedroom. After these times, the temperatures, at different heights within the rooms, started increasing. This increase was greater for the SW bedroom than the SE bedroom because the door to the SW bedroom was open. Smoke entered the SE bedroom mainly through gaps around the door. Maximum temperatures between 160ºC and 170ºC were reached at the 2.4 m height above the floor level for the SW bedroom. For the SW bedroom, the temperatures first peaked around 240 s and subsequently decreased probably due to fresh air coming from the opening of the exterior door on the first storey. The temperatures started increasing again around 400 s due to the intensive burning in the basement.

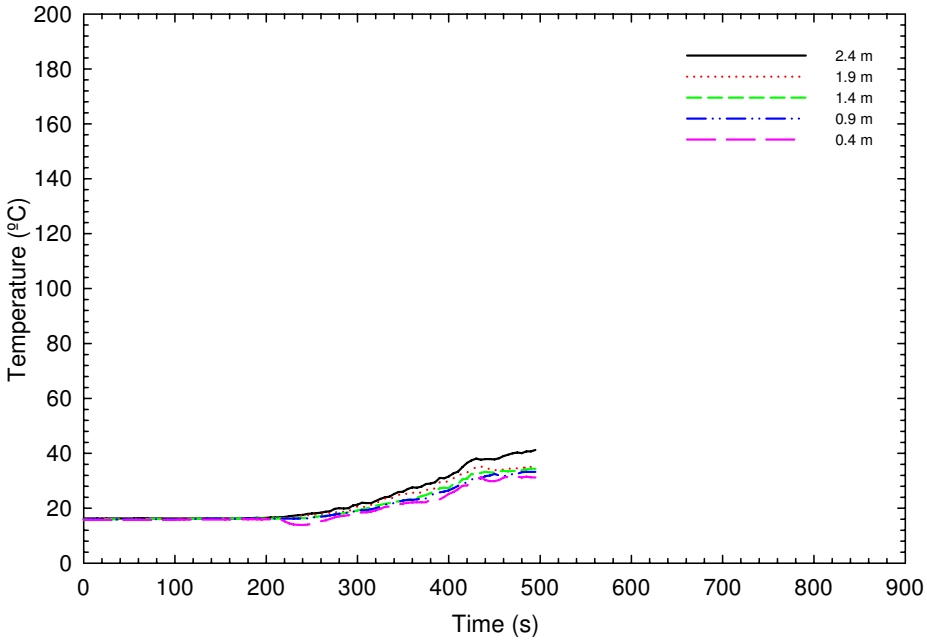


a) 2nd Storey SE bedroom

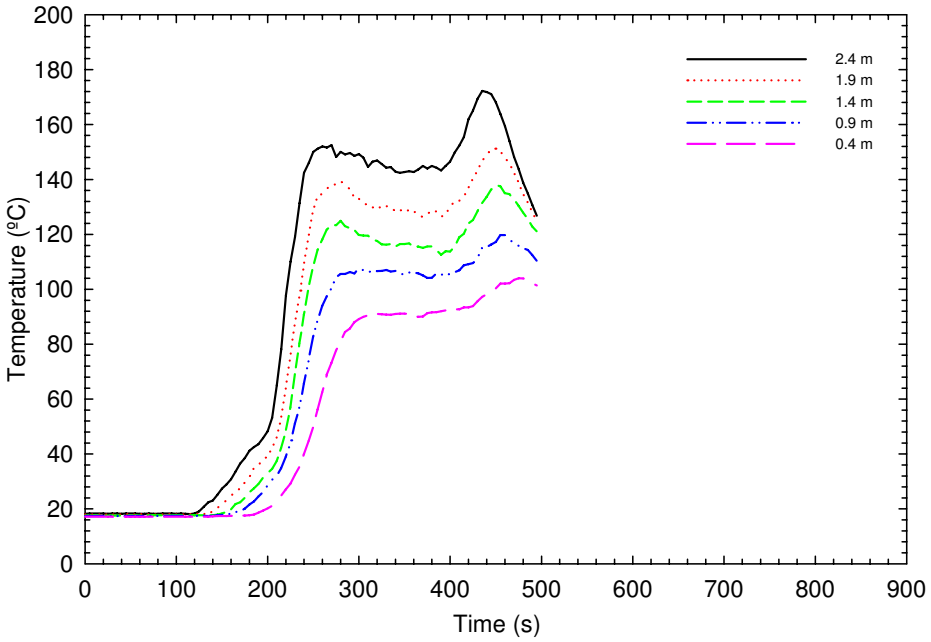


b) 2nd Storey SW bedroom

**Figure 22 (a and b). TC trees in the second storey bedrooms – Test UF-06**

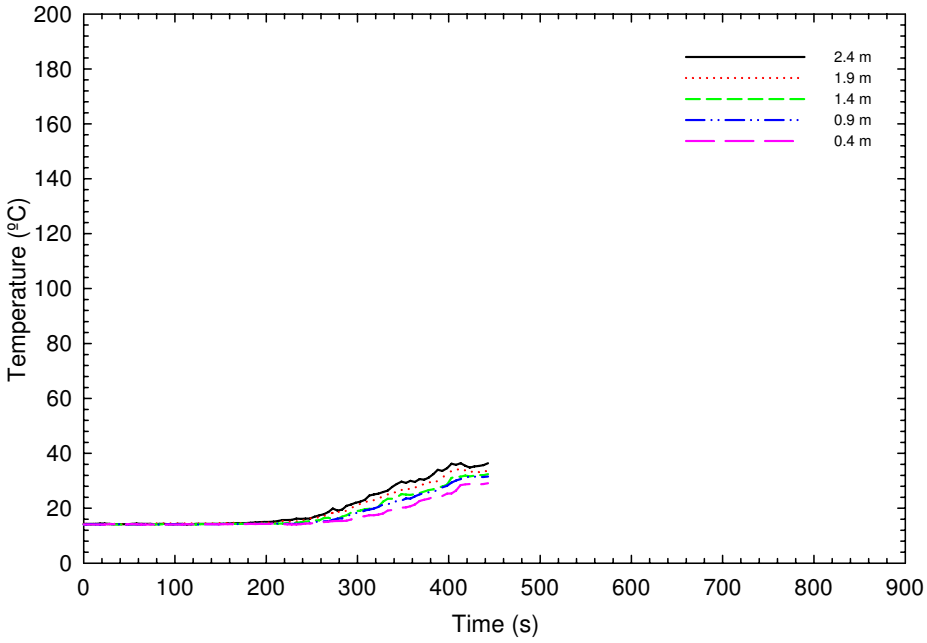


a) 2nd Storey SE bedroom.

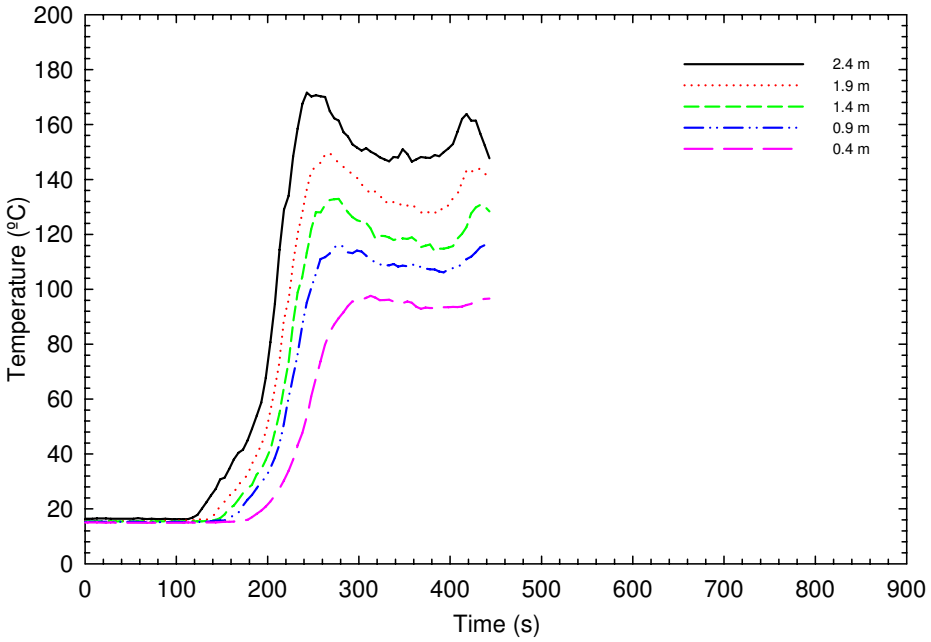


b) 2nd Storey SW bedroom.

**Figure 22 (R-a and R-b). TC trees in the second storey bedrooms – Test UF-06R**

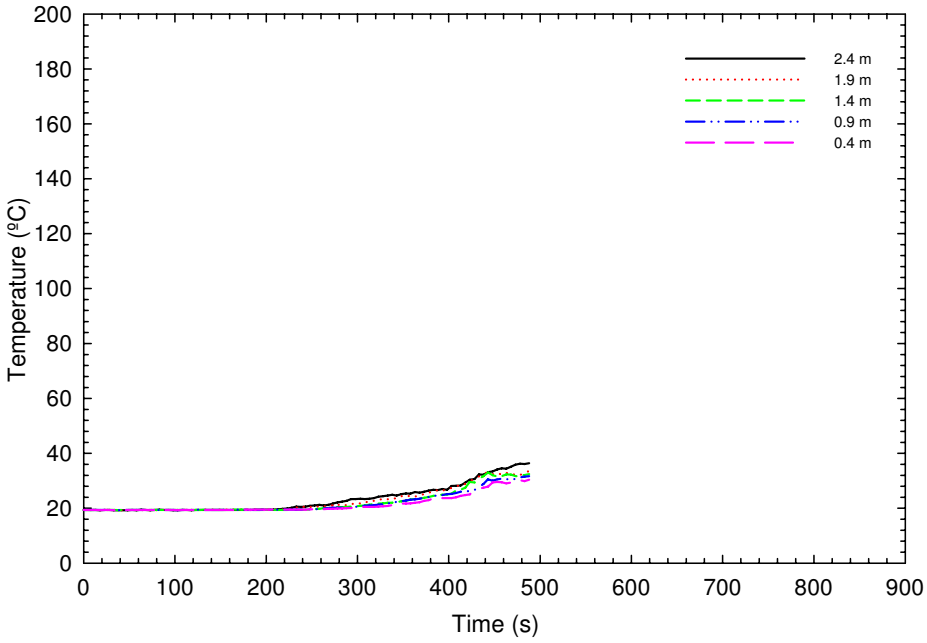


a) 2nd Storey SE bedroom

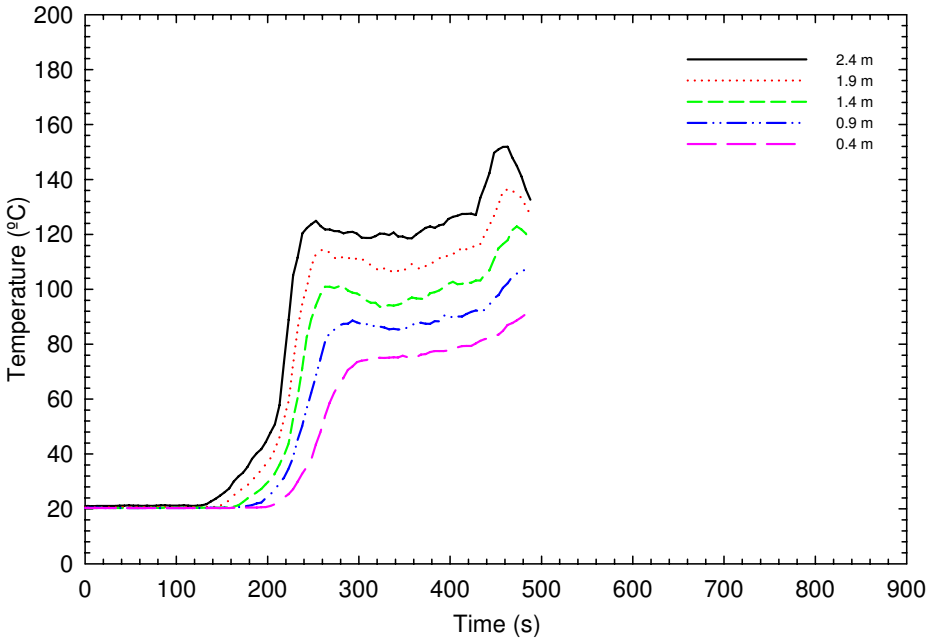


b) 2nd Storey SW bedroom

**Figure 22 (RR-a and RR-b). TC trees in the second storey bedrooms – Test UF-06RR**

### 3.3.2 Temperatures at the Window in the Basement

Five thermocouples were located in the basement window opening. Three were located along the vertical centreline of the opening, 125 mm from the bottom, 250 mm from the bottom and 375 mm from the bottom, respectively. The remaining two thermocouples were located 375 mm up from the bottom of the opening and 500 mm in from each side of the opening.

Figure 23 (a, b, c) shows the temperatures recorded at the basement window for Tests UF-06, UF-06R and UF-06RR, respectively. For all the tests, the temperatures increased to 600ºC in the first 120 s. The window was opened after 100 s for UF-06, 88 s for UF-06R, and 109 s for and UF-06RR, when the temperatures reached 300ºC at the window. After 120 s, due to air entering and smoke exiting the basement through the window opening, the temperatures varied depending on whether or not the flames touched the thermocouples (the bottom TC was probably below the neutral plane).

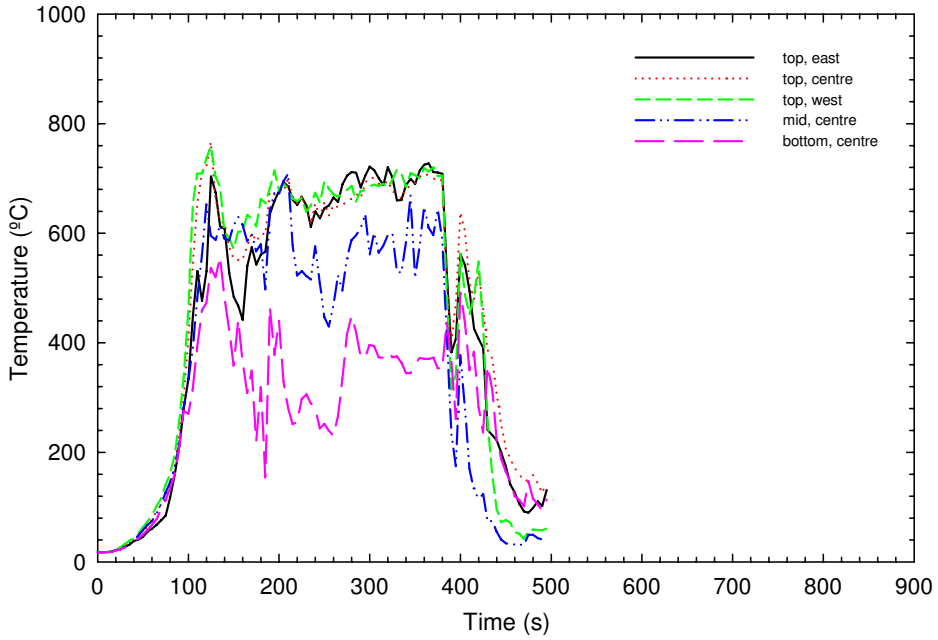


**Figure 23 (a). Temperatures at the window in the basement – Test UF UF-06**

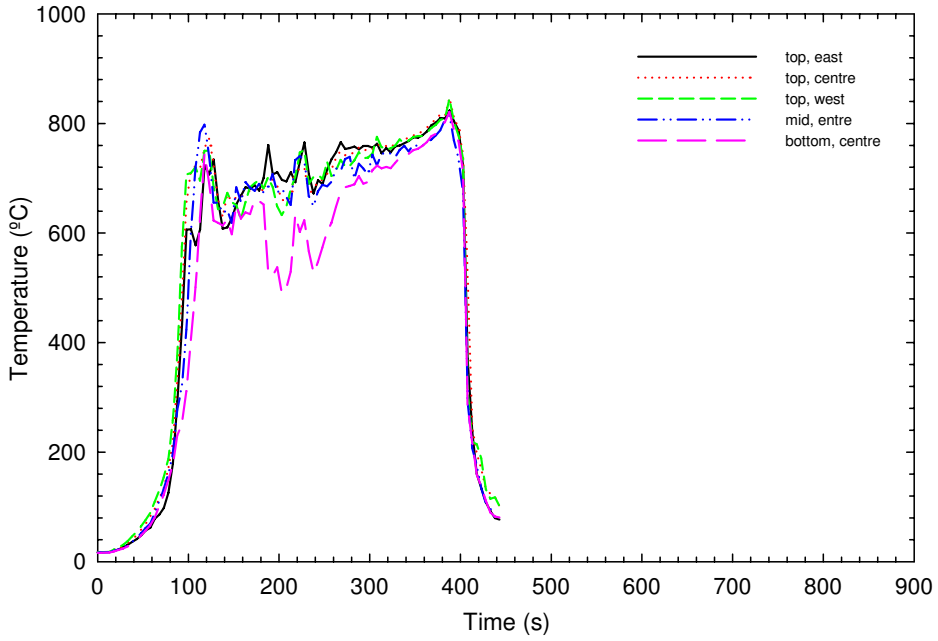


**Figure 23 (b). Temperatures at the window in the basement – Test UF-06R**

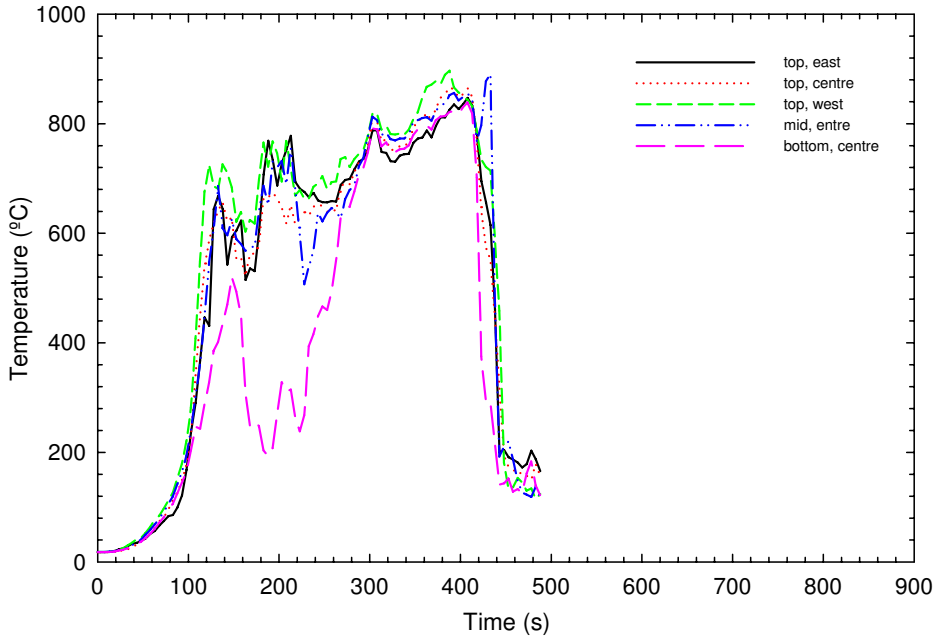


**Figure 23 (c). Temperatures at the window in the basement – Test UF-06RR**

### 3.3.3 Temperatures on the First Storey at the Top of the Stairs from the Basement

Figure 24 (a, b, c) shows the temperatures at the top of the stairs on the first storey at different heights for Tests UF-06, UF-06R and UF-06RR, respectively. The conditions remained at ambient temperature for about the first 60 s. After this, temperatures, at different heights, started increasing due to the migration of hot gases and smoke from the basement to the upper storeys. A maximum temperature of about 900ºC was reached. Then, there was a decline in temperatures after the exterior door on the first storey was open and there was an influx of fresh air. The temperatures then remained constant, for each height, for about 150 s. Near the end of the tests, the temperatures started increasing again due to the extensive burning of the wood cribs and flame penetration through the floor. The temperatures started decaying after the extinguishment of the fire was initiated.

The maximum temperatures were not reached at the 2.4 m level but at the 0.9, 1.4 and 1.9 m levels. This is probably an indication that cooler air was entering the basement at both the upper level and lower level of the doorway.

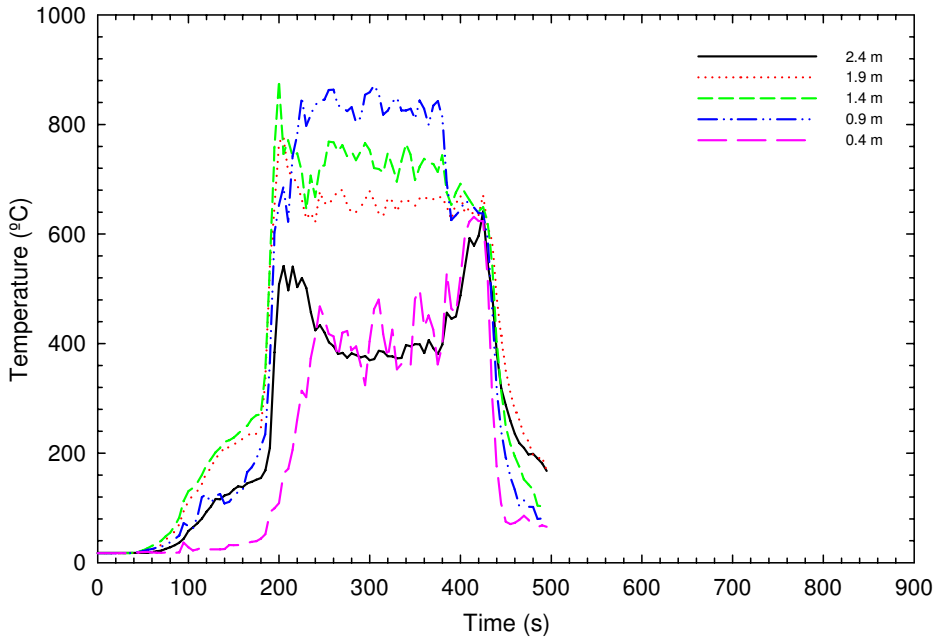


**Figure 24 (a). Temperatures on the first storey at the top of the stairs from the basement – UF-06**

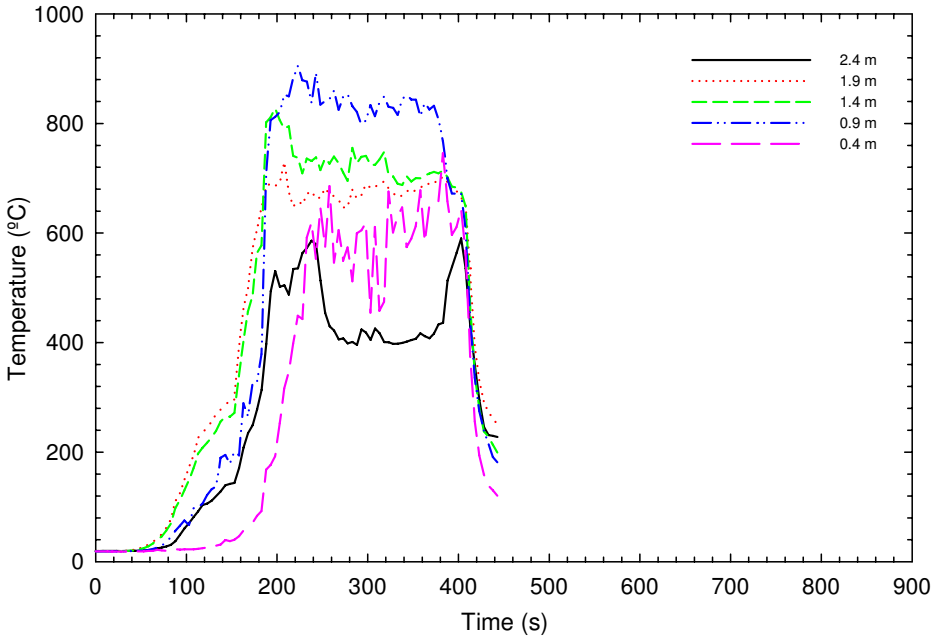


**Figure 24 (b). Temperatures on the first storey at the top of the stairs from the basement – Test UF-06R**

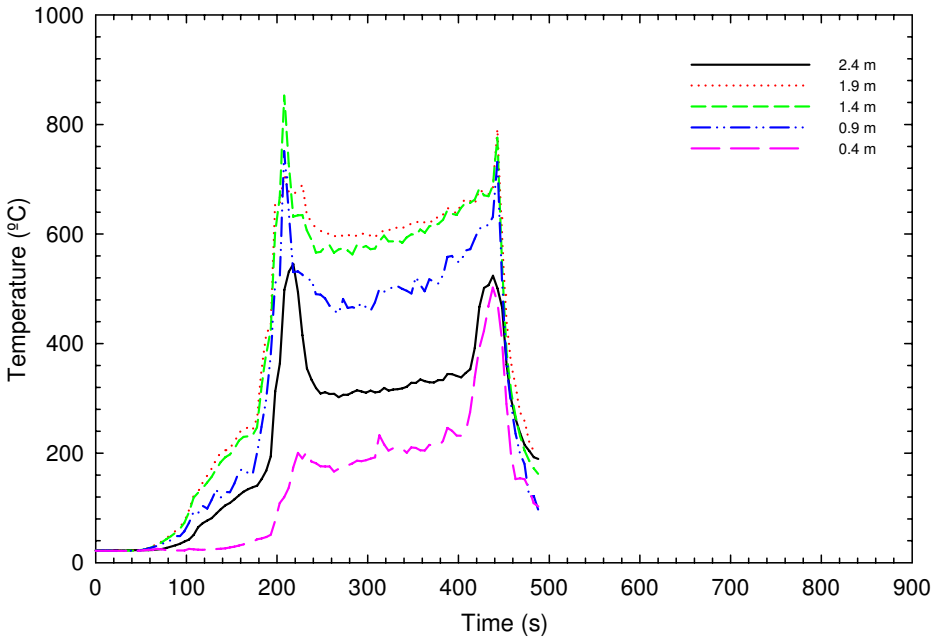


**Figure 24 (c). Temperatures on the first storey at the top of the stairs from the basement – Test UF-06RR**

### 3.3.4 Temperatures on the Second Storey at the Top of the Stairs

Figure 25 (a, b, c) shows the temperatures at the top of the stairs on the second storey at different heights for Tests UF-06, UF-06R and UF-06RR, respectively. The conditions remained at ambient temperature for about the first 120 s. After this, temperatures, at different heights, started increasing due to the migration of hot gases and smoke from the basement to the upper storeys. A maximum temperature of about 250ºC was reached at the 2.4 m height. The temperatures started decaying after the extinguishment of the fire was initiated.

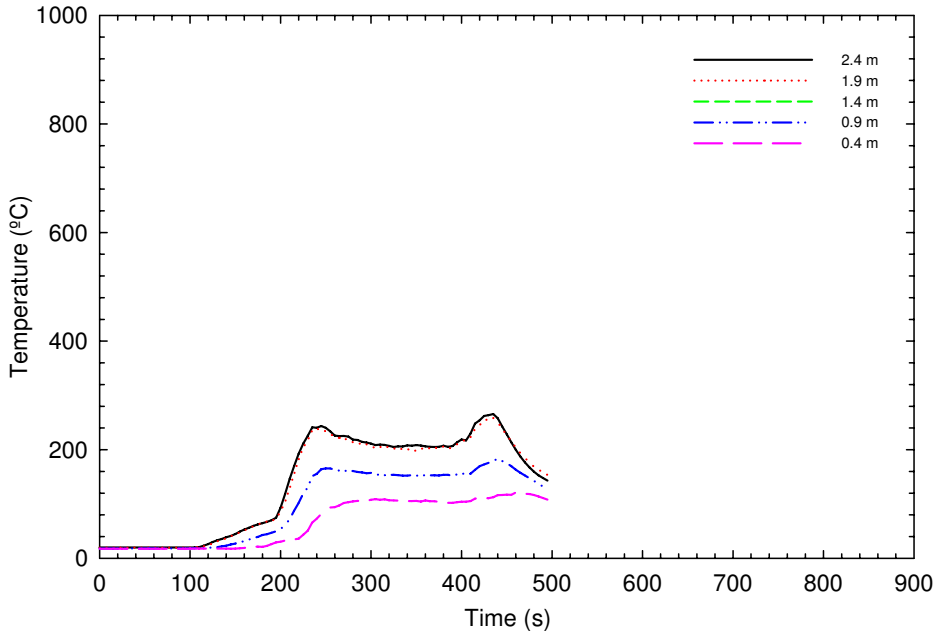


**Figure 25 (a). Temperatures on the second storey at the stairs – Test UF-06**

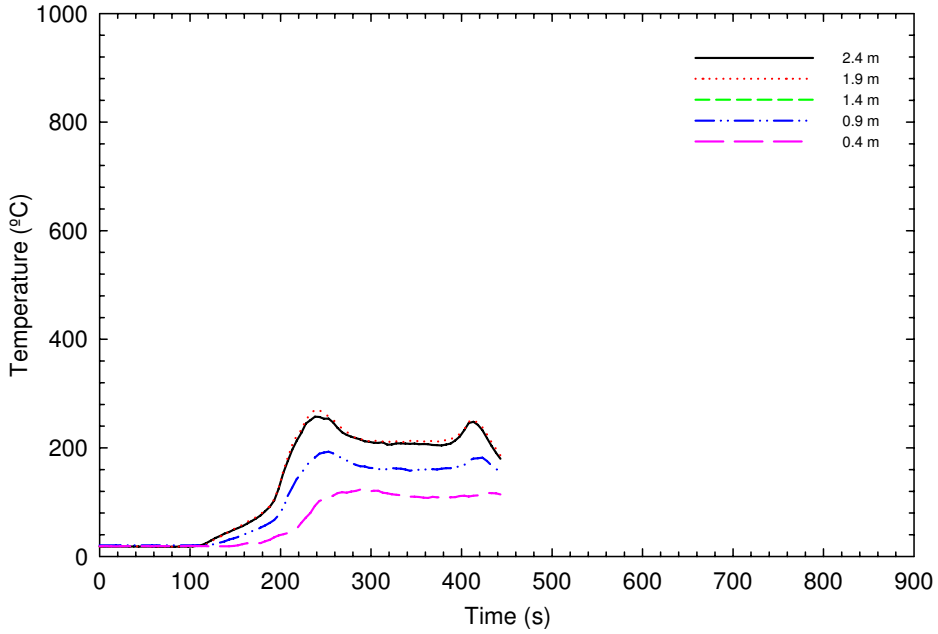


**Figure 25 (b). Temperatures on the second storey at the stairs – Test UF-06R**

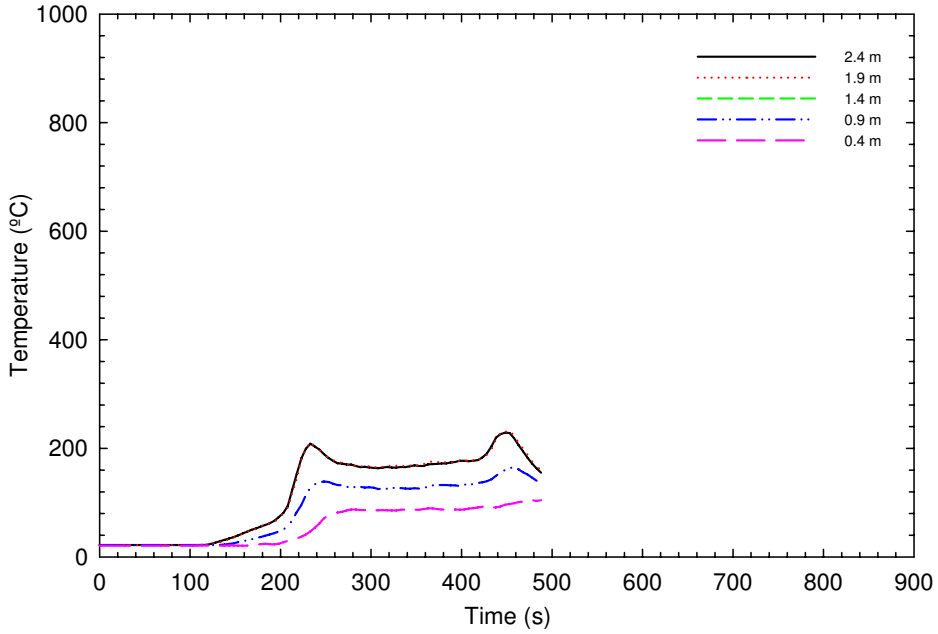


**Figure 25 (c). Temperatures on the second storey at the stairs – Test UF-06RR**

### 3.3.5 Temperatures at the Outside Doorway on the First Storey

Figure 26 (a, b, c) shows the temperatures at the exterior doorway on the first storey for Tests UF-06, UF-06R and UF-06RR, respectively. Ambient temperature was measured for about the first 100 s for the three tests. After this time, the temperatures increased reaching 340ºC in Test UF-06, 360°C in Test UF-06R, and 300ºC in Test UF-06RR at 230 s due to smoke and hot fire gases exiting through the open exterior door. Near the end of the tests, there was an increase in temperatures (due probably to flame penetration through the floor producing more radiation and hot gases in the vicinity of the exterior door). The maximum temperatures reached were about 500ºC for UF-06, 440°C for UF-06R, and 400ºC for UF-06RR. The temperatures started decaying after the extinguishment of the fire was initiated.

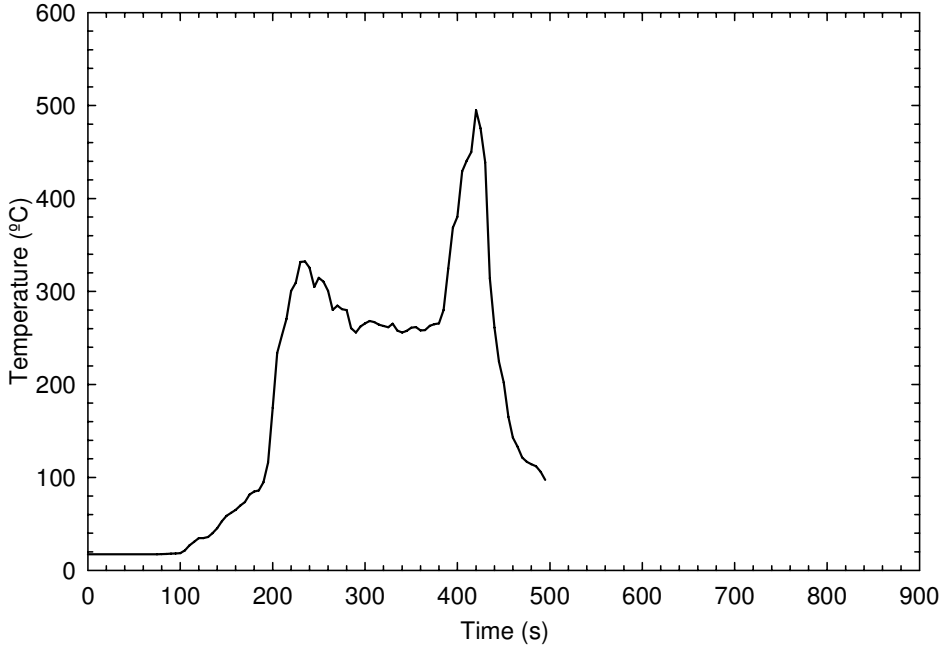


**Figure 26 (a). Temperatures at the outside doorway on the first storey – Test UF-06**

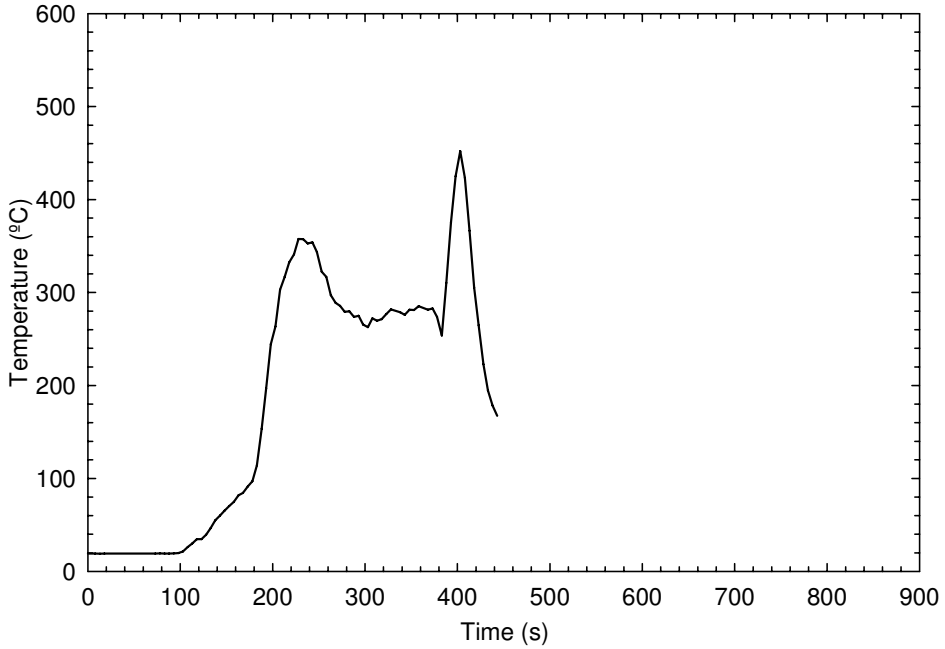


**Figure 26 (b). Temperatures at the outside doorway on the first storey – Test UF-06R**

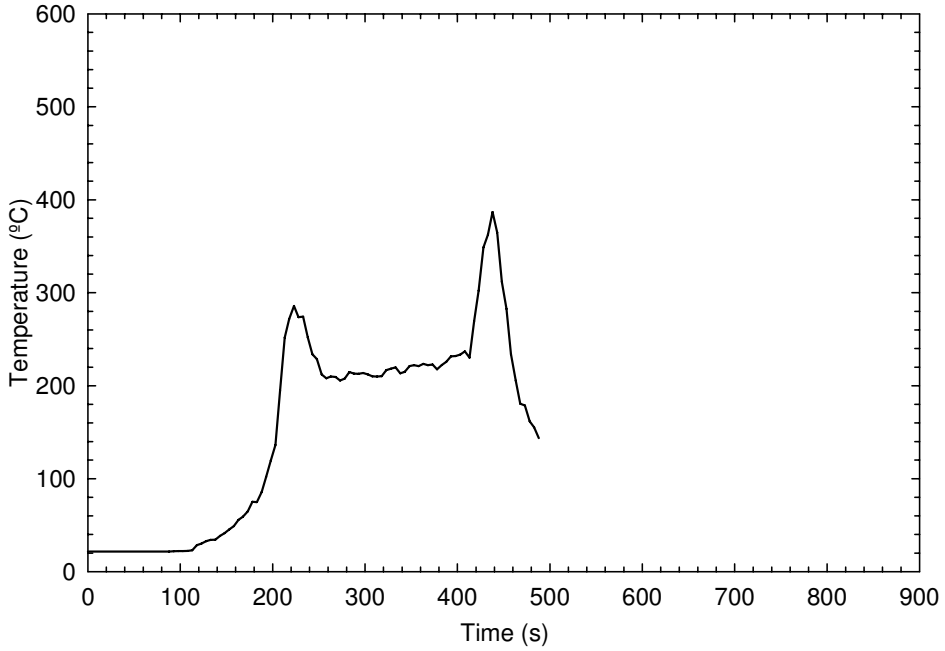


**Figure 26 (c). Temperatures at the outside doorway on the first storey – Test UF-06RR**

### 3.3.6 Temperatures on the First Storey on the Unexposed Side of the Floor Assembly

#### 3.3.6.1 Test UF-06, UF-06R and UF-06RR

Figure 27 (a and b), Figure 27 (R-a and R-b) and Figure 27 (RR-a and RR-b) show the temperatures measured by thermocouples (TCs) No. 1 to 9 and No. 89 through 94 located on the unexposed side (top) of the OSB subfloor of the floor assembly (see Figure 15 and Figure 16) for Tests UF-06, UF-06R and UF-06RR. For TCs 1 to 9, the temperatures remained at ambient temperature for the first 200 s. After this, the temperatures increased gradually until 390 s for Test UF-06, 380 s for Test UF-06R, and 410 s for Test UF-06RR. Thereafter, the temperatures show a faster rate of increase at all locations. This faster increase in temperature rise was due to the positioning of the thermocouples in the vicinity of the fire. This is also an indication that flames penetrated through the floor and the floor was being breached at many locations. Subsequently, the temperatures decreased during the extinguishment of the fire. Temperatures at locations 89 to 94 show a similar trend.

It is worth mentioning that failure under standard fire test conditions [14], on the basis of temperature, is defined as a temperature rise of 140°C above ambient temperature for the average of the nine padded thermocouples or a temperature rise of 180°C above ambient temperature at any single point on the unexposed side.

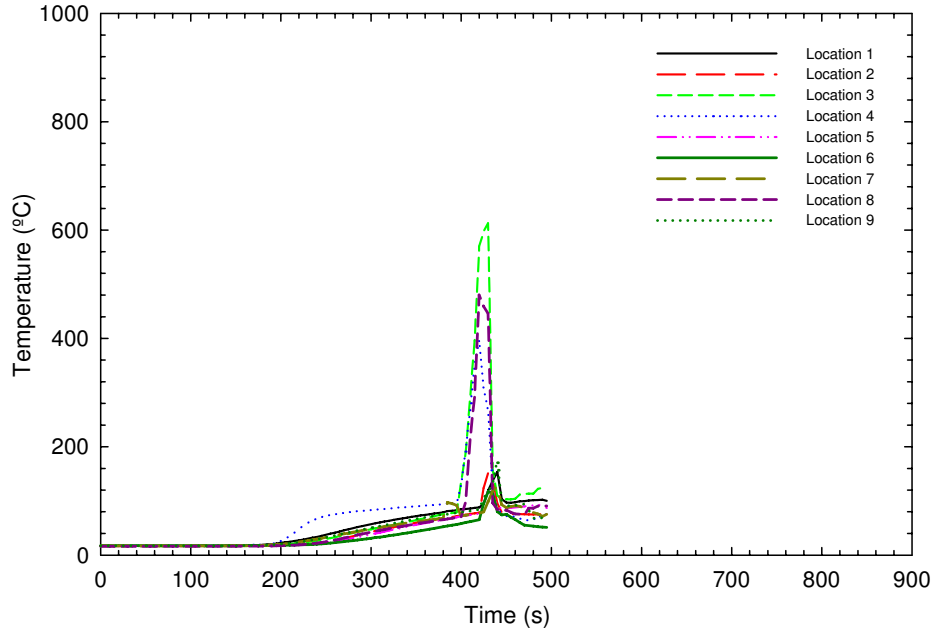


a) Unexposed TCs under insulated pad on top of subfloor

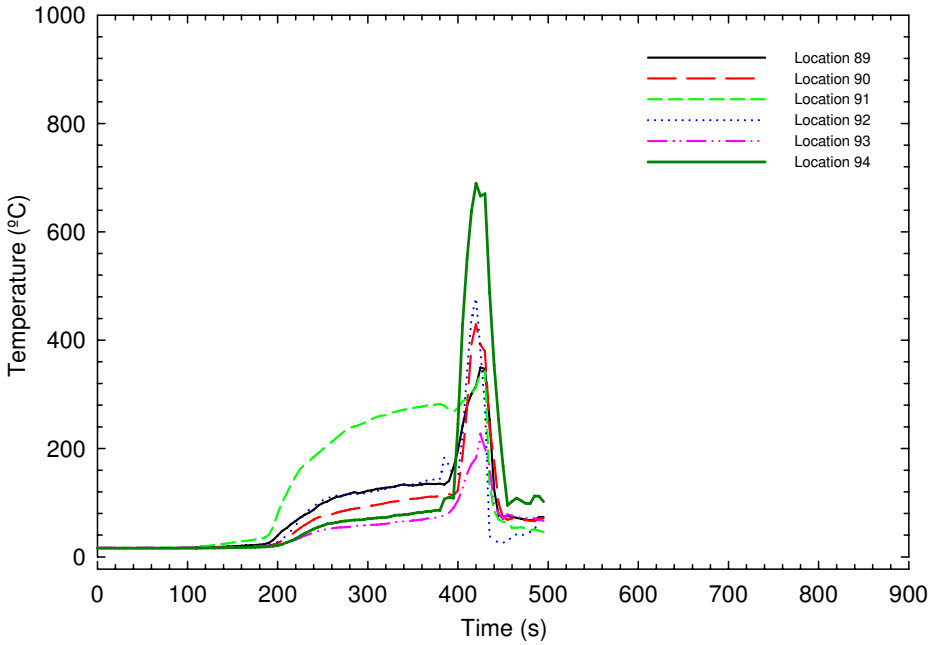


b) Bare TCs on the unexposed (top) side of the subfloor

**Figure 27(a and b). Temperatures at the unexposed side of subfloor – Test UF-06**

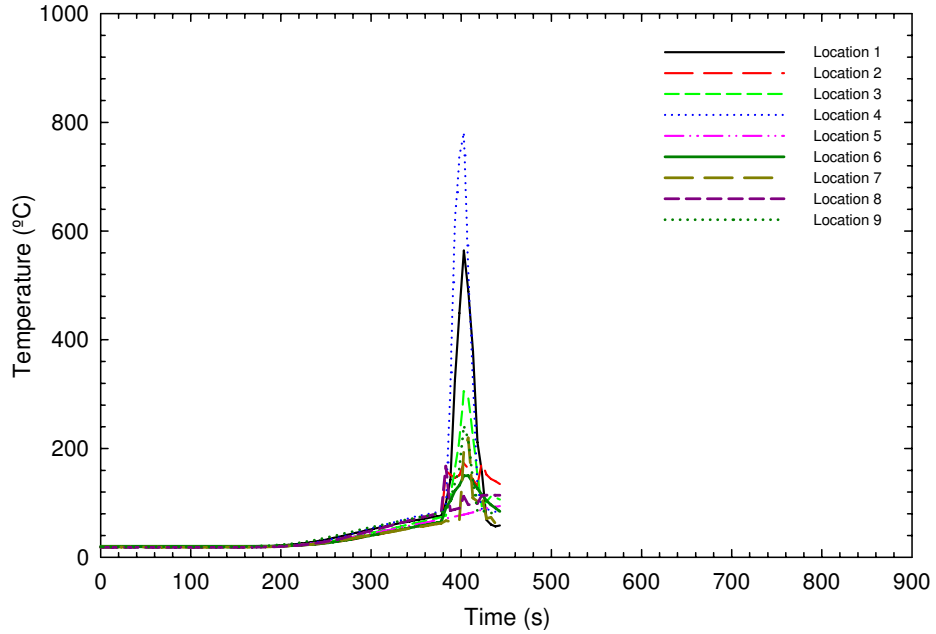


a) Unexposed TCs under insulated pad on top of the subfloor

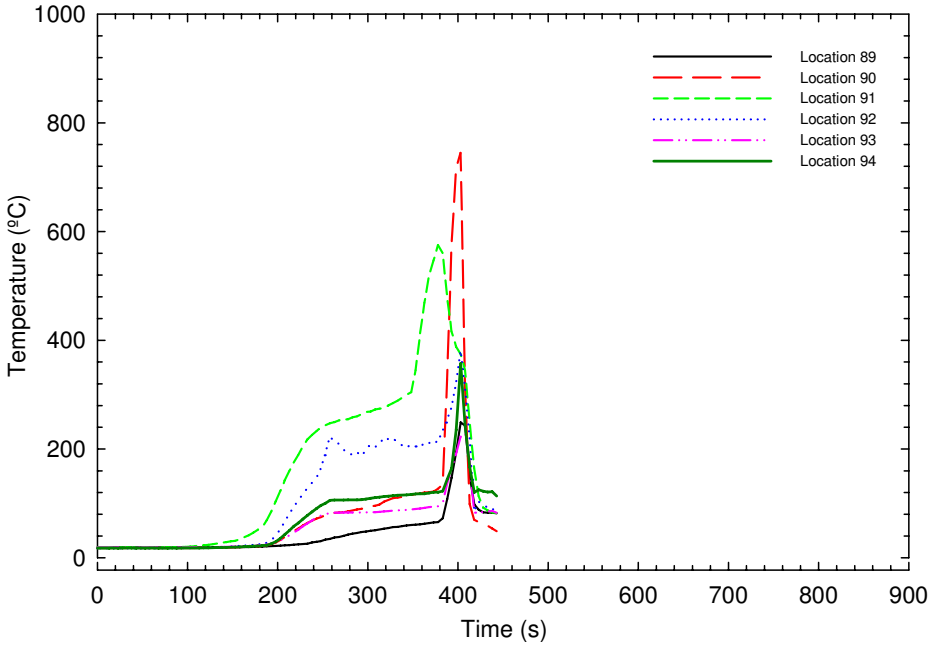


b) Bare TCs on the unexposed (top) side of the subfloor

**Figure 27 (R-a and R-b). Temperatures at the unexposed side of subfloor – Test UF-06R**

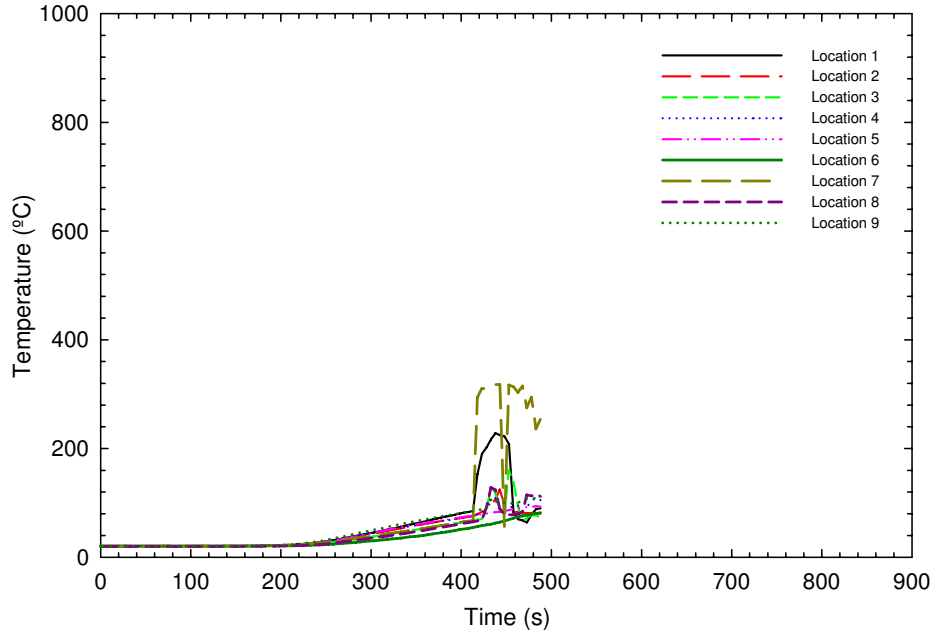


a) Unexposed TCs under insulated pad on top of subfloor

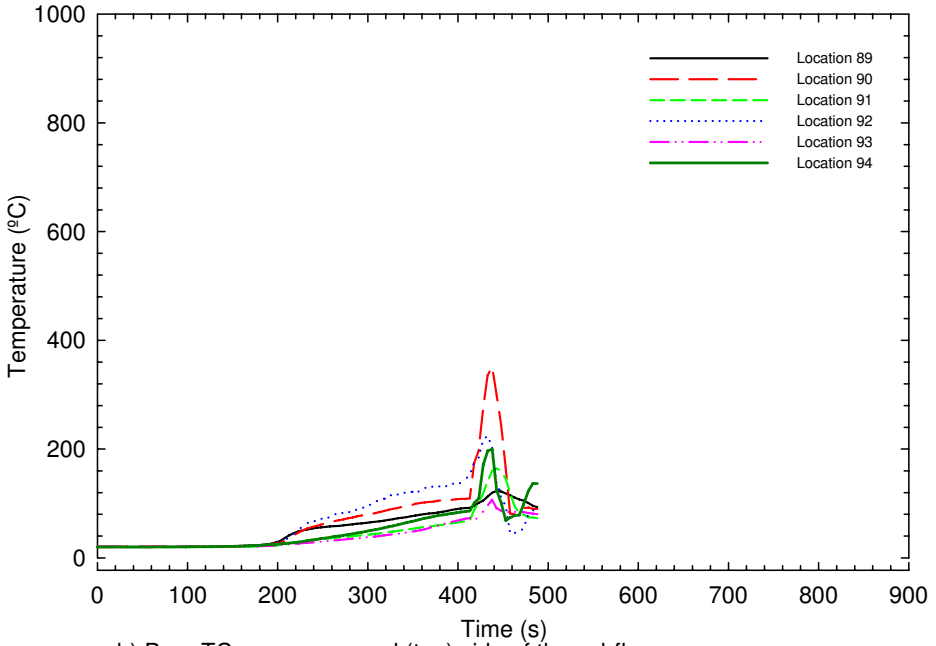


b) Bare TCs on unexposed (top) side of the subfloor

**Figure 27 (RR-a and RR-b). Temperatures at the unexposed side of subfloor – Test UF-06RR**

### 3.3.7 Temperatures on the Exposed Side of the Floor Assembly

The location of each grouping of thermocouples is identified by the Section label (A, B, C, D and E) and the I-joist space shown on Figure 15 and Figure 16. For example, C-1 is the group of thermocouples located along Section C in I-joist Cavity 1.

The temperatures on the exposed side of the floor assembly were measured at a number of locations distributed in such a way as to learn, as much as possible, the effect of the fire on the floor assemblies. As shown in Figure 15 and Figure 16 (Location of Thermocouples), in the locations at Sections A, B, C and E, seven thermocouples were installed: 2 at the bottom of two adjacent I-joists, 2 in the cavity at mid-height of the two I-joists, 2 between the subfloor and the two I-joists, and 1 in the cavity at the subfloor at mid-distance between the 2 I-joists. Section D had only 1 thermocouple in the cavity at the subfloor at mid-distance between the 2 I-joists.

#### 3.3.7.1 Tests UF-06, UF-06R and UF-06RR

Figure 28 (a to l), Figure 28 (R-a to R-l) and Figure 28 (RR-a to RR-l) show the temperatures measured by the thermocouples located on the exposed side of the floor. For all the locations with 7 thermocouples (A-2, A-7, A-12, B-7, C-1, C-5, C-7, C-9, C-11, C-13, and E-1), in almost every case the trend was similar with a sharp increase in temperatures for all the exposed thermocouples in the first 100 s to 140 s. For the thermocouples located at the interface between the top of an I-joist and the subfloor (SF/WIJ), the temperature rise in most cases was relatively slow and gradual due to the shielding of the thermocouples by the I-joists. When the temperatures for SF/WIJ North (3) and SF/WIJ South (5) show a temperature increase, which is sudden in some cases, it is an indication that gaps were forming between the top of the I-joists and the subfloor at these points and that the thermocouples were being exposed to the hot gases from the fire.

The increase in temperature happened at different times for different locations. The difference in time between the two SF/WIJ (North and South) thermocouples is partly due to the view factor relative to the burning fuel package. In some cases, the bulk of the fuel package was 'positioned' South of the thermocouple grouping. Consequently, the thermocouple at the top of the North I-joist experienced a greater heat insult from both the convective and radiative effects from the burning fuel. For the thermocouple groupings with the bulk of the fuel package located to the North, the reverse effect occurred.

Of particular mention is Section C-9 where the temperatures at SF/WIJ North (3) and SF/WIJ South (5) reached almost the same peak values as the temperatures at the exposed thermocouples in the first 110 s. This is an indication that gaps due to structural movement and charring of the wood at the interface of the I-joists and subfloor occurred much earlier at this location than other locations. It was located directly above the mock-up sofa and very close to the wood cribs.

For the exposed thermocouples, the first peak temperature (a value of 820 to 840ºC) was recorded at section C-9 (located very close or directly over the burning mock-up sofa and the wood cribs). In most cases, there was a drop in temperature measured by the exposed thermocouples just after about 100 to 120 s, due to fresh air coming through the open basement window; the temperatures dropped further after the exterior door on the first storey was opened at 180 s. After this short period of temperature decrease, the temperatures started increasing again.

There were cases where there was no obvious drop in the temperature at 100 to 120 s (C-1). This is because these locations were not in the proximity of the fuel package and thus had limited radiative impact from the fuel.

For Section D, points D-2 and D-12 have the same trend as the exposed thermocouples in sections A-2, A-7 and E-1.

Near the end of the tests, the temperatures at some locations show a slight increase probably because the flames penetrated the floor and allowed more fresh air to enter and slightly more burning to occur in the basement. The temperatures decayed after the extinguishment of the fire was initiated.

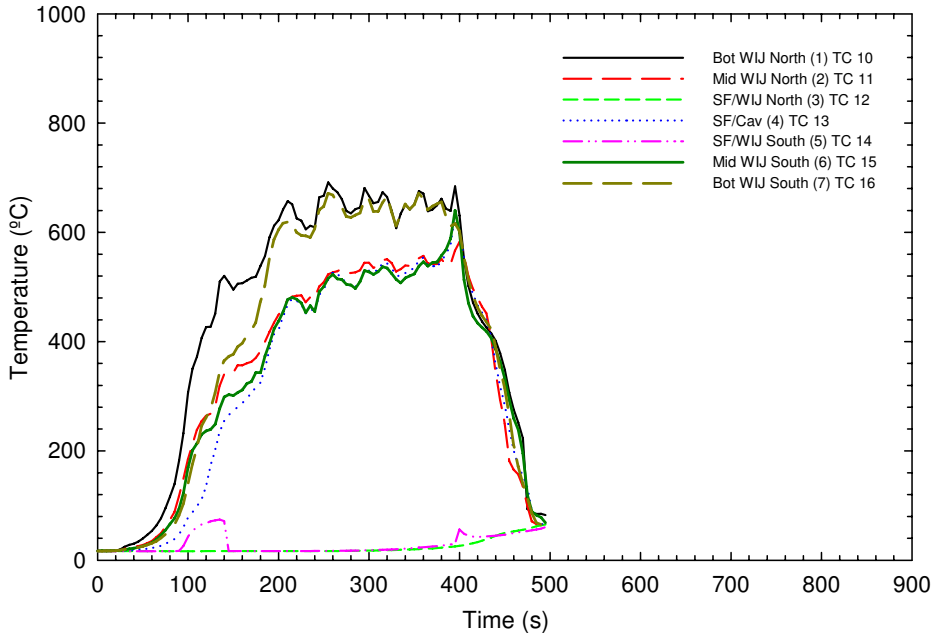


a) Thermocouples in cavity A-2

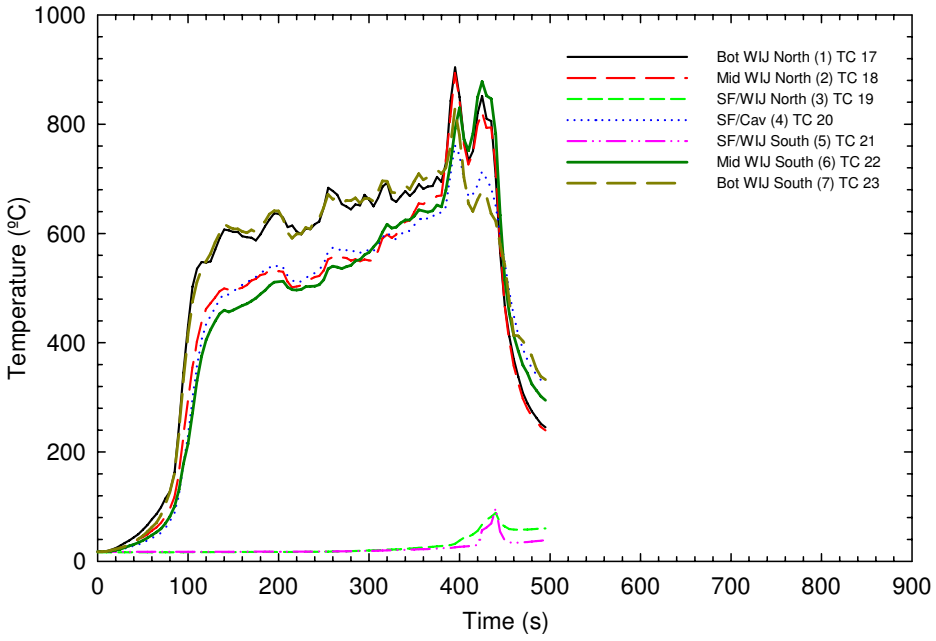


b) Thermocouples in cavity A-7

**Figure 28 (a and b). Temperatures at the exposed side – Test UF-06 in cavities A-2, A-7**

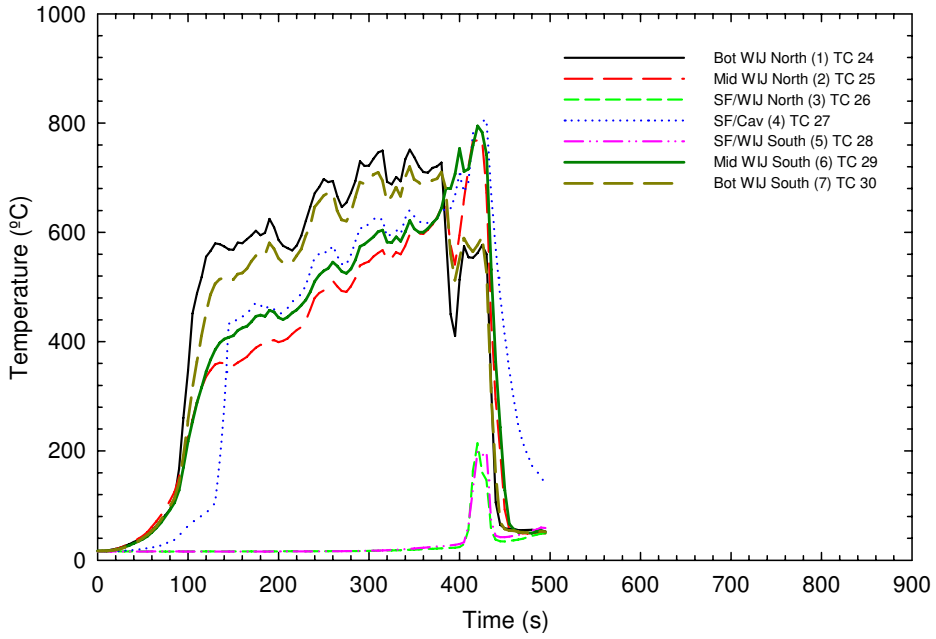


c) Thermocouples in cavity A-12

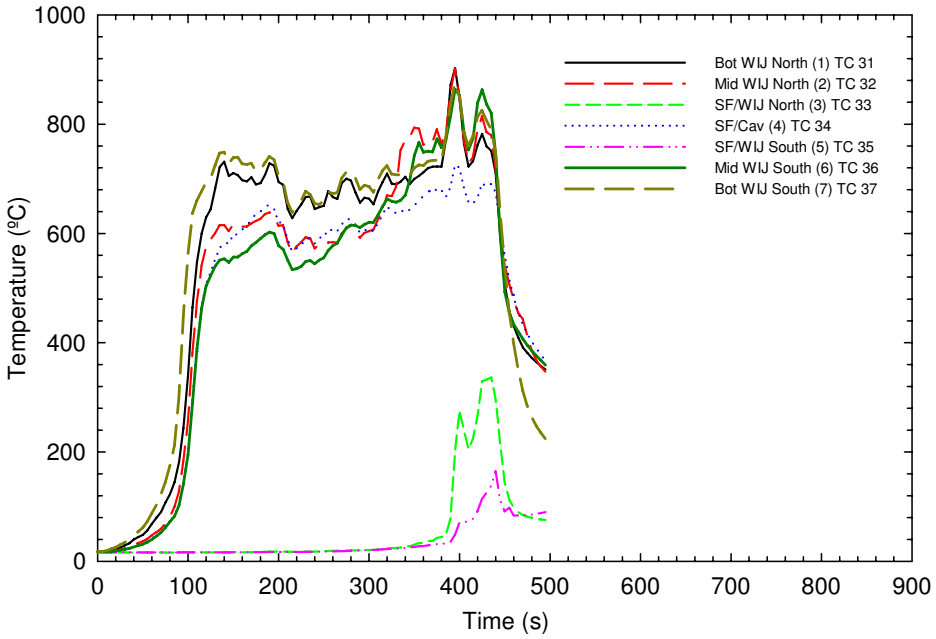


d) Thermocouples in cavity B-7

**Figure 28 (c and d). Temperatures at the exposed side – Test UF-06 in cavities A-12, B-7**

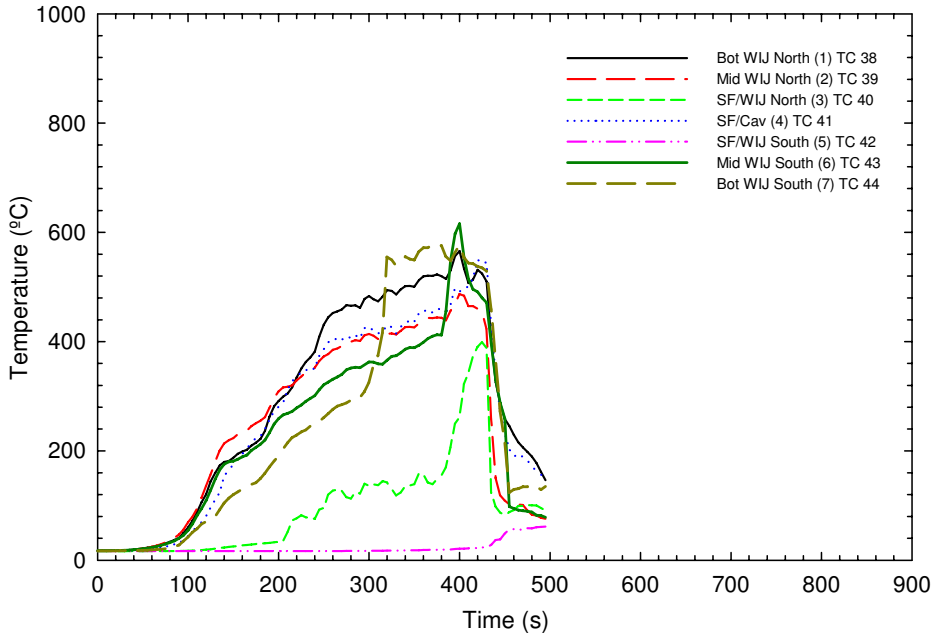


e) Thermocouples in cavity C-1

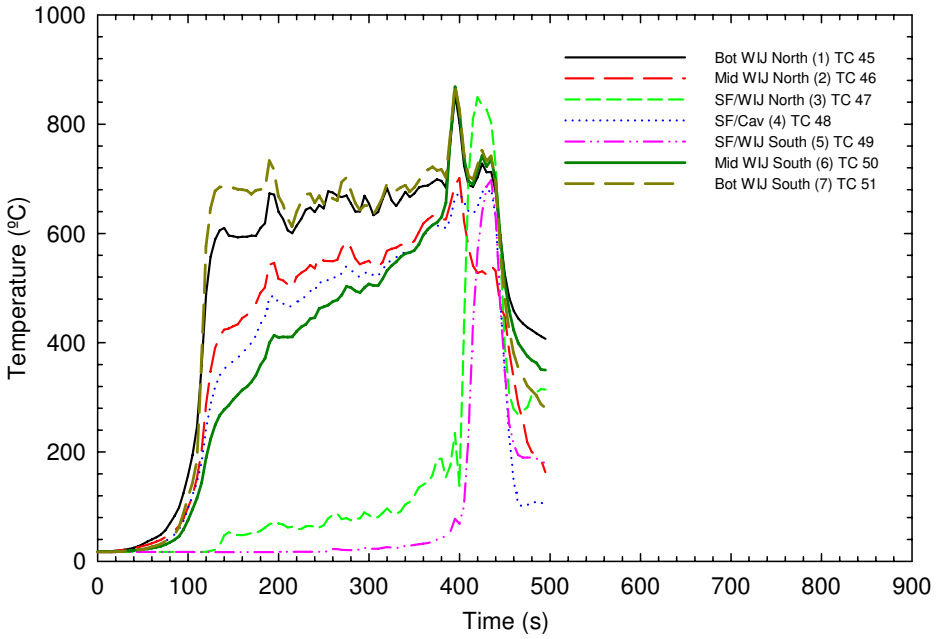


f) Thermocouples in cavity C-5

**Figure 28 (e and f). Temperatures at the exposed side – Test UF-06 in cavities C-1, C-5**

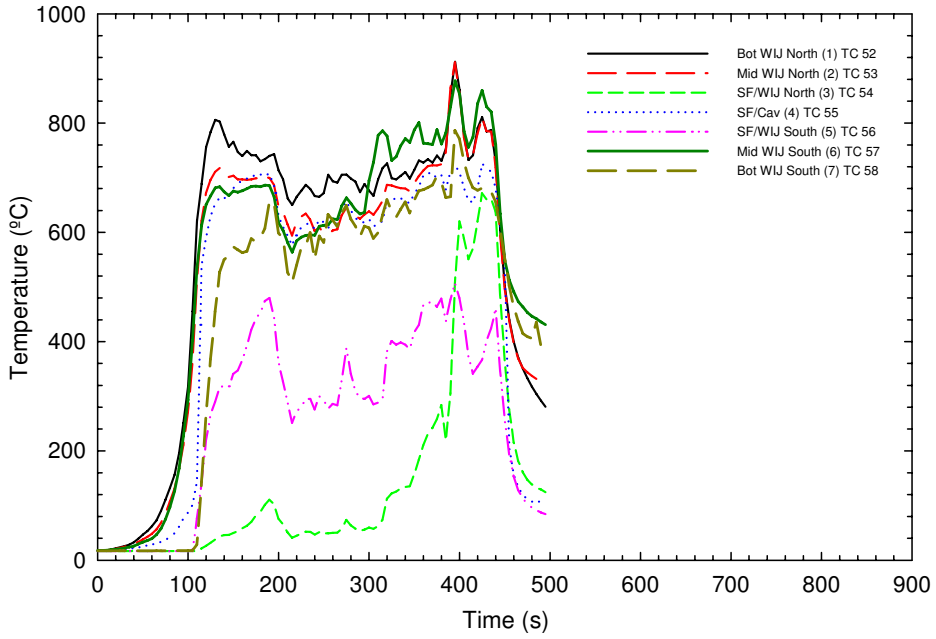


g) Thermocouples in cavity C-7

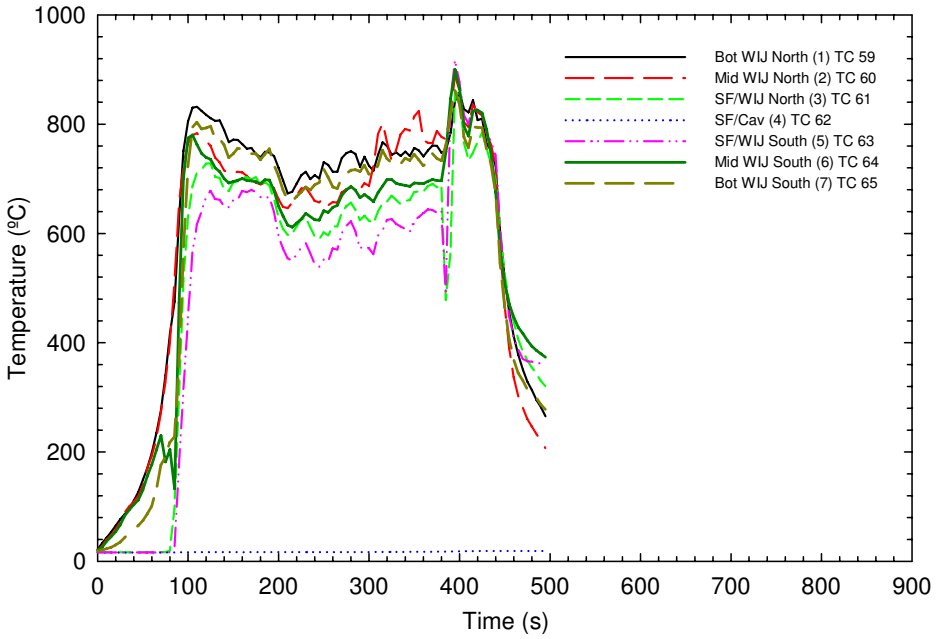


h) Thermocouples in cavity C-9

**Figure 28 (g and h). Temperatures at the exposed side – Test UF-06 in cavities C-7, C-9**

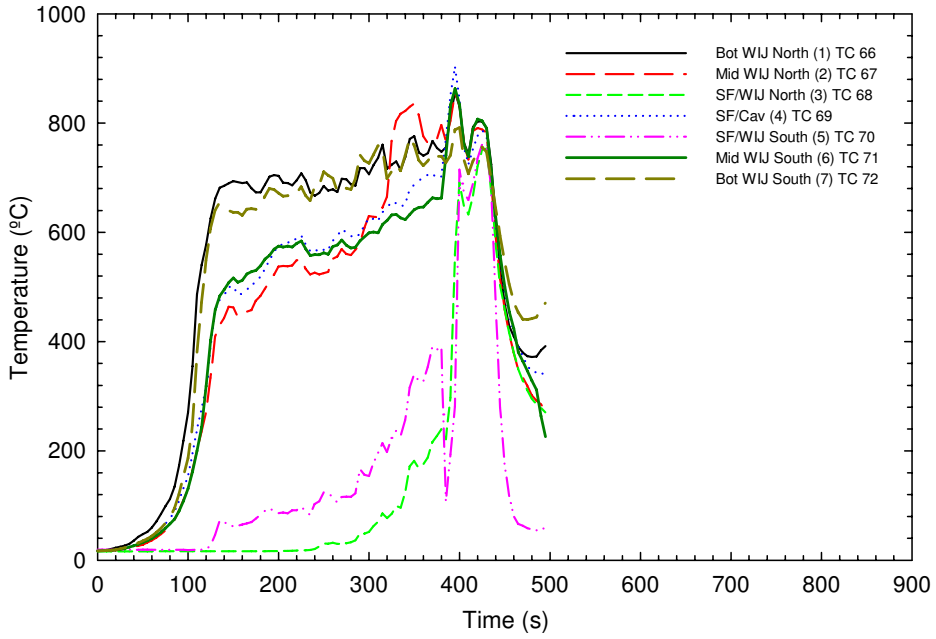


i) Thermocouples in cavity C-11

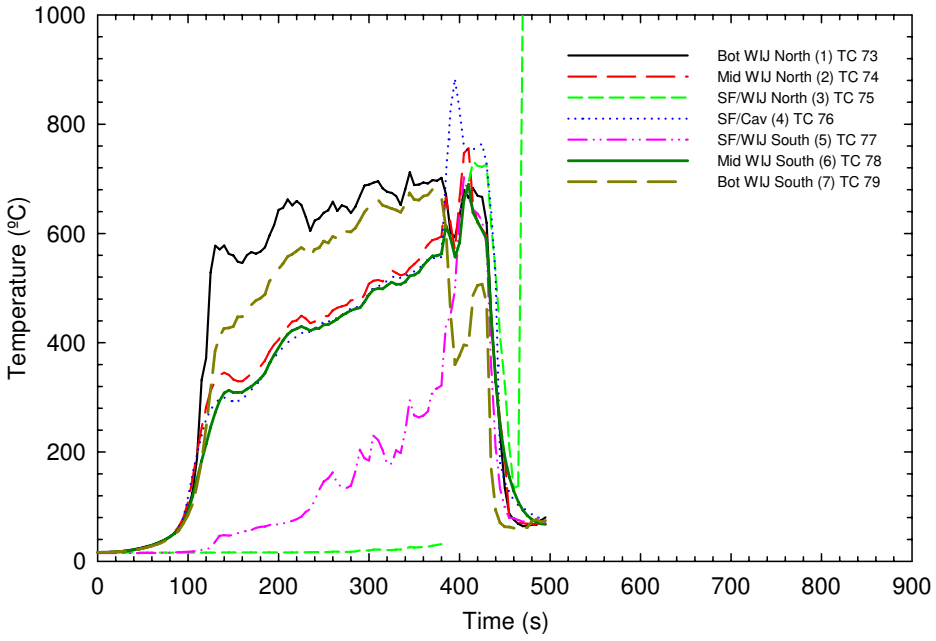


j) Thermocouples in cavity C-13

**Figure 28 (i and j). Temperatures at the exposed side – Test UF-06 in cavities C-11, C-13**

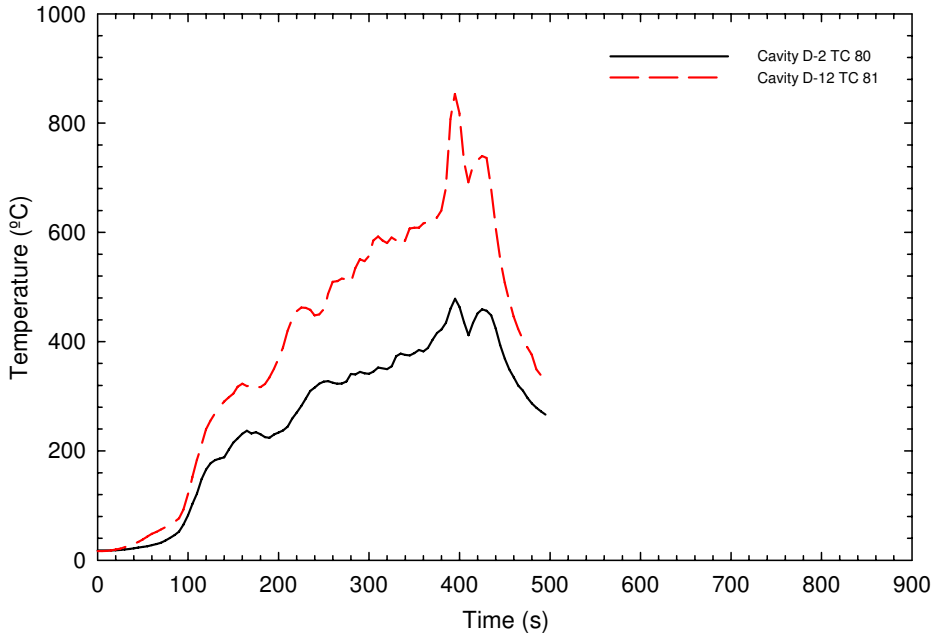


k) Thermocouples in cavity D-2 and D-12

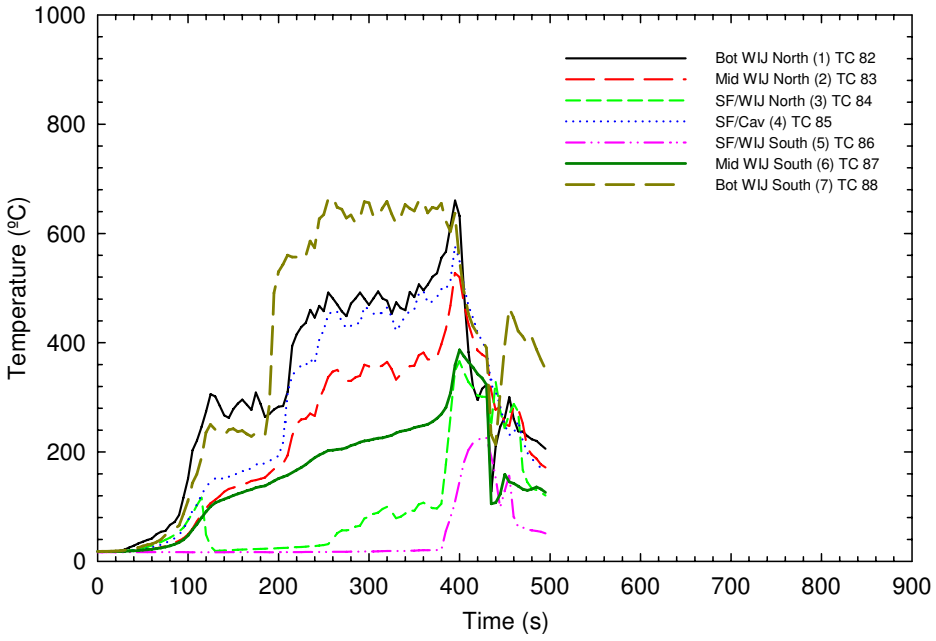


l) Thermocouples in cavity E-1.

**Figure 28 (k and l). Temperatures at the exposed side – Test UF-06 in cavities D-2, D-12, E-1**

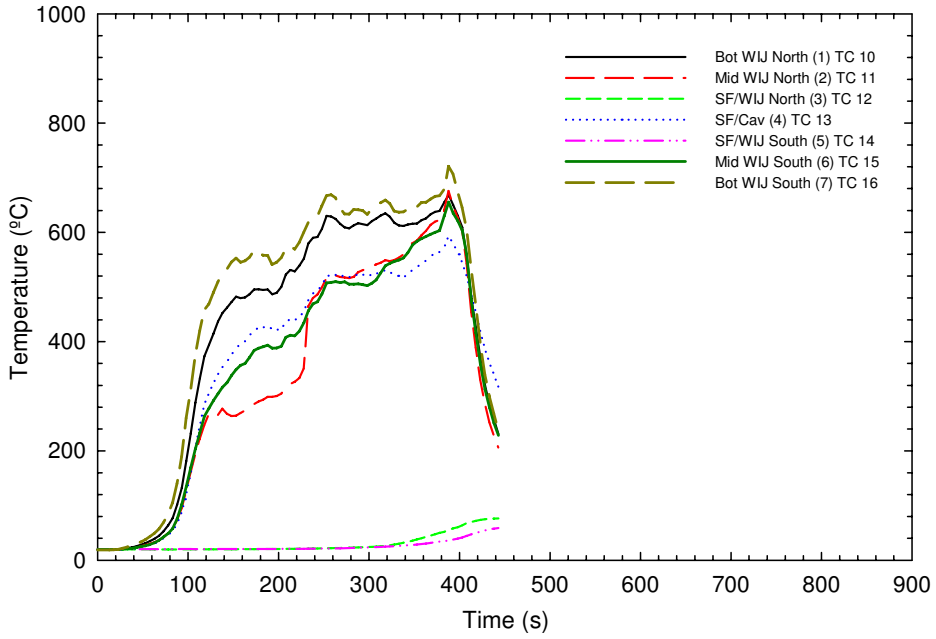


a) Thermocouples in cavity A-2

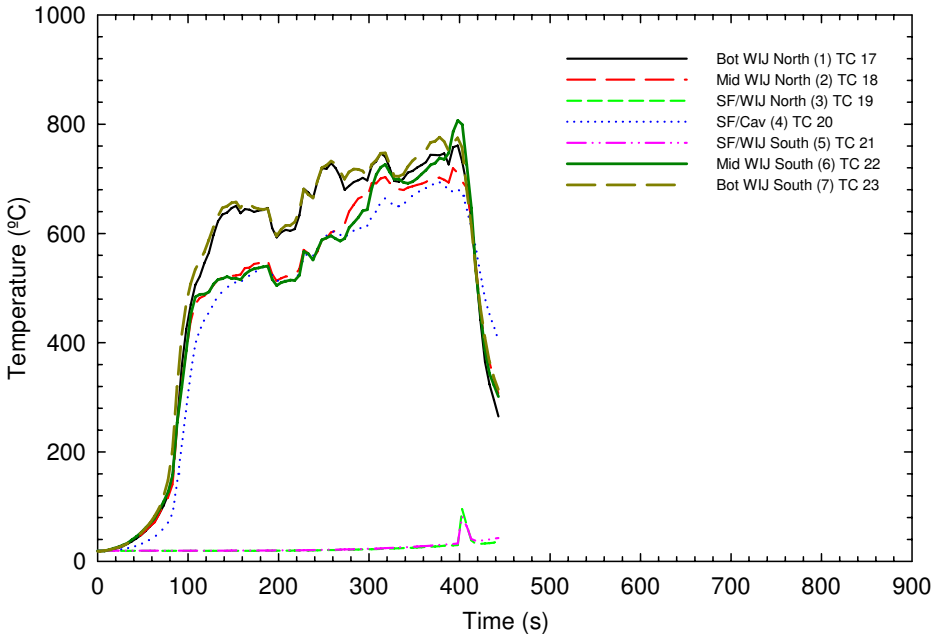


b) Thermocouples in cavity A-7

**Figure 28 (R-a and R-b). Temperatures at the exposed side – Test UF-06R in cavities A-2, A-7**

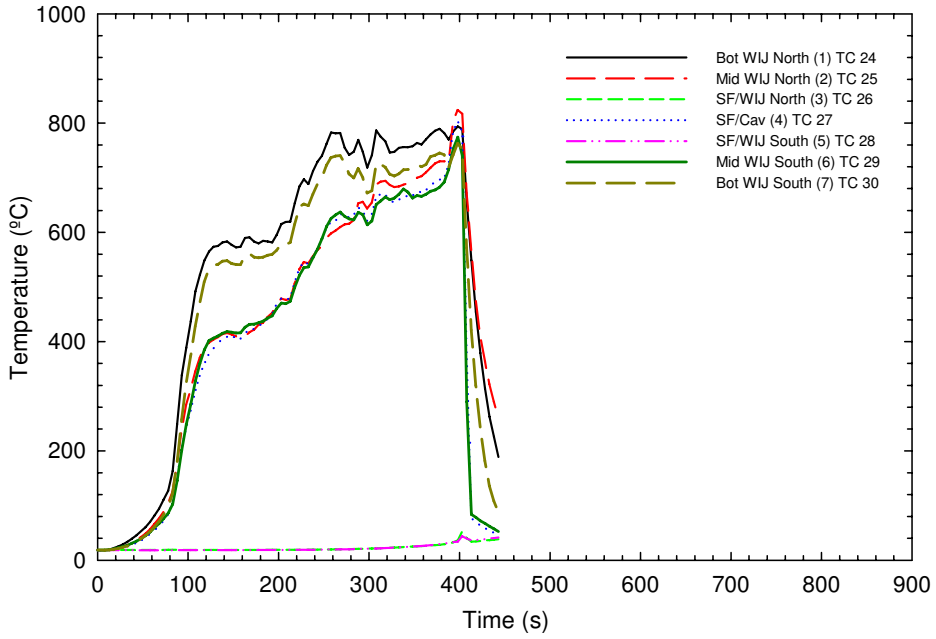


c) Thermocouples in cavity A-12

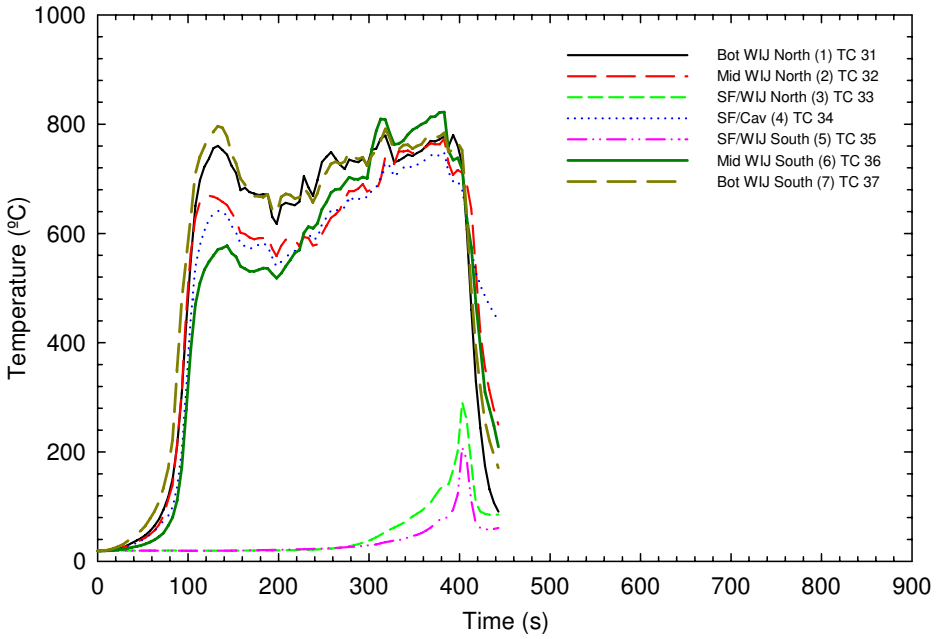


d) Thermocouples in cavity B-7

**Figure 28 (R-c and R-d). Temperatures at the exposed side – Test UF-06R in cavities A-12, B-7**

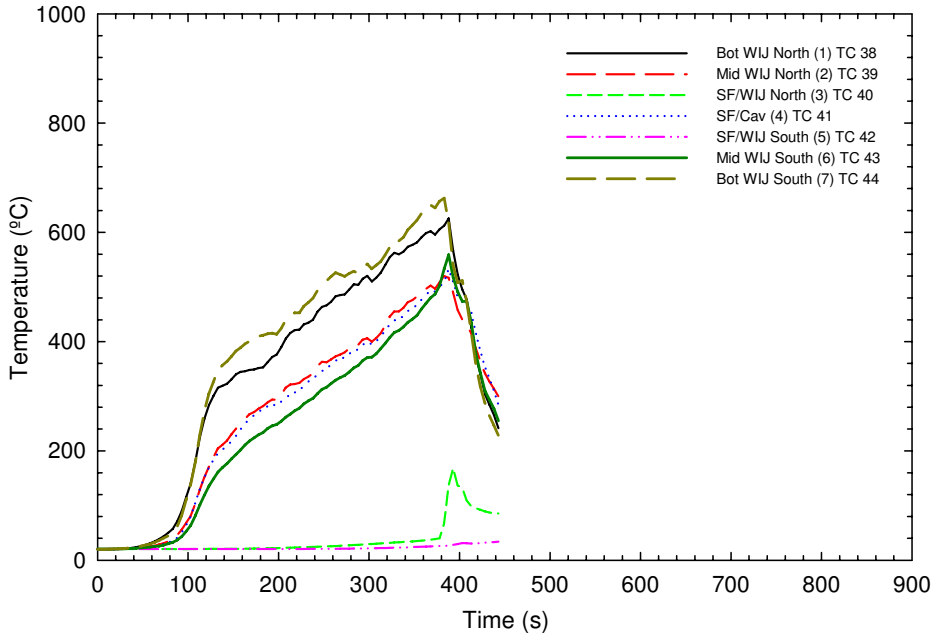


e) Thermocouples in cavity C-1

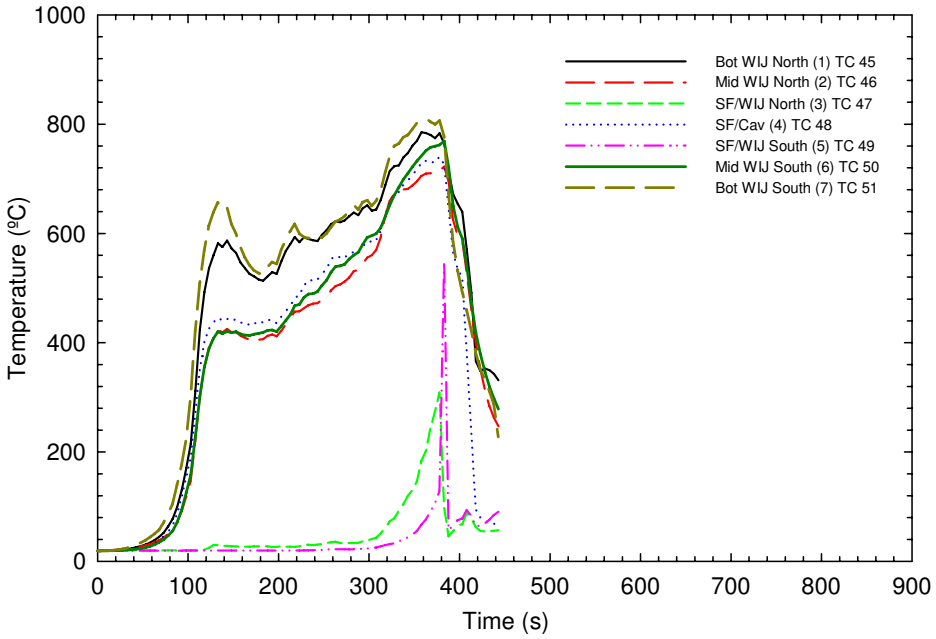


f) Thermocouples in cavity C-5

**Figure 28 (R-e and R-f). Temperatures at the exposed side – Test UF-06R in cavities C-1, C-5**

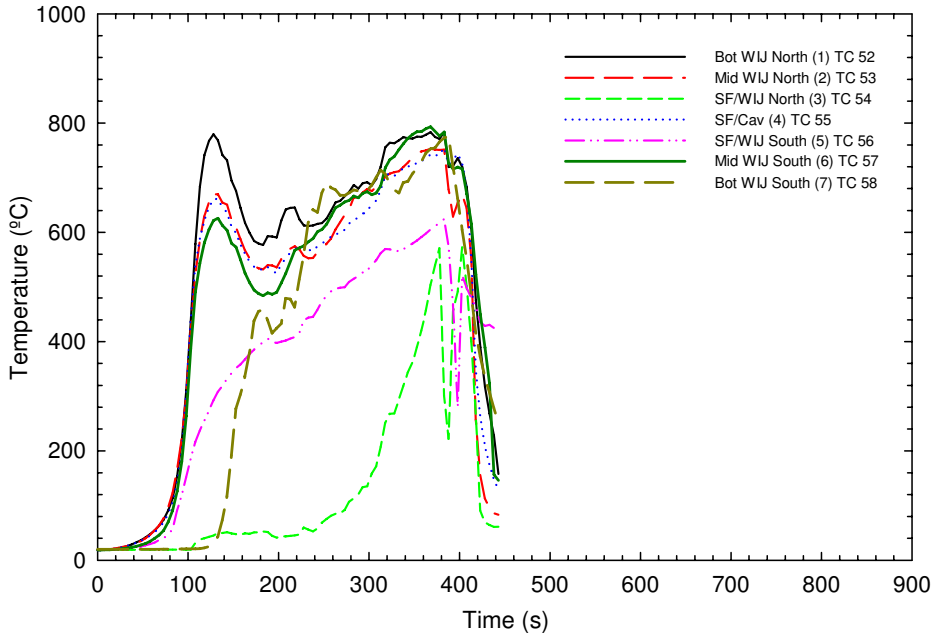


g) Thermocouples in cavity C-7

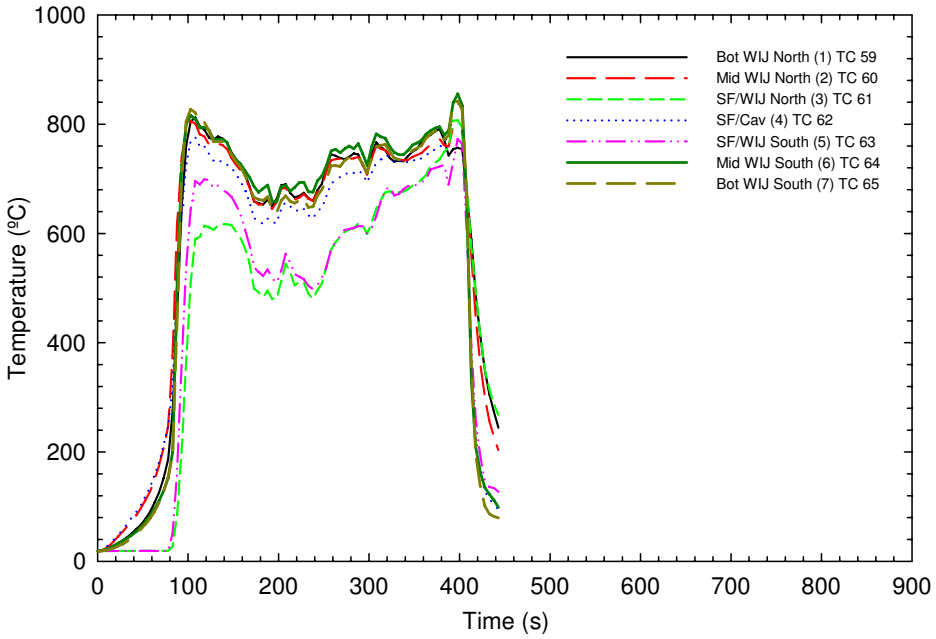


h) Thermocouples in cavity C-9

**Figure 28 (R-g and R-h). Temperatures at the exposed side – Test UF-06R in cavities C-7, C-9**

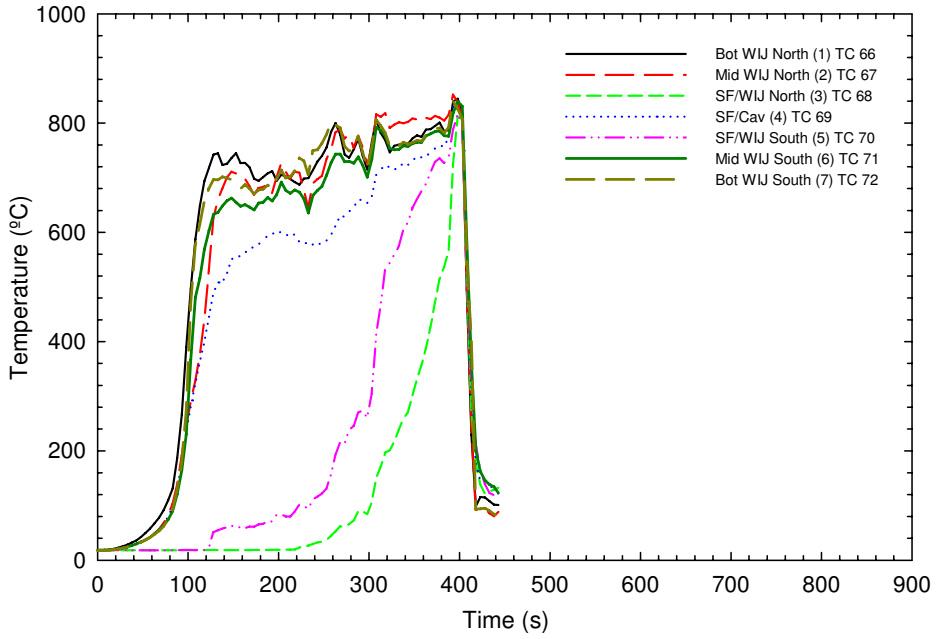


i) Thermocouples in cavity C-11

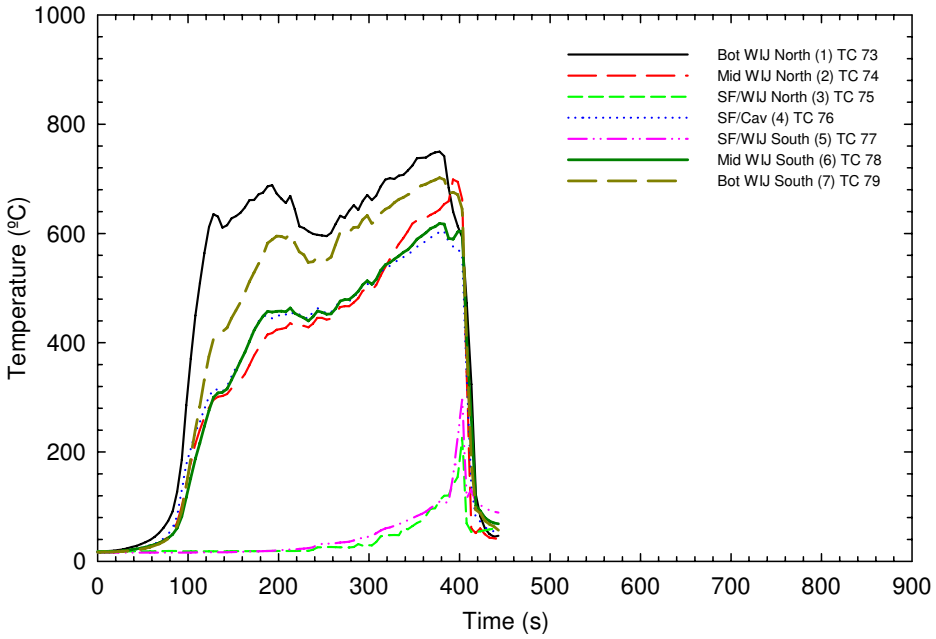


j) Thermocouples in cavity C-13

**Figure 28 (R-i and R-j). Temperatures at the exposed side – Test UF-06R in cavities C-11, C13**

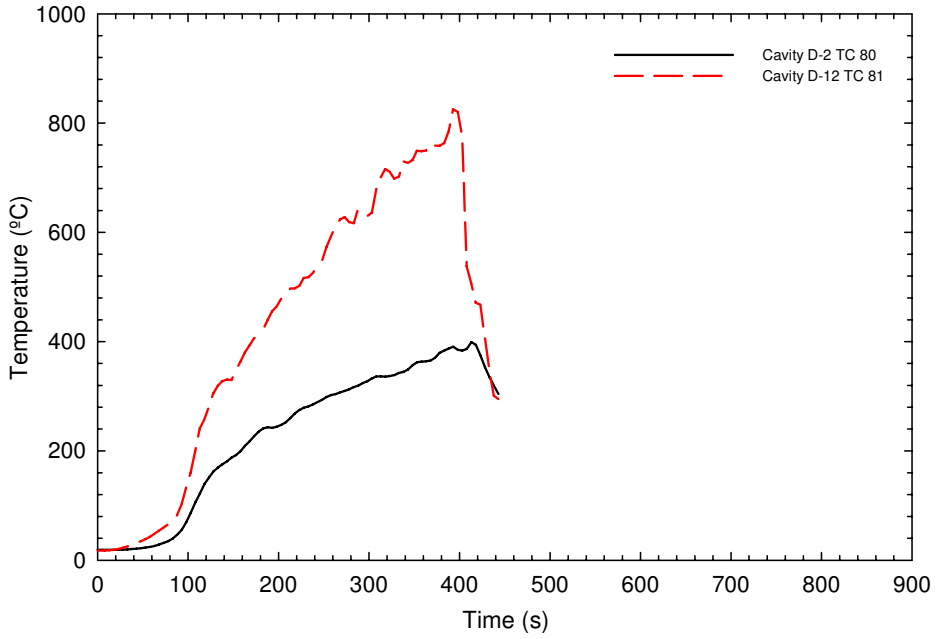


k) Thermocouples in cavity D-2 and D-12

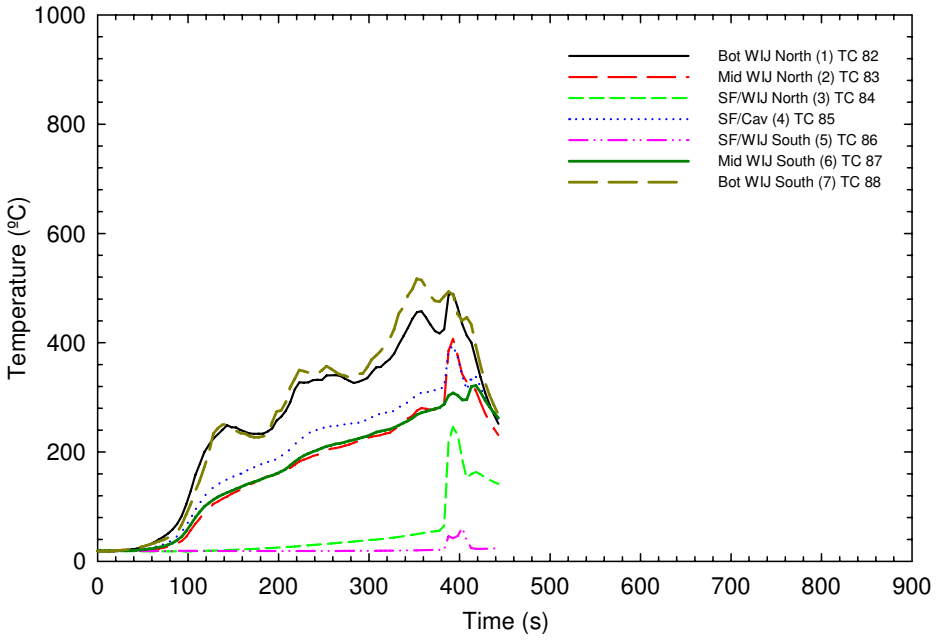


l) Thermocouples in cavity E-1

**Figure 28 (R-k and R-l). Temperatures at the exposed side – Test UF-06R in cavities D-2, D-12, E-1**

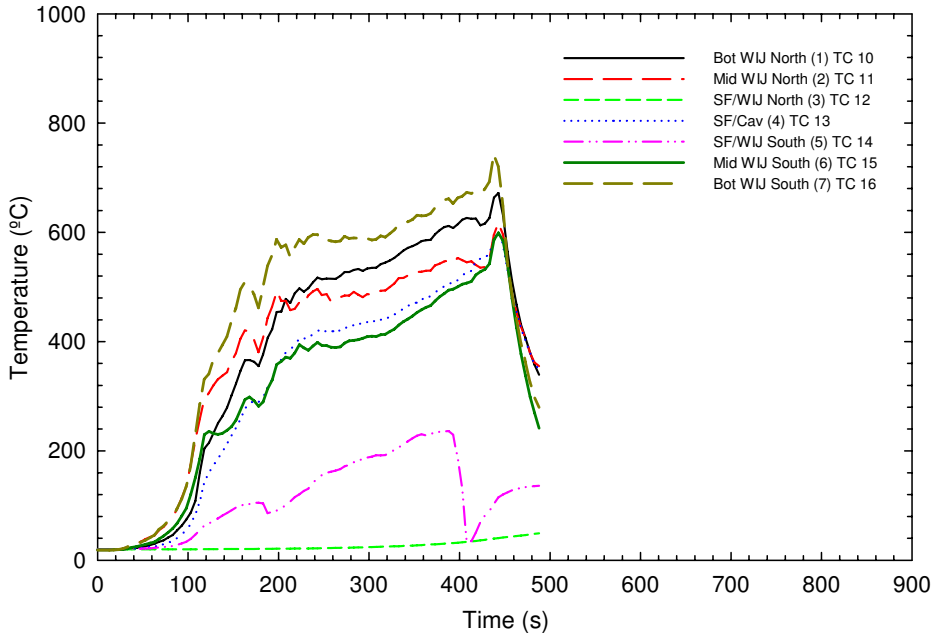


a) Thermocouples in cavity A-2

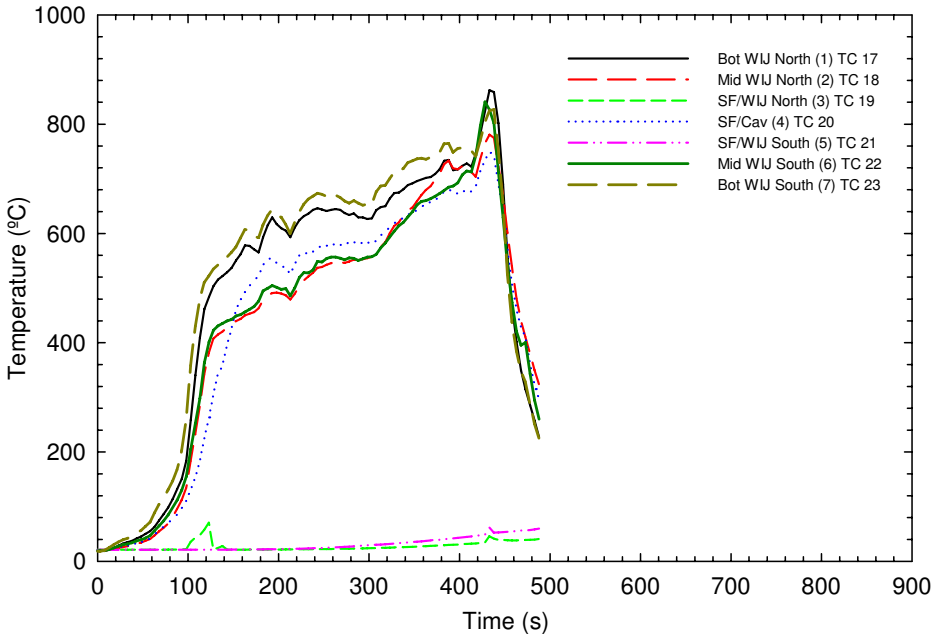


b) Thermocouples in cavity A-7

**Figure 28 (RR-a and RR-b). Temperatures at the exposed side – Test UF-06RR in cavities A-2, A-7**

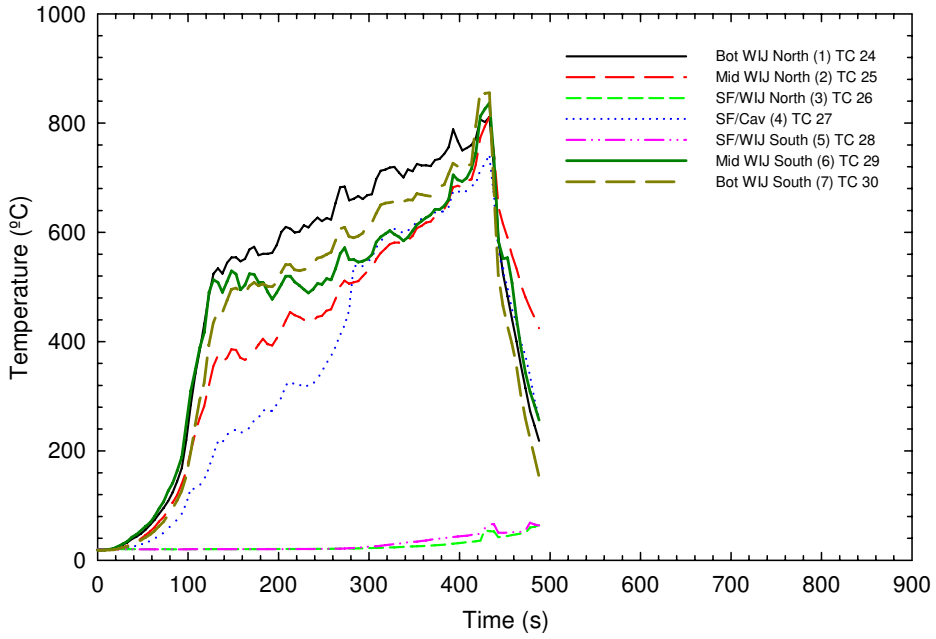


c) Thermocouples in cavity A-12

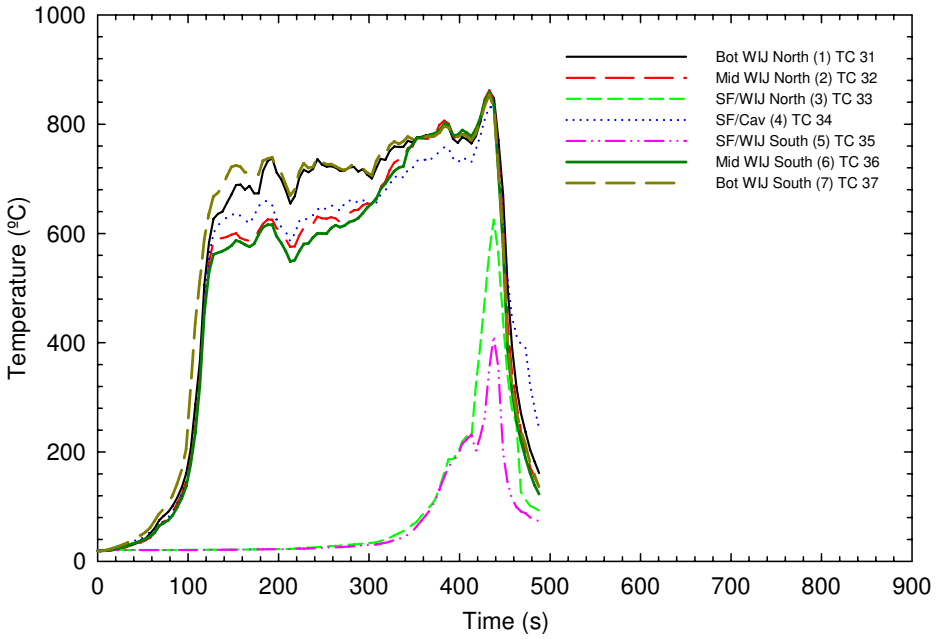


d) Thermocouples in cavity B-7.

**Figure 28 (RR-c and RR-d). Temperatures at the exposed side – Test UF-06RR in cavities A-12, B-7**

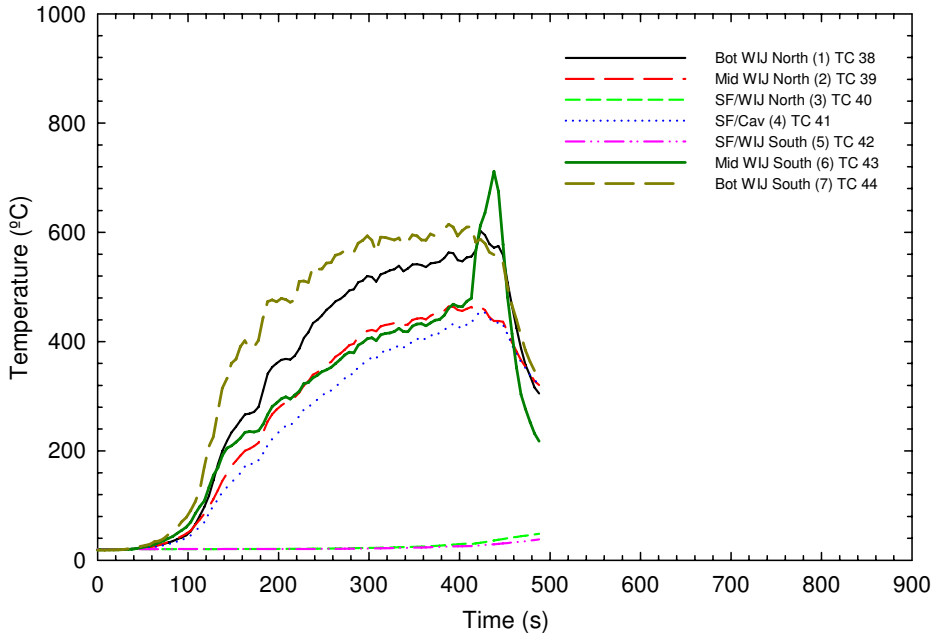


e) Thermocouples in cavity C-1

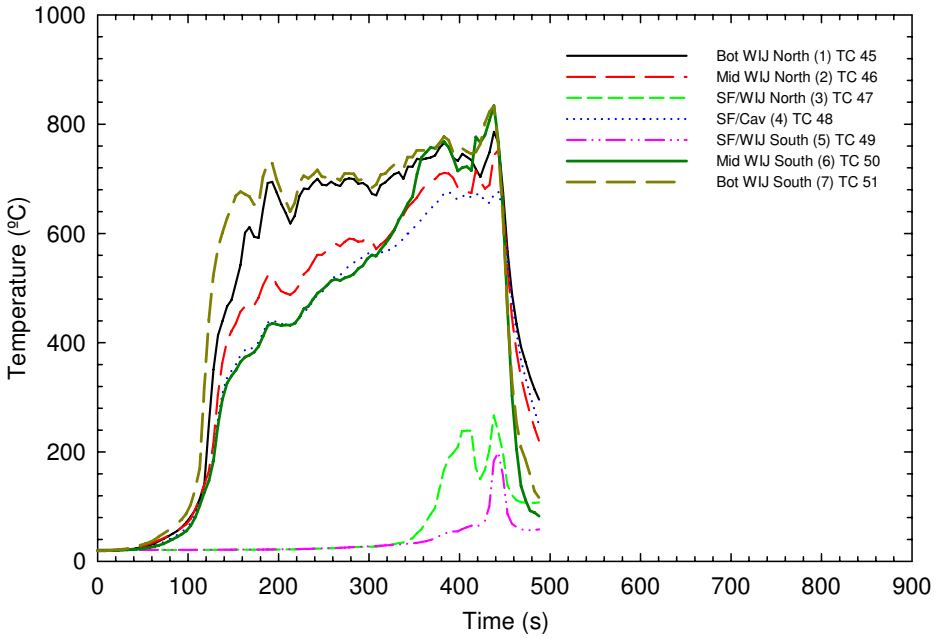


f) Thermocouples in cavity C-5

**Figure 28 (RR-e and RR-f). Temperatures at the exposed side – Test UF-06RR in cavities C-1, C-5**

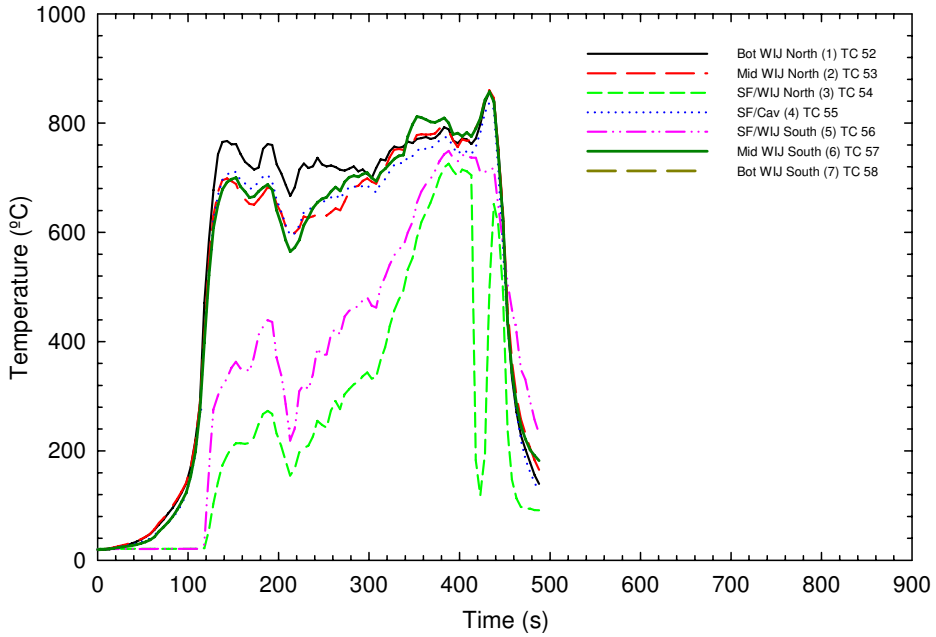


g) Thermocouples in cavity C-7

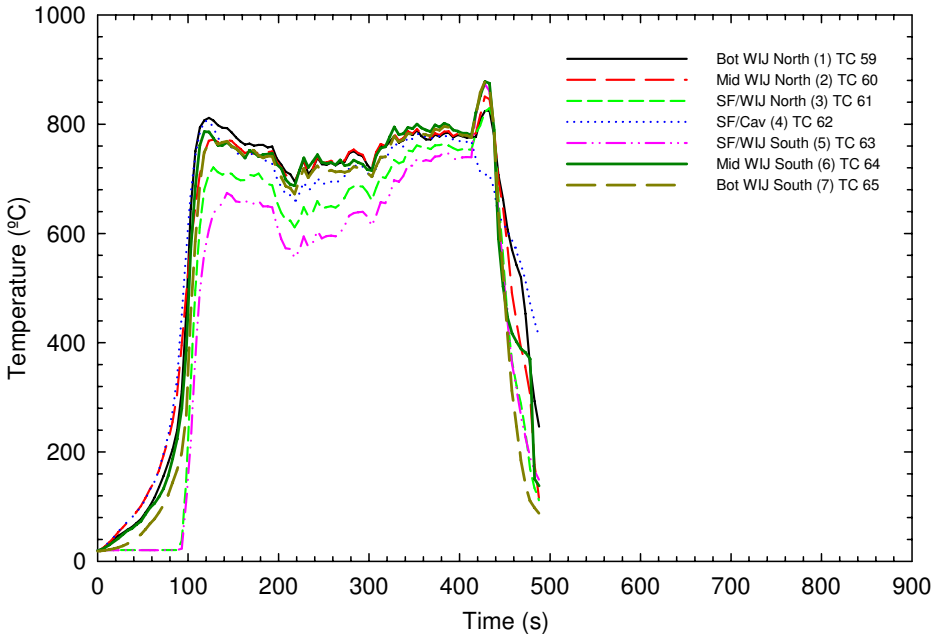


h) Thermocouples in cavity C-9

**Figure 28 (RR-g and RR-h). Temperatures at the exposed side – Test UF-06RR in cavities C-7, C-9**

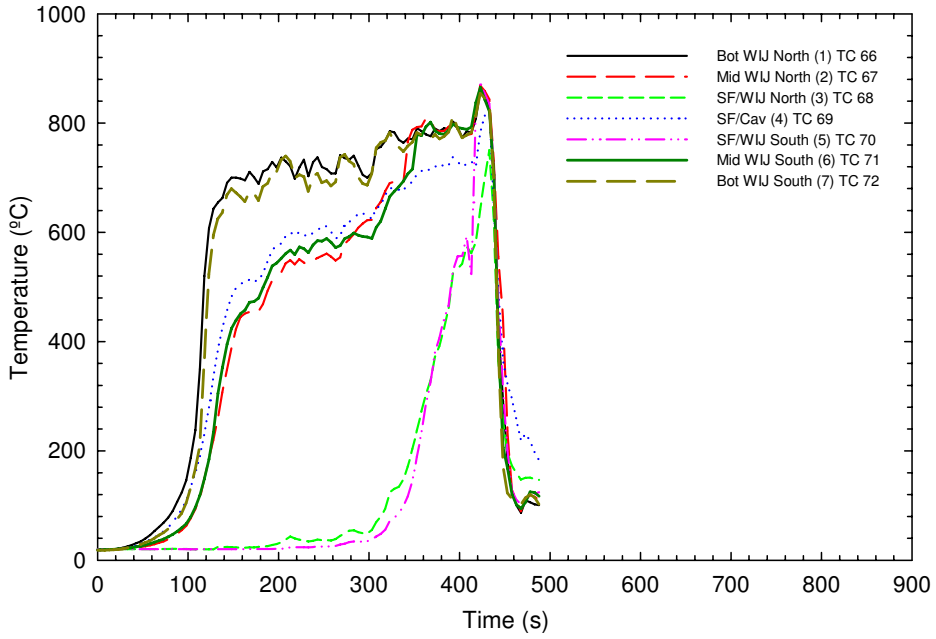


i) Thermocouples in cavity C-11

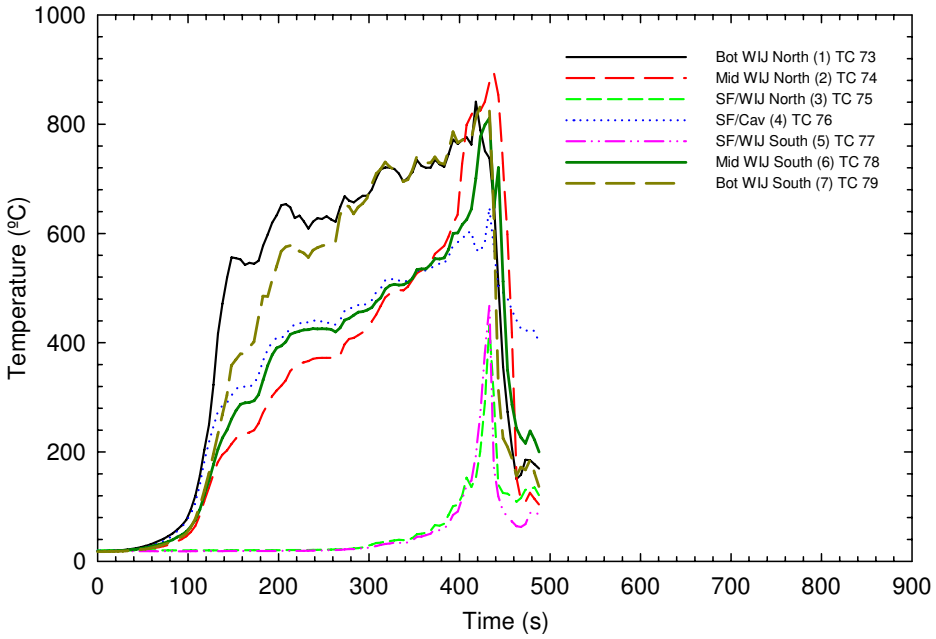


j) Thermocouples in cavity C-13

**Figure 28 (RR-i and RR-j). Temperatures at the exposed side – Test UF-06RR in cavities C-11, C-13**

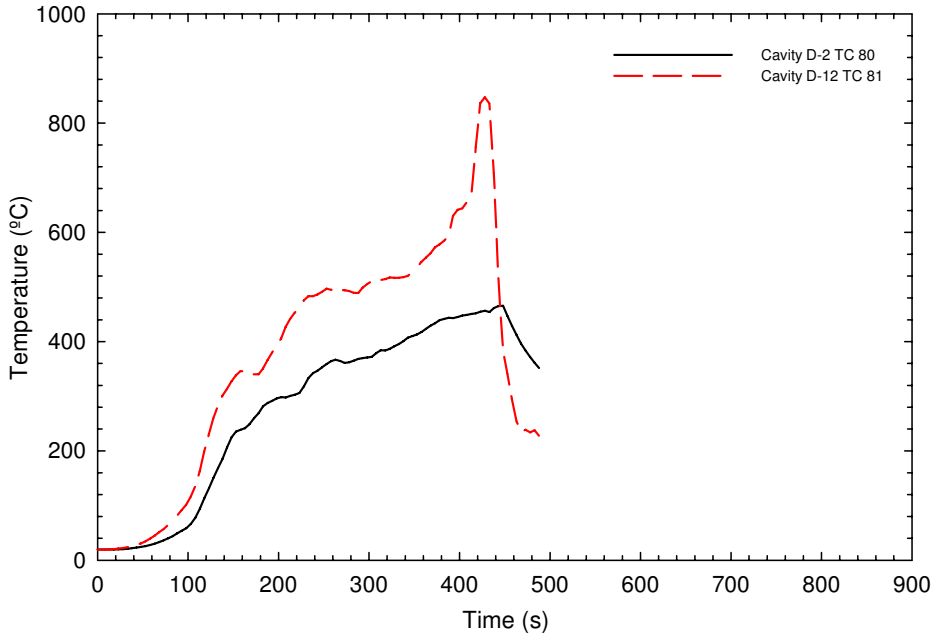


k) Thermocouples in cavity D-2 and D-12

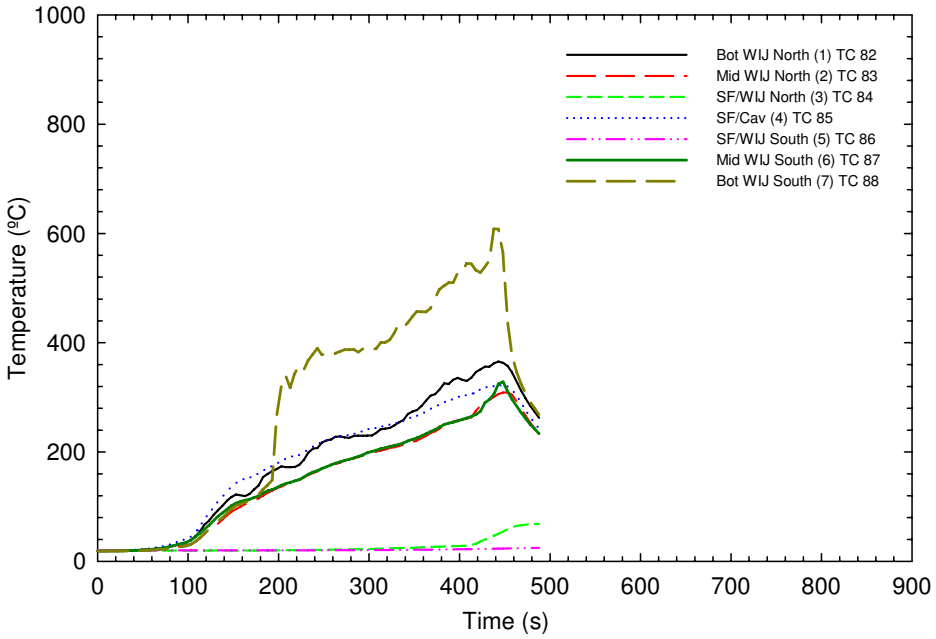


l) Thermocouples in cavity E-1

**Figure 28 (RR-k and RR-l). Temperatures at the exposed side – Test UF-06RR in cavities D-2, D-12, E-1**

## 3.4 Deflection Measurements Results and Structural Performance

Figure 29 shows the 9 deflection measurement points (as well as explained previously; see also Figure 11 for the closest I-joist to the deflection points). The points of measurement were chosen as they were located in the middle of the fire compartment just above the fire load where the impact of the fire on the structural integrity of the floor assembly was anticipated to be the greatest. Some measurement points were aligned with one of the joists, while the other row was positioned between joists.

### 3.4.1 For Tests UF-06, UF-06R and UF-06RR

Figure 30 (a, b, c) shows the deflections measured for Tests UF-06, UF-06R and UF-06RR, respectively. For Test UF-06, up to 200-260 s, the deflections were very small. After this time, the deflections increased from a moderate to a fast rate reaching deflections of over 100 mm at 380 s. After this time, the deflections show a very fast increase indicating that the concrete blocks were falling as the floor started to collapse. The time of floor collapse was 382 s.

For Test UF-06R, up to 200 s, the deflections were very small. After this time, the deflections increased from a moderate to a fast rate reaching deflections of over 160 mm at 380 s. After this time, the deflections show a very fast increase indicating that the concrete blocks were falling as the floor started to collapse. The time of floor collapse was 380 s.

For Test UF-06RR, up to 220-260 s, the deflections were very small. After this time, the deflections increased from a moderate to a fast rate reaching deflections of over 100 mm around 400 s. After this time, the deflections show a very fast increase indicating that the concrete blocks were falling as the floor started to collapse. The time of floor collapse was 414 s.

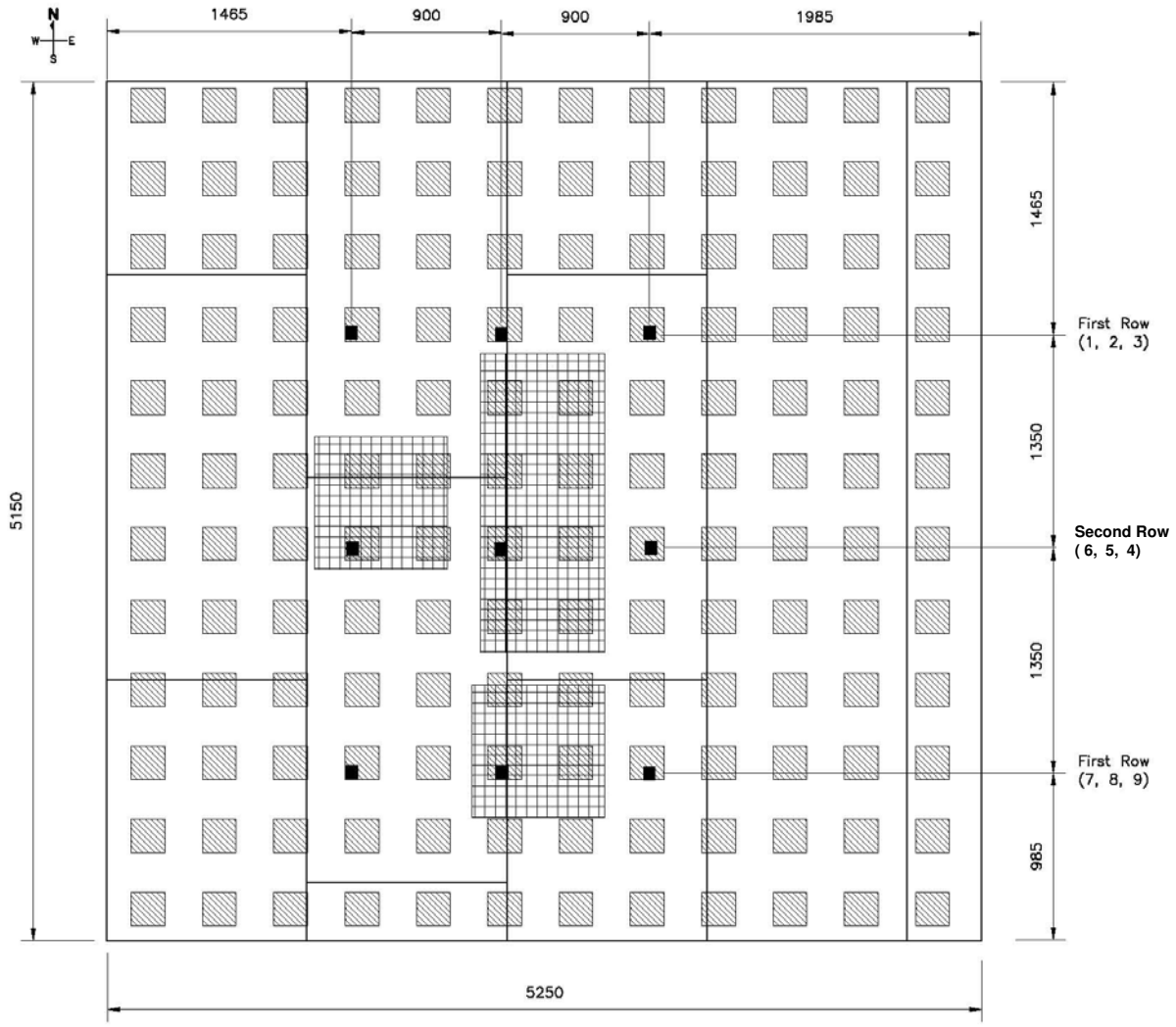


**Figure 29. Deflection points measured (all dimensions in mm)**

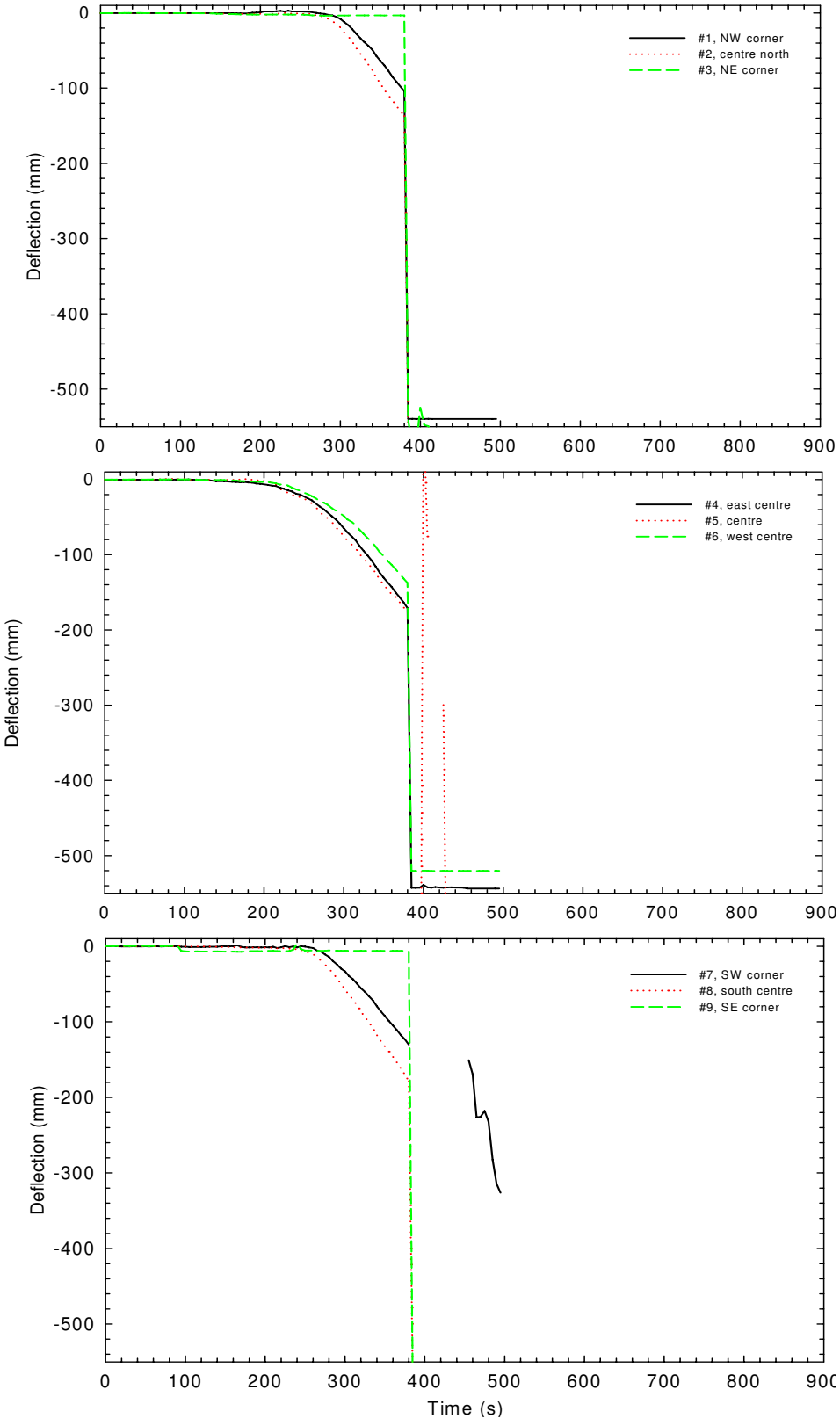


**Figure 30 (a). Deflection measurements for rows 1, 2 and 3 – Test UF-06**

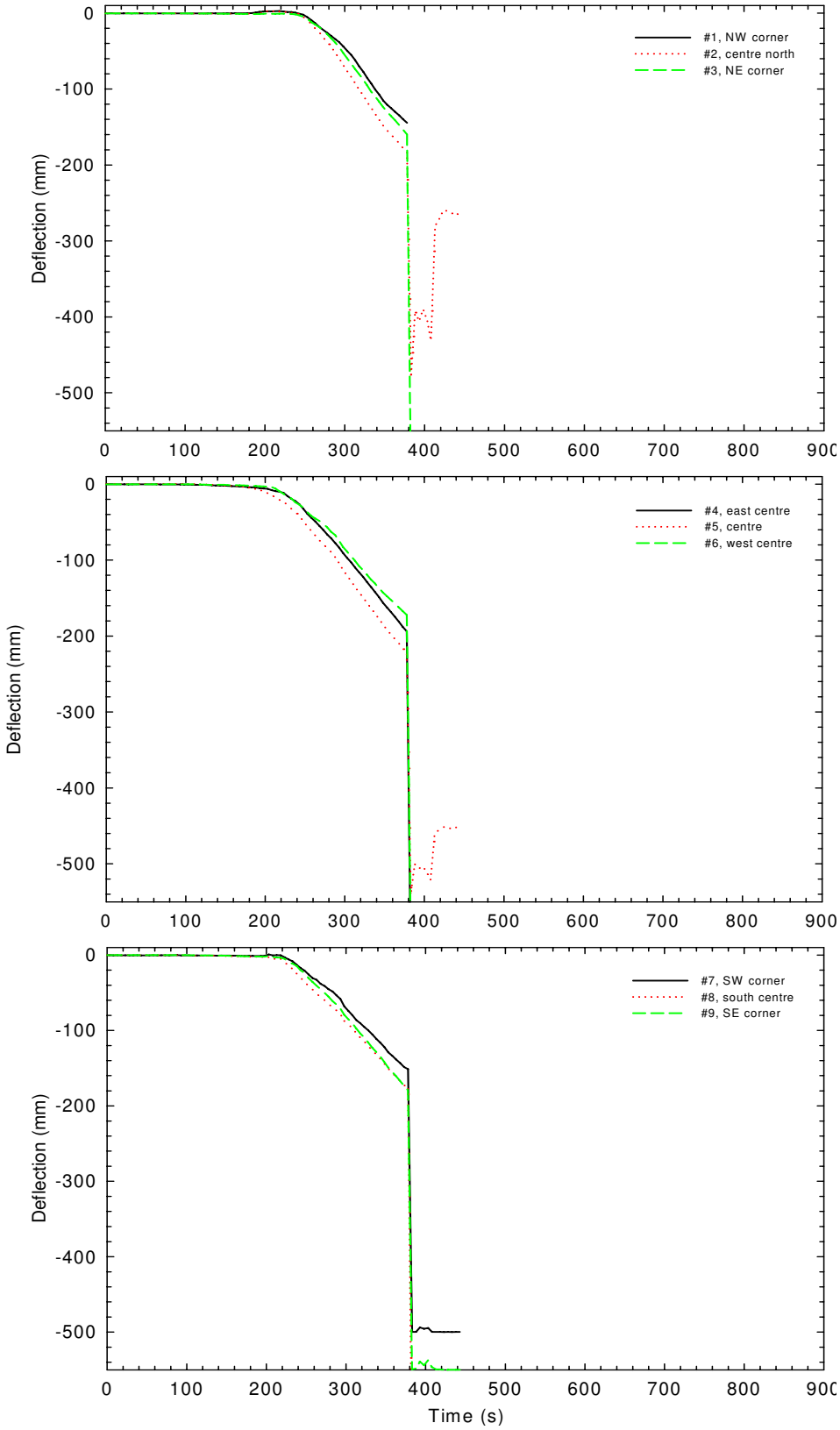


**Figure 30 (b). Deflection measurements for rows 1, 2 and 3 – Test UF-06R**

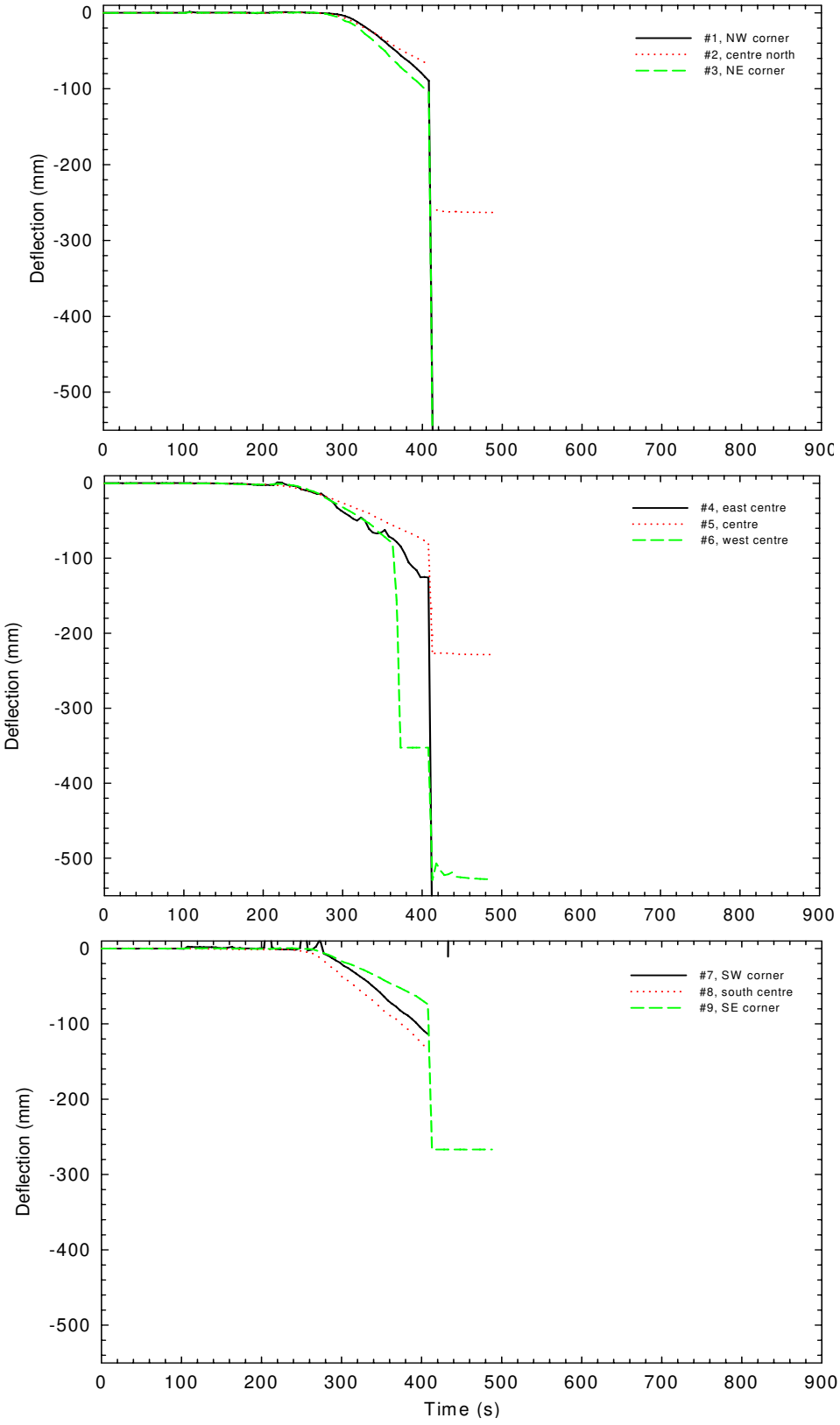


**Figure 30 (c). Deflection measurements for rows 1, 2 and 3 – Test UF-06RR**

## 3.5 Flame Penetration Results

Flame penetration through the floor assembly is one of the important aspects of fire performance that is of interest in this project since this is also a failure criterion in standard fire resistance testing. Flames and combustion products penetrating through the floor can impact on the time available for evacuation. Any opening(s) created by the flames penetrating the subfloor or excessive deflection would also provide a means for hot fire gases to migrate from the basement fire room to the upper storey(s). As well, the holes would add to the overall weakening of the subfloor. To determine whether there was flame penetration through the floors, both a flame-sensing device and the time-temperature curves on the unexposed side of the floors were used.

### 3.5.1 For Tests UF-06, UF-06R and UF-06RR

Figure 31 shows the results of the flame-sensing devices. Three wire meshes were installed on the top of three joints (East, Centre and West) on the unexposed side of the floor as shown in Figure 17 (instrumentation figure). There was a sudden increase in the voltage output of the flame-sensing device when flames penetrated through the floor and struck the wire meshes. As indicated by Figure 31, heavy flame penetration occurred at the joints at the times that are very close to the time of floor collapse (382 s for Test UF-06, 380 s for Test UF-06R, and 414 s for Test UF-06RR).

These times are also similar to the times that indicate potential flame penetrations in Figure 21 and Figure 27.

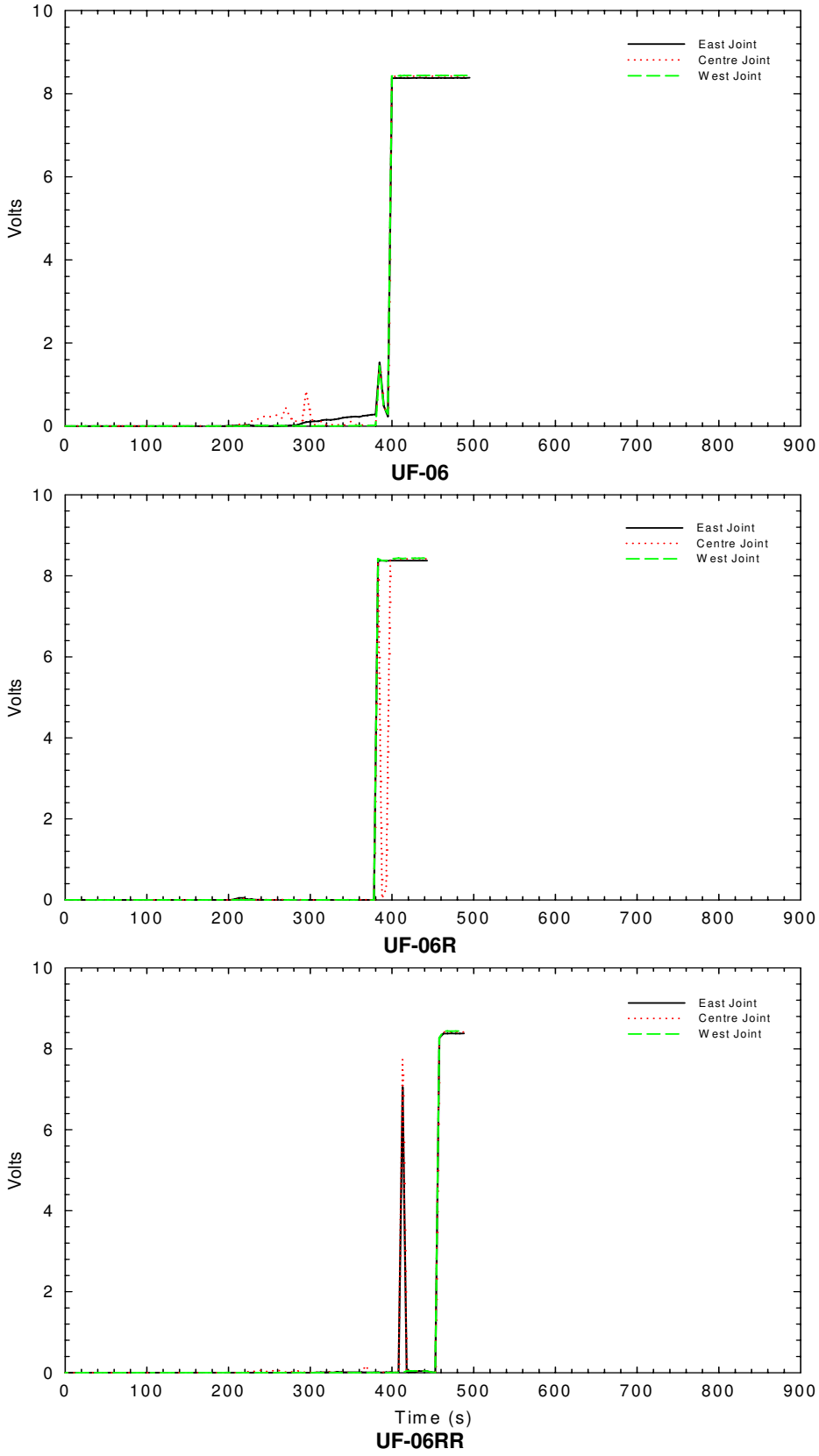


**Figure 31. Results of flame sensors at different joints**

### 3.6 Detection Times

Residential photoelectric and ionization smoke alarms were installed on the ceiling in each bedroom, second storey corridor, first storey and the basement fire compartment. These smoke alarms were powered by batteries and were not interconnected. The ionization smoke alarm was not installed in the basement fire room in order to avoid dealing with radioactive materials in the cleanup of debris after the fire tests. Since photoelectric smoke alarms are generally slower in detecting flaming fires than ionization smoke alarms, using the photoelectric smoke alarms in the basement resulted in more conservative estimates for activation times for the fire scenarios used in the experiments. New smoke alarms were used in each experiment.

Table 2 shows the activation times of the smoke alarms installed in the test facility. The photoelectric smoke alarms in the basement fire compartment took 38-45 s to activate. It took up to 95 s longer for the smoke alarms in the second storey corridor to activate and up to 210 s longer for the smoke alarms in the closed bedroom to activate. This highlights the importance of having the smoke alarms interconnected to activate simultaneously when one of them detects a fire. The results also show that the activation times are quite repeatable in most of the locations.

**Table 2. Smoke Alarm Activation Times after Ignition (in seconds)**

| Location | Basement fire room | First storey | | Second storey corridor | | SE bedroom (door closed) | | SW bedroom (door open) | |
|---|---|---|---|---|---|---|---|---|---|
| Alarm Type | P | I | P | I | P | I | P | I | P |
| UF-06 | 45 | 75 | 85 | 115 | 125 | 230 | 255 | 130 | 200 |
| UF-06R | 38 | 58 | 78 | 113 | 123 | 198 | 223 | 138 | 163 |
| UF-06RR | 43 | 73 | 78 | 128 | 138 | 223 | 248 | 143 | 153 |

Notes:
1. See section on instrumentation in compartment (Figure 8 to Figure 10)
2. I: ionization, P: photoelectric, SE: South East, SW: South West

### 3.7 Results of Smoke and Gas Measurements and Tenability Analysis

Fires produce heat, narcotic and irritant gases, and smoke that obscures vision. The temperature and the production of combustion products depend upon the fire characteristics, enclosure geometry and ventilation. The increased temperature and combustion products can, either individually or collectively, create conditions that are potentially untenable for occupants.

Tenability analysis involves examination of the production of heat and toxic products of combustion during the fire tests. It also involves estimation of the potential exposure of occupants, who would have been in the test house, to heat and toxic smoke and of the potential effects as a result of the exposure. The purpose of tenability analysis is to

provide an estimation of the time available for escape — the calculated time interval between the time of ignition and the time after which conditions become untenable for an individual occupant.

There are various endpoints for tenability analysis, such as incapacitation, lethality/fatality, etc. For this project, *incapacitation* – a state when people lose the physical ability to take effective action to escape from a fire – was chosen as the endpoint for the tenability analysis related to heat and toxic products of combustion. The time available for escape thus calculated is the interval between the time of ignition and the time after which conditions become incapacitating for an individual occupant.

ISO/TS 13571 and the SFPE Handbook of Fire Protection Engineering provide guidance and methodologies for evaluating the time available for occupants to escape from a fire [15, 16]. These methodologies are used in this report to calculate the time available for escape as an input to the hazard analysis for each fire scenario used in the project. The methodologies include a fractional effective dose (FED) approach to quantify the time at which the accumulated exposure to each fire effluent exceeds a specified threshold criterion for incapacitation. This time then is taken to represent the time available for escape relative to the specified threshold.

The calculated time available for escape depends not only on the time-dependent temperatures, concentrations of combustion gas products and density of smoke in the test house, but also on the characteristics of occupants. The age and health of the occupants (such as body weight and height, lung and respiratory system function, blood volume and hemoglobin concentration, skin, vision, etc.) as well as the degree of activity at the time of exposure have an effect on the consequences of exposure to fire effluents and heat. Since the general population has a wide range of susceptibility to fire effluents and heat, the exposure thresholds for incapacitation can change from subpopulation to subpopulation. Thus, each occupant is likely to have a different time available for escape.

This section of the report does not try to debate what FED criterion should be used as the incapacitation threshold but rather to present the results of the analysis for 2 typical FED values (e.g. FED = 1 and FED = 0.3). The methodology can be used to estimate the time available for escape associated with other FED values, if required.

The time available for escape calculated based on FED =1 represents the time available for a healthy adult of average susceptibility. The distribution of human responses to the fire effluents is unknown but is assumed to be a logarithmic normal distribution [15]. Under this distribution, the time available for escape calculated at FED =1 also represents statistically the time by which 50% of the general population would have been incapacitated but the conditions would still be tenable for the other 50% of the population.

For a more susceptible person, the threshold can be lower and the time available for escape would be shorter than for an average healthy adult. If FED = 0.3 is used as a criterion to determine the time available for escape, it would statistically represent the time by which 11% of the population would have been incapacitated but the conditions would still be tenable for the other 89% of the population [15].

The location of the occupant who would have been in the test house has an effect on the time available for escape. The analysis focused on the fire conditions affecting tenability, as measured on the first and second storeys of the test facility, and the impact on any occupant assumed to be present on the upper storeys of the test house at the time of ignition. In real fire situations, the occupant would move through different locations during egress. Therefore, the time to incapacitation would be in-between the times calculated for different locations. The conditions in the basement fire room would not be survivable once flashover occurred.

The methodology used does not address quantitatively any interaction (combined effects) between heat, combustion gas products and smoke obscuration. Each component is treated as acting independently on the occupants to create incapacitating conditions and the time available for escape is the shortest of the times estimated from consideration of exposure to combustion gas products, heat and visual obscuration.

It is necessary to recognize that 2 types of uncertainty exist in the tenability analysis: the uncertainties associated with the experimental data and the uncertainties associated with the equations used for FED calculations. Fortunately, with the fast-growing fire used in the project, the resulting uncertainty in the estimated time available for escape is much smaller than the uncertainty in the calculated FED due to their non-linear relationship. More details are provided in the following sections.

### 3.7.1 Exposure to Toxic Gases

Exposure to toxic products of combustion from fires has been a major cause of death and injury in many fire incidents. Understanding the toxic effect of the smoke products and predicting the exposure time necessary to cause incapacitation are complex problems.

In regards to the fuel package used in this study, with the combined flaming combustion of polyurethane foam and wood cribs, the primary gas products were toxic carbon monoxide (CO) and asphyxiant carbon dioxide ($CO_2$) in a vitiated oxygen ($O_2$) environment. Given the amount of polyurethane foam in the fuel package and the volume of the test house, hydrogen cyanide (HCN) produced from the combustion of polyurethane foam would not reach a concentration of concern for occupant life safety. A literature review by Beyler concluded that exposure to products of flaming combustion of flexible polyurethane foam would result in CO levels in the blood of test animals generally consistent with simple CO exposure, despite the toxicological role of HCN [17]. The fuel package contained no chemical components that would produce acid halides in the combustion gases. In this report, the analysis involved CO and $CO_2$ and oxygen vitiation only.

Table 3 shows the maximum CO and $CO_2$ concentrations and the minimum $O_2$ concentrations for Tests UF-06, UF-06R and UF-06RR. Not that gas analyzers used for the first storey at the 0.9 m height had an upper limit of 10% for $CO_2$ measurements and/or an upper limit of 1% for CO measurements.

Figure 32 to Figure 34, Figure 36 to Figure 38 and Figure 40 to Figure 42 (figures commence on page 96) show the CO, $CO_2$ and $O_2$ concentration-time profiles measured

during Tests UF-06, UF-06R and UF-06RR. The gases were well mixed in the test house.

The SFPE Handbook of Fire Protection Engineering contains information on the tenability limits for incapacitation or death after a 5-min exposure [16], shown in Table 4, which indicate the test results that need to be analyzed. In the following sections, tenability due to each gas is first analyzed independently; the interaction between the gases is then considered.

**Table 3. Maximum CO and $CO_2$ Concentrations and Minimum $O_2$ Concentration (%)**

| | | Test UF-06 | Test UF-06R | Test UF-06RR |
|---|---|---|---|---|
| 2nd storey 1.5 m high | CO | 4.5 | 5.2 | 5.6 |
| | $CO_2$ | 14.6 | 14.9 | 13.0 |
| | $O_2$ | 4.5 | 3.9 | 6.2 |
| 2nd storey 0.9 m high | CO | 4.2 | 4.8 | 5.4 |
| | $CO_2$ | 14.6 | 15.1 | 13.5 |
| | $O_2$ | 5.0 | 4.7 | 6.4 |
| 1st storey 1.5 m high | CO | 4.6 | 5.5 | 5.6 |
| | $CO_2$ | 14.7 | 15.4 | 13.1 |
| | $O_2$ | 4.3 | 3.5 | 5.7 |
| 1st storey 0.9 m high | CO | >1.0 | >1.0 | 5.5 |
| | $CO_2$ | >10.0 | >10.0 | >10.0<br>13.0* |
| | $O_2$ | 4.3 | 4.0 | 6.2 |

Notes:
1. ">" indicating the concentration beyond the measurement range of the gas analyzer;
2. All concentrations before the structural failure;
3. *calculated: $CO_2\% = 20.9\% - O_2\% - ½\ CO\%$.

**Table 4. Tenability Limits for Incapacitation or Death after 5-min Exposure [16]**

| Gas | Incapacitation | Death |
|---|---|---|
| CO | 6000 – 8000 ppm (0.6 – 0.8%) | 12,000 – 16,000 ppm (1.2 – 1.6%) |
| Low $O_2$ | 10 – 13% | < 5% |
| $CO_2$ | 7 – 8% | > 10% |

3.7.1.1 Exposure to $O_2$ vitiation

Fires consume oxygen and create a low oxygen atmosphere. Past human experiments in an oxygen-depleted atmosphere indicated that most people could tolerate a 15% $O_2$ atmosphere [16]. Healthy individuals could also tolerate a 12% $O_2$ level for a short period (<5 min) [18]. When oxygen diminished to below 10%, unconsciousness could occur rapidly. For healthy adults, the following equation was derived from the experiments with human subjects [16] and can be used to predict the time, $t_{in,O_2}$ *(minute)*, to loss of consciousness due to lack of oxygen alone.

$$t_{in,O_2} = \exp[8.13 - 0.54(20.9 - \%O_2)]$$

With the changing $O_2$ concentration, the fractional effective dose approach has to be used in the analysis. The incapacitation dose for oxygen vitiation can be expressed by *(20.9 - %$O_2$)* $\times t_{in,O_2}$. The fractional effective dose is the accumulation of the ratio of the actual exposure dose *(20.9 - %$O_2$)* $\times \Delta t$ and the incapacitation dose at each discrete increment of time:

$$F_{in,O_2} = \sum_{t1}^{t2} \frac{(20.9 - \%O_2) \cdot \Delta t}{(20.9 - \%O_2) \cdot t_{in,CO_2}} = \sum_{t1}^{t2} \frac{\Delta t}{\exp[8.13 - 0.54(20.9 - \%O_2)]}$$

where $\Delta t$ *(minute)* is the discrete increment of time, i.e. the time interval for data sampling. Table 5 shows the calculated times for the fractional effective dose reaching 0.3 and 1.0 for exposure to $O_2$ vitiation alone.

In Test UF-06 (see Figure 33), the $O_2$ concentration on both the first and second storeys dropped to below 10% in 230 s and to 4% at 380 s after ignition. The $O_2$ vitiation alone would cause incapacitation after 325 s using $F_{in,O_2}$ = 1 as a criterion, or after 275 s using $F_{in,O_2}$ = 0.3.

In Test UF-06R (see Figure 37), the $O_2$ concentration on both the first and second storeys dropped to below 10% in 220 s and to 4% at 380 s after ignition. The $O_2$ vitiation alone would cause incapacitation after 278-294 s using $F_{in,O_2}$ = 1 as a criterion, or after 250 s using $F_{in,O_2}$ = 0.3.

In Test UF-06RR (see Figure 41), the $O_2$ concentration on both the first and second storeys dropped to below 10% in 270 s and to 6% at 410 s after ignition. The $O_2$ vitiation alone would cause incapacitation after 413 s using $F_{in,O_2}$ = 1 as a criterion, or after 343 s using $F_{in,O_2}$ = 0.3.

#### 3.7.1.2 Exposure to $CO_2$

$CO_2$ is not toxic at concentrations of up to 5%. Above 7%, $CO_2$ becomes an asphyxiant gas; the danger of loss of consciousness of an exposed person increases. Loss of consciousness could occur in approximately 2 minutes at 10% $CO_2$, for example. The following equation can be used to predict the time, $t_{in,CO_2}$ *(minute)*, to loss of consciousness due to the $CO_2$ asphyxiant effect [16]:

$$t_{in,CO_2} = \exp(6.1623 - 0.5189 \cdot \%CO_2)$$

With the changing $CO_2$ concentration, the fractional effective dose approach has to be used. The incapacitation dose for $CO_2$ exposure can be expressed by *%$CO_2$* $\times$ $t_{in,CO_2}$ above which loss of consciousness would occur for people of average

susceptibility. At each discrete increment of time, the increment of the fractional effective dose was calculated as the actual exposure dose ($CO_2$ concentration × time increment) divided by the incapacitation dose. The fractional effective dose values expressed in Table 5 are the accumulation of this ratio of each time increment:

$$F_{in,CO_2} = \sum_{t1}^{t2} \frac{\%CO_2 \cdot \Delta t}{\%CO_2 \cdot t_{in,CO_2}} = \sum_{t1}^{t2} \frac{\Delta t}{\exp(6.1623 - 0.5189 \cdot \%CO_2)}$$

In Test UF-06 (see Figure 34), the $CO_2$ concentration exceeded 10% in 230 s. The increased concentration of $CO_2$ alone would cause incapacitation after 283 s using $F_{in,CO_2}$ = 1 as a criterion, and after 246 s using $F_{in,CO_2}$ = 0.3.

In Test UF-06R (see Figure 38), the $CO_2$ concentration exceeded 10% in 220 s. The increased concentration of $CO_2$ alone would cause incapacitation after 253 s using $F_{in,CO_2}$ = 1 as a criterion, and after 234 s using $F_{in,CO_2}$ = 0.3.

In Test UF-06RR (see Figure 42), the $CO_2$ concentration exceeded 10% in 270 s. The increased concentration of $CO_2$ alone would cause incapacitation after 353 s using $F_{in,CO_2}$ = 1 as a criterion, and after 288 s (1st storey-2nd storey) using $F_{in,CO_2}$ = 0.3.

#### 3.7.1.3 Exposure to CO

CO is known to be the most important toxicant of the fire gases. The lowest CO concentration in air that has been reported to cause human death is 5,000 ppm for a 5 min exposure [19]. The toxic effect of CO is due to its affinity with the hemoglobin in human blood to form carboxyhemoglobin (COHb), which reduces the transport of oxygen in the blood to various parts of the body. When COHb in the blood increases to a threshold concentration, loss of consciousness or death may occur. The time for the toxic effect to occur depends on the uptake rate of CO into the blood of a victim and the threshold COHb concentration for that victim.

The CO uptake rate is determined by the difference between the CO concentration inhaled and that already in the body, and varies with the breathing rate, the degree of activity, the lung function, the body size, the blood volume and hemoglobin concentration of the victim and the exposure duration. The complexity of the CO uptake is described by the theoretical Coburn-Forster-Kane (CFK) equation, which takes account of a wide range of variables to predict the COHb concentration [20]. For high-concentration and short-duration exposures such as the fire scenarios used in the FPH tests, one can use a simpler equation that was derived from human exposure experiments with healthy adults [16, 21]:

$$\%COHb = 3.317 \times 10^{-5} [CO]^{1.036} RMV \cdot t$$

where *[CO]* is the inhaled carbon monoxide concentration in *parts per million*, *RMV* (respiratory minute volume) is the volume of air breathed in *litres per minute*, and *t* is the exposure duration in *minutes*. This equation gives equally good predictions as the CFK

equation for average healthy adults. Since the CO concentration in the experiments varied with time, %COHb was calculated as a summation of the CO uptake at each discrete time step:

$$\%COHb = \sum_{t_0}^{t} 3.317 \times 10^{-5} [CO]^{1.036} RMV \cdot \Delta t$$

For an average adult, the normal breathing rate is 20 L/min with light activity. The breathing rate is affected by the presence of $CO_2$ in a fire situation. In the concentration range of 2 to 6%, $CO_2$ can stimulate breathing. A $CO_2$-induced hyperventilation factor, $VCO_2$, for breathing can be estimated using [16]:

$$VCO_2 = \exp(\frac{\%CO_2}{5})$$

The hyperventilation increases the uptake rate of other toxic gases, such as CO, from the fire. This effect should be considered when $CO_2$ concentration is above 2%. The presence of 5% $CO_2$ could triple the normal breathing rate, for example. Considering the $CO_2$-induced hyperventilation in a fire situation, the breathing rate would be

$$RMV = 20 \cdot \exp(\frac{\%CO_2}{5})$$

For the same individual, the CO uptake rate changes if the breathing rate changes, which also depends on the degree of activity of that individual. The CO uptake rate varies from person to person for a given smoke atmosphere.

The COHb incapacitating concentration at which loss of consciousness may occur is in the range of 25-40% depending on the degree of activity of the occupant among other variables [16, 22]. The threshold of 40% is more appropriate for those at rest and 30% for those engaged in light activity [16]. Certain susceptible populations may be incapacitated at lower COHb concentrations.

With the rate of CO uptake and the likely incapacitating concentration of COHb, time to incapacitation due to CO exposure can be predicted. For those engaged in light activity, the fractional effective dose for incapacitation due to the CO uptake can be expressed as the COHb concentration in the blood divided by the incapacitating COHb concentration

$$F_{in,CO} = \frac{\%COHb}{30} = 2.2113 \times 10^{-5} \sum_{t_0}^{t} [CO]^{1.036} \Delta t \cdot \exp(\frac{\%CO_2}{5})$$

Alternatively, the fractional effective dose for incapacitation due to CO can also be calculated using the approach given in ISO TS 13571 for short exposure to CO at high concentrations [15]:

$$F_{in,CO} = \sum_{t1}^{t2} \frac{[CO] \cdot \Delta t}{35000} \exp\left(\frac{\%CO_2}{5}\right)$$

where the incapacitation dose is 35000 ppm·min, which is consistent with the tenability limits of 6000 to 8000 ppm for incapacitation for 5-min exposure given in the SFPE Handbook of Fire Protection Engineering [16]. For the FPH tests, the difference between the incapacitation times predicted using these two equations is relatively small.

The time to incapacitation determined using $F_{in,CO}$ = 1 as a criterion represents the time available for escape for healthy adults of average susceptibility. For more susceptible people, the exposure thresholds could be lower. The CO uptake and the COHb increase are known to be faster in small children than in adults [23]. Therefore, the incapacitation time for small children or a more susceptible subpopulation would be shorter than for average healthy adults. These can be addressed, to a certain degree, by using $F_{in,CO}$ =0.3 as a criterion to determine the incapacitation time. Table 5 shows the calculated times for the fractional effective dose reaching 0.3 and 1.0. Calculation for the CO fractional effective dose was done with and without the $CO_2$ hyperventilation factor *exp(%$CO_2$/5)*.

In Test UF-06 (see Figure 32), the maximum CO concentration prior to failure of the floor assembly was 48000 ppm at 380 s. The increased concentration of CO alone would cause incapacitation after 230-235 s (1st storey-2nd storey) using $F_{in,CO}$ = 0.3 as a criterion, and after 300-310 s (1st storey-2nd storey) using $F_{in,CO}$ = 1.0. With $CO_2$-induced hyperventilation, these times were reduced to 198-208 s (1st storey-2nd storey) for $F_{in,CO}$ = 0.3 and 233-241 s (1st storey-2nd storey) for $F_{in,CO}$ = 1.0.

In Test UF-06R (see Figure 36), the maximum CO concentration prior to failure of the floor assembly was 56000 ppm at 380 s. The increased concentration of CO alone would cause incapacitation after 233-253 s (1st storey-2nd storey) using $F_{in,CO}$ = 0.3 as a criterion, and after 288-308 s (1st storey-2nd storey) using $F_{in,CO}$ = 1.0. With $CO_2$-induced hyperventilation, these times were reduced to 198-207 s (1st storey-2nd storey) for $F_{in,CO}$ = 0.3 and 228-241 s (1st storey-2nd storey) for $F_{in,CO}$ = 1.0.

In Test UF-06RR (see Figure 40), the maximum CO concentration prior to failure of the floor assembly was 56000 ppm at 410 s. The increased concentration of CO alone would cause incapacitation after 228-248 s (1st storey-2nd storey) using $F_{in,CO}$ = 0.3 as a criterion, and after 293-308 s (1st storey-2nd storey) using $F_{in,CO}$ = 1.0. With $CO_2$-induced hyperventilation, these times were reduced to 203-218 s (1st storey-2nd storey) for $F_{in,CO}$ = 0.3 and 233-248 s (1st storey-2nd storey) for $F_{in,CO}$ = 1.0.

The times to untenable conditions due to CO exposure were quite repeatable for the three tests.

**Table 5. Time (in seconds) to the Specified Fractional Effective Dose for Exposure to $O_2$ Vitiation, $CO_2$ and CO**

| | Test UF-06 | | Test UF-06R | | Test UF-06RR | |
|---|---|---|---|---|---|---|
| **Fractional Effective Dose** | **FED = 0.3** | **FED = 1.0** | **FED = 0.3** | **FED = 1.0** | **FED = 0.3** | **FED = 1.0** |
| CO alone – 1st storey | 230 | 300 | 233 | 288 | 228 | 293 |
| CO with $CO_2$ hyperventilation – 1st storey | 198 | 233 | 198 | 228 | 203 | 233 |
| Low $O_2$ hypoxia – 1st storey | 275 | 330 | 251 | 294 | 343 | 413 |
| CO alone – 2nd storey corridor | 235 | 310 | 253 | 308 | 248 | 308 |
| CO with $CO_2$ hyperventilation – 2nd storey corridor | 208 | 241 | 207 | 241 | 218 | 248 |
| Low $O_2$ hypoxia – 2nd storey corridor | 275 | 325 | 250 | 278 | 343 | 413 |
| High $CO_2$ hypercapnia – 1st storey | 246 | 290 | 234 | 256 | 298 | 358 |
| High $CO_2$ hypercapnia – 2nd storey corridor | 251 | 283 | 237 | 253 | 288 | 353 |

Note:

1. Based on concentrations at 1.5 m height

3.7.1.4 Interaction of CO, $CO_2$ and $O_2$ vitiation

Interactions between these gases and their combined effect are not well understood. The asphyxiant effect of $CO_2$ is generally treated as being independent of other gases; the effect of $O_2$ vitiation (low oxygen hypoxia) is generally treated as being additive with the effect of CO [16]. The effect of the smoke gases is determined by $F_{in,CO_2}$ or $(F_{in,CO} + F_{in,O_2})$, whichever is larger (with $F_{in,CO}$ including the effect of $CO_2$-induced hyperventilation).

Table 6 shows examples of this treatment. The calculation shows that the $O_2$ vitiation did not add much to the effect at the time when CO was capable of producing incapacitation. CO was the most important toxicant of the smoke gases; increased CO uptake by $CO_2$-induced hyperventilation was the most important interaction. Therefore, the exposure to CO with $CO_2$-induced hyperventilation determined the incapacitation time for the gases analyzed. Assuming the rate of CO uptake remains unchanged, the time required from the incapacitation dose to the lethal dose for an average adult is estimated to be within 1 minute under the conditions of Tests UF-06, UF-06R and UF-06RR.

A recent paper by Gann includes an analysis of incapacitation by exposure to CO alone for a susceptible subpopulation such as people with coronary artery disease or small children; incapacitation could occur at an FED range of 0.14-0.21 (CO alone) [24]. As

shown in Table 6, when the FED due to CO exposure with $CO_2$ hyperventilation reached 0.3, the FED due to CO exposure alone already reached this range. This shows consistency in the estimation of time to incapacitation.

For exposure to the gases, each calculation for estimating incapacitation in this section was associated with a particular position where the concentrations were measured – each calculated time applies to an occupant who would stay at that particular location. In real fire situations, the occupant would move through different locations during egress. Therefore, the time to incapacitation would be in-between the times calculated for different locations.

**Table 6. FED due to CO, $CO_2$, $O_2$ Vitiation at Specified Time**

| Test | UF-06 | | UF-06R | | UF-06RR | |
|---|---|---|---|---|---|---|
| Time | **198 s** | **233 s** | **198 s** | **228 s** | **203 s** | **233 s** |
| CO alone | 0.18 | 0.30 | 0.16 | 0.25 | 0.16 | 0.33 |
| CO × $CO_2$ hyperventilation | 0.30 | 1.0 | 0.30 | 1.0 | 0.30 | 1.0 |
| Low $O_2$ hypoxia | 0.003 | 0.03 | 0.003 | 0.05 | 0.003 | 0.02 |
| CO × $CO_2$ hyperventilation + low $O_2$ hypoxia | 0.3 | 1.0 | 0.3 | 1.0 | 0.3 | 1.0 |
| High $CO_2$ hypercapnia | 0.015 | 0.12 | 0.019 | 0.18 | 0.015 | 0.07 |

Note:
1. Calculated based on concentrations at 1st storey SW quadrant at 1.5 m height

### 3.7.2 Exposure to Heat

Convected heat is the most important source of heat exposure for occupants in the first and second storeys. Figure 21 to Figure 22 and Figure 24 to Figure 25 show the temperature-time profiles measured on the two upper storeys during the tests. The temperatures at the 1.4 m height above the floor were used for the analysis of convected heat exposure.

The rate of convective heat transfer from hot gases to the skin depends on temperature, ventilation, humidity of the enclosure and clothing over the skin [16]. The tolerable time of exposure to convected heat is 15 min for dry air of 100°C or saturated air of 80°C. For hot air at temperatures above 120°C and with water vapour of less than 10%, pain and skin burns would be likely to occur in minutes; assuming unclothed or lightly clothed subjects, the time to incapacitation due to exposure to convected heat, $t_{in,conv}$ *(minutes)*, can be estimated for a constant temperature *T (°C)* using [15, 16]:

$$t_{in,conv} = 5 \times 10^7 T^{-3.4}$$

Since the temperatures in the FPH experiments were changing, the exposure was estimated using the fractional effective dose analogy at each discrete increment of time, $\Delta t$ *(minutes*):

$$\frac{\Delta t}{t_{in,conv}} = \frac{T^{3.4}}{5\times 10^{7}}\Delta t$$

When the temperature is increasing or stable, the fractional effective dose for incapacitation due to the convected heat exposure can be calculated using the following equation:

$$F_{in,heat} = \sum_{t1}^{t2} \frac{\Delta t}{t_{in,conv}} = \sum_{t1}^{t2} \frac{T^{3.4}}{5\times 10^{7}}\Delta t$$

The calculated time to incapacitation due to the convected heat exposure is given in Table 7. Radiant heat is important when the hot smoke layer is over 200°C, which corresponds to the threshold radiant heat flux of 2.5 kW·m$^{-2}$ required to produce the second degree burning of skin [25]. The calculation indicated that the convected heat exposure would result in incapacitation before the radiant heat began to play a major role on the first and second storeys.

Each calculation was associated with a particular position where the temperature was measured; in other words, each calculated time applies to an occupant who would stay at the location of a particular thermocouple tree. In real fire situations, the occupant would move through different locations during egress. Therefore, the time to incapacitation would be in-between the times calculated for different locations.

The convective heat exposure alone would produce incapacitation, but the time depended on the location in the test house. For Test UF-06, in the corridor on the second storey, the incapacitation time would be 229 s and 254 s for $F_{in,heat}$= 0.3 and $F_{in,heat}$= 1, respectively. In the open bedroom, the incapacitation time would be 315 s for $F_{in,heat}$= 0.3 but $F_{in,heat}$ did not reach 1. Heat exposure would not contribute to incapacitation in the closed bedroom. On the first storey, the incapacitation time would be 201-210 s using $F_{in,heat}$= 0.3 as a criterion, and 207-219 s using $F_{in,heat}$= 1.

For Test UF-06R, in the corridor on the second storey, the incapacitation time would be 217 s and 238 s for $F_{in,heat}$= 0.3 and $F_{in,heat}$= 1, respectively. In the open bedroom, the incapacitation time would be 293 s for $F_{in,heat}$= 0.3 but $F_{in,heat}$ did not reach 1. Heat exposure would not contribute to incapacitation in the closed bedroom. On the first storey, the incapacitation time would be 190-199 s using $F_{in,heat}$= 0.3 as a criterion, and 195-208 s using $F_{in,heat}$= 1.

For Test UF-06RR, in the corridor on the second storey, the incapacitation time would be 234 s and 298 s for $F_{in,heat}$= 0.3 and $F_{in,heat}$= 1, respectively. In the open bedroom, the incapacitation time would be 393 s for $F_{in,heat}$= 0.3 but $F_{in,heat}$ did not reach 1.. Heat exposure would not contribute to incapacitation in the closed bedroom. On the first storey, the incapacitation time would be 205-215 s using $F_{in,heat}$= 0.3 as a criterion, and 211-223 s using $F_{in,heat}$= 1.

The times to untenable conditions on the first storey due to exposure to the convective heat were also quite repeatable for the three tests.

**Table 7. Time (in seconds) to the Specified FED for Exposure to Convected Heat**

| | Test UF-06 | | Test UF-06R | | Test UF-06RR | |
|---|---|---|---|---|---|---|
| **Fractional Effective Dose** | **FED = 0.3** | **FED = 1.0** | **FED = 0.3** | **FED = 1.0** | **FED = 0.3** | **FED = 1.0** |
| 1st storey SE quadrant | 201 | 207 | 190 | 195 | 205 | 211 |
| 1st storey SW quadrant | 202 | 211 | 193 | 199 | 209 | 216 |
| 1st storey NE quadrant | 207 | 216 | 196 | 206 | 212 | 221 |
| 1st storey NW quadrant | 210 | 219 | 199 | 208 | 215 | 223 |
| 2nd storey corridor | 229 | 254 | 217 | 238 | 234 | 298 |
| 2nd storey open bedroom | 315 | n.r. (FED < 0.8) | 293 | n.r. (FED<0.8) | 393 | n.r. (FED<0.4) |
| 2nd storey closed bedroom | n.r. (FED < 0.008) | n.r. (FED < 0.008) | n.r. (FED < 0.005) | n.r. (FED < 0.005) | n.r. (FED < 0.008) | n.r. (FED < 0.008) |

Notes:
1. Based on temperatures at 1.4 m height;
2. n.r. – not reached.

### 3.7.3 Visual Obscuration by Smoke

Visual obscuration by the optically dense smoke tended to be the first hazard to arise that could impede evacuation by the occupants. Although visual obscuration would not directly cause incapacitation, it would cause delays in movement by the occupants and thus prolong exposure of occupants to other hazards. In this report, the smoke obscuration is expressed as the optical density per meter (*OD* in $m^{-1}$):

$$OD = \frac{1}{L}\log_{10}\left(\frac{I_0}{I}\right)$$

where $I_0$ is the intensity of the incident light, $I$ is the intensity of the light transmitted through the path length, $L$ (m), of the smoke. The optical density is related to the extinction coefficient ($k$ in $m^{-1}$) by $OD = k/2.303$.

Studies by Jin indicated that the optical density of smoke and visibility through smoke are related (the visibility is proportional to the reciprocal of the *OD* for non-irritating smoke, for example) [26]. Various threshold *OD* values related to the loss of visibility have been suggested for small buildings with occupants familiar with the egress route. The limiting *OD* value was suggested to be 0.5 $m^{-1}$ for non-irritating smoke and 0.2 $m^{-1}$ for irritating smoke [16,26]. A limiting OD value of 0.5 $m^{-1}$ was also set by Babrauskas using the results of full-scale burns of upholstered chairs and mattresses [22,27]. A recent home smoke alarm study used an *OD* of 0.25 $m^{-1}$ as the tenability limit for smoke obscuration [28]. In ISO 13571[15], the minimum visible brightness difference between an object and a background is used to estimate the smoke obscuration limit at which occupants cannot see their hands in front of their faces (a distance of 0.5 m or less). These calculations indicate that occupants cannot see their hands in front of their faces and become disoriented at an optical density of 3.4 $m^{-1}$. For an occupant whose vision is impaired, this can happen at an optical density of 2 $m^{-1}$ or less.

Video records were also analyzed for visual obscuration. The video images became completely obscure when the optical density was approaching 2 $m^{-1}$. Note that there were at least 2 halogen lamps (2 x 500 Watts) providing lighting in the view direction of each video camera on the first and second storey. This lighting condition was much better than that in a real house.

In this report, a tenability limit for optical density is set at $OD_{Limit}$ = 2 $m^{-1}$, recognizing that this limit could be lower for people with impaired vision. The time to untenable smoke obscuration is the moment when the optical density reaches this limit. Times to reach other smoke levels are also provided for discussion.

Figure 35, Figure 39 and Figure 43 show the optical density-time profiles measured on the first and second storeys. The times to reach various optical density levels at different locations for this series of the tests are listed in

Table 8. It must be pointed out that the smoke density meters used for the first storey had a narrower range of signal output (0.15 to 0 V) while the smoke density meters used for the second storey had a wider working range (1 to 0 V). The starting voltage (0.15 or 1 V when there was no smoke) decreased due to smoke residue left over from the preceding tests on the light source and the detector inside the meters. This reduced the working range particularly for the smoke density meters used for the first storey, which became saturated at a lower OD level than the meters used for the second storey. The smoke density meters used for the first storey were not able to measure the smoke obscuration of $OD = 2\ m^{-1}$ and beyond. The analysis of video records indicated that by the time when $OD = 2\ m^{-1}$ was reached in the corridor on the second storey, there was complete smoke obscuration in the test house.

In a separate study, fire scenario (FS) tests were conducted in the test facility with the ceiling of the basement fire room lined with two layers of non-combustible cement board (no structural floor was installed above the fire room). Ventilation and door openings in Test FS-1 were the identical to those in Tests UF-06, UF-06R and UF-06RR. Information about Test FS-1 can be found in data compilation and analysis reports [6, 29].

In Tests UF-06, UF-06R and UF-06RR, the increase in the optical density at each measurement location was quite fast. The times to reach various optical density levels of interest were very similar to the fire scenario Test FS-1. The combustion of the polyurethane foam produced sufficient smoke for conditions to reach the smoke obscuration limit. Both the optical density measurements and video records indicate that complete visual obscuration occurred around 160-190 s in the test house.

Psychological effects of smoke on occupants may accelerate the loss of visibility [26]. Possible reduction of time to untenable smoke level due to psychological effect is not addressed in this report.

**Table 8. Time (in seconds) to the Specified Smoke Optical Density**

| | Test UF-06 | | | | Test UF-06R | | | | Test UF-06RR | | | |
|---|---|---|---|---|---|---|---|---|---|---|---|---|
| **OD ($m^{-1}$) =** | **0.25** | **0.50** | **1.0** | **2.0** | **0.25** | **0.50** | **1.0** | **2.0** | **0.25** | **0.50** | **1.0** | **2.0** |
| 1st storey SW quadrant 1.5 m height | 120 | 130 | 147 | n.a. | 120 | 123 | 133 | n.a. | 130 | 154 | 168 | n.a. |
| 1st storey SW quadrant 0.9 m height | 145 | 160 | 180 | n.a. | 140 | 148 | 158 | n.a. | 153 | 173 | 183 | n.a. |
| 2nd storey corridor 1.5 m height | 130 | 145 | 160 | 170 | 126 | 140 | 150 | 161 | 148 | 158 | 168 | 184 |
| 2nd storey corridor 0.9 m height | 150 | 160 | 167 | 181 | 140 | 149 | 158 | 169 | 158 | 168 | 178 | 193 |

Note:
n.a.– not available due to limited measurement range of smoke meters used on the first storey.

### 3.7.4 Summary of Estimation of Time to Incapacitation

Tenability was analyzed independently for gas exposure, heat exposure and smoke obscuration to estimate the time available for escape, using incapacitation as the endpoint. The combined incapacitating effect as a result of simultaneous exposure to the combustion gases, heat and smoke obscuration is not well understood. Table 9 summarizes the estimated times to the onset of untenable conditions, where each value is the shortest time among each set of values from Table 5, Table 7 and

Table 8.

The uncertainty in the calculation of the FED is estimated to be ±25% for the heat exposure and ±40% for the CO exposure (with $CO_2$ induced hyperventilation) [15]. With the fast-growing fire used in the FPH project, the resulting uncertainty in the estimated time is much smaller than the uncertainty in the calculated FED due to the non-linear relationship. The uncertainty in the timing of the optical density measurement is ±5 s. Table 9 lists the uncertainty in the estimated time.

**Table 9. Summary of Estimation of Time to Specified FED and OD (in seconds)**

| Test | OD = 2 $m^{-1}$ | FED = 0.3 | | FED = 1 | |
|---|---|---|---|---|---|
| | 2nd storey | 1st storey | 2nd storey | 1st storey | 2nd storey |
| Tests with open basement doorway | | | | | |
| FS-1 | 190±5 | *245±15* | *260±15* | *290±20* | *325±30* |
| UF-06 | 170±5 | *198±10* | *208±12* | **211±3** | *241±10* |
| UF-06R | 161±5 | *198±10* | *207±15* | **199±2** | *241±10* |
| UF-06RR | 184±5 | *203±10* | *218±10* | **216±2** | *248±15* |

Notes:

1. Values determined using the measurements at 1.5 m height (for gas concentrations and OD) or 1.4 m height (for temperatures);
2. The number with the *Italic* font represents the calculated time for reaching the CO incapacitation dose, while the number with the bold Arial font represents the calculated time for reaching the heat incapacitation dose, whichever occurred first.

Smoke obscuration was the first hazard to arise. Although smoke obscuration would not directly cause incapacitation, it could impede evacuation and prolong exposure of occupants to other hazards. In Tests UF-06, UF-06R and UF-06RR, the times to reach various optical density levels of interest were similar to that of Test FS-1 and the combustion of polyurethane foam was mainly responsible for reaching the smoke obscuration limit. It must be pointed out that people with impaired vision could become disoriented at a lower optical density.

Because of the variation in susceptibility to heat and/or gas exposure, the time to untenable conditions was not a single value. The times corresponding to FED = 0.3 and FED = 1 in Table 9 represent this variation to a certain extent. There was also a slight variation of the corresponding time on the 2 different storeys, which is reflected by the time range for each FED in Table 9. It should be pointed out that the heat exposure and the CO exposure (with hyperventilation) would cause incapacitation at a similar time on each storey, independently.

For the closed bedroom, only heat exposure could be estimated. Based on the temperature measurements and the heat exposure calculation, the conditions in the closed bedroom on the second storey would not reach untenable conditions associated with FED = 0.3 or 1.

The analysis so far addressed a potential exposure that started at the time of ignition, which applies to occupants who would have been in the open spaces of the house.

Further analysis was also conducted for exposure starting at times later than ignition. This further analysis is important for occupants who would have been in the closed bedroom but tried to open the bedroom door to escape through the normal routes. Figure 44, Figure 45 and Figure 46 show the time remaining to incapacitation calculated from the convected heat and hyperventilated CO exposure for people of average susceptibility (FED=1) and for more susceptible occupants (FED=0.3) as a function of onset of exposure. Again, this calculation was associated with particular positions where the concentrations or temperatures were measured (each calculated time applies to an occupant who would have stayed at that particular location). The actual time to incapacitation would be in between the times calculated for different locations since an occupant would have moved through different locations during egress.

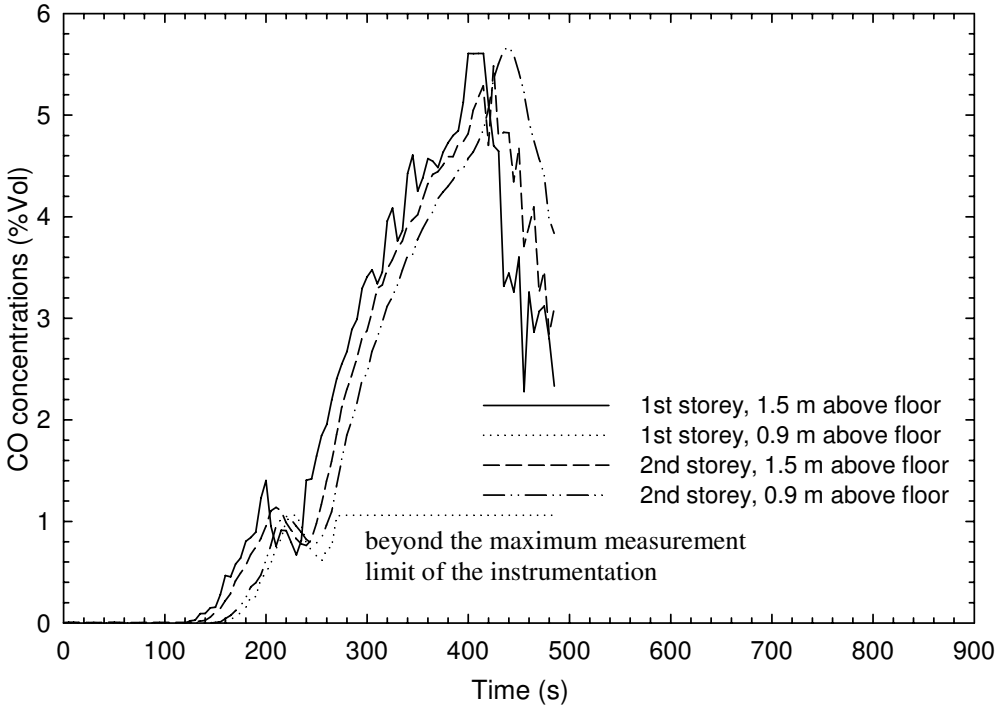


**Figure 32. CO measurements for Test UF-06**

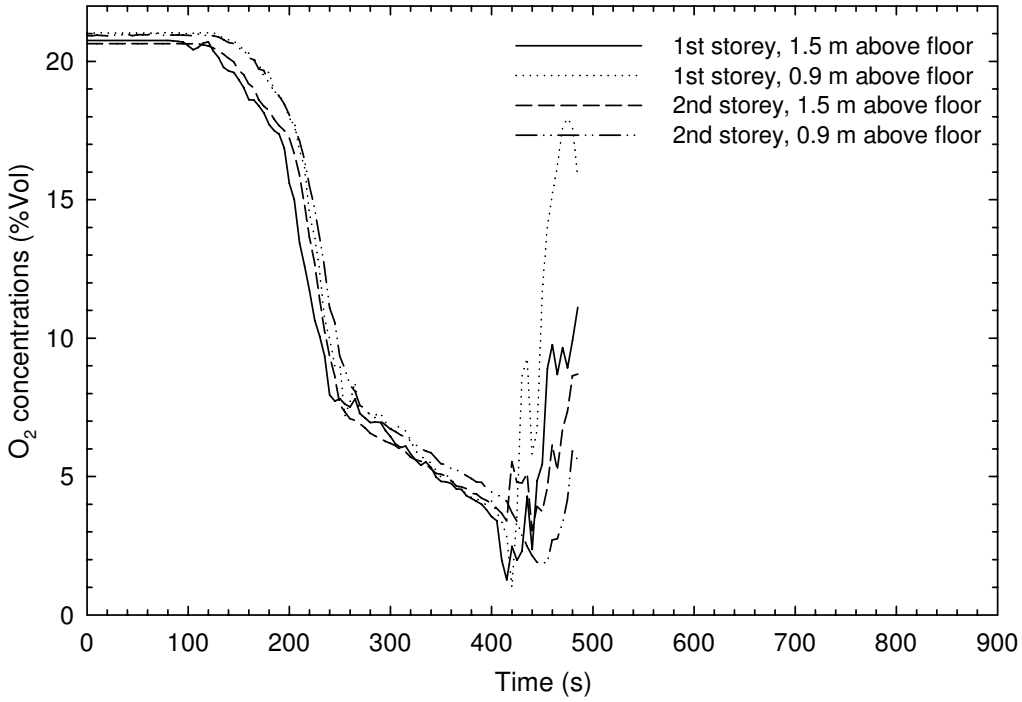


**Figure 33. $O_2$ measurements for Test UF-06**

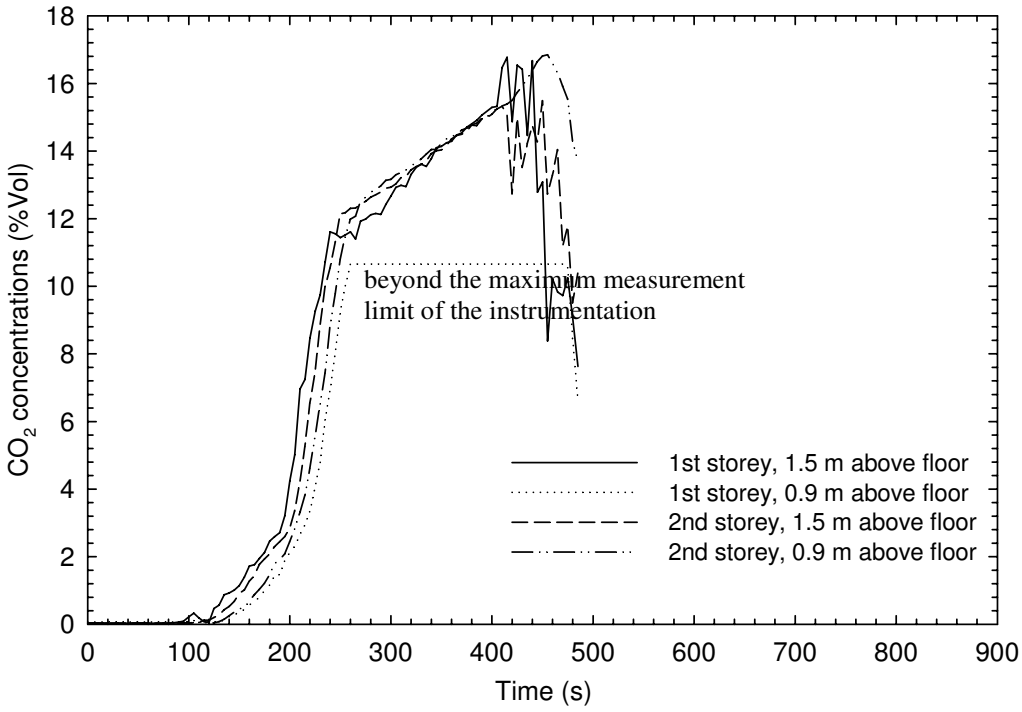


**Figure 34. $CO_2$ measurements for Test UF-06**

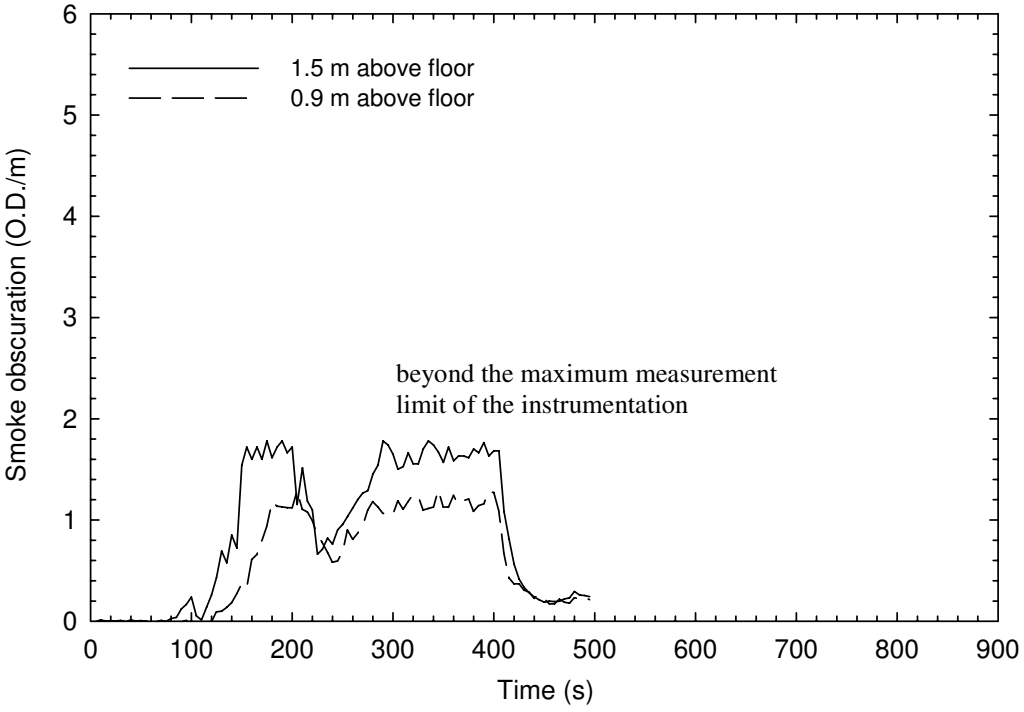


a) Smokemeters - 1st storey SW quadrant

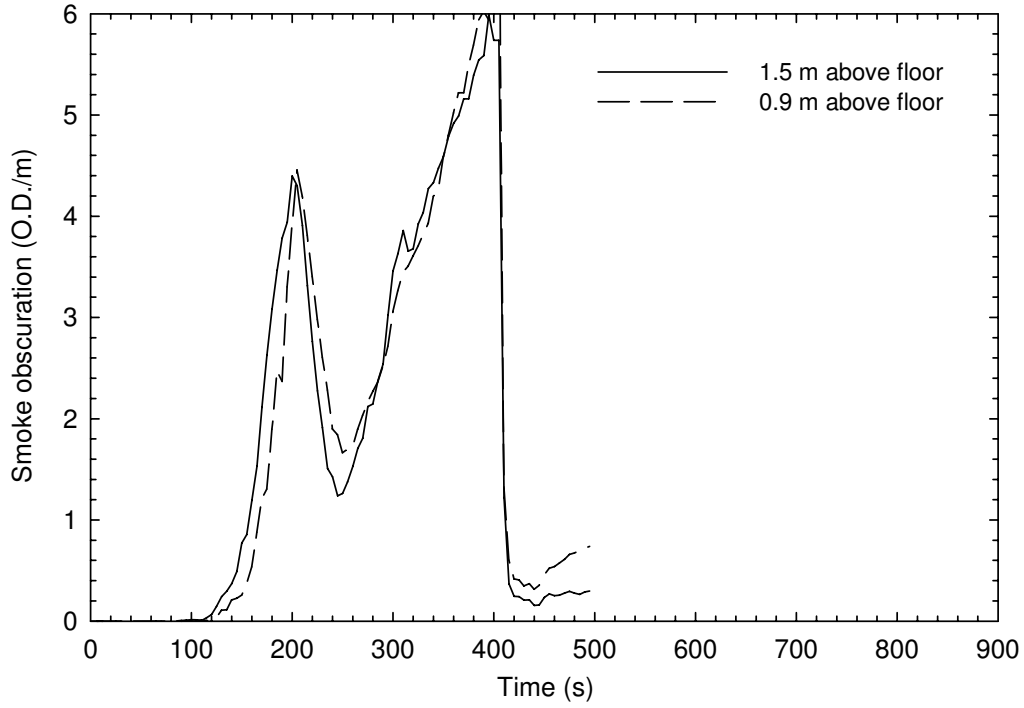


b) Smokemeters - 2nd storey corridor

**Figure 35. Optical density measurements for Test UF-06**

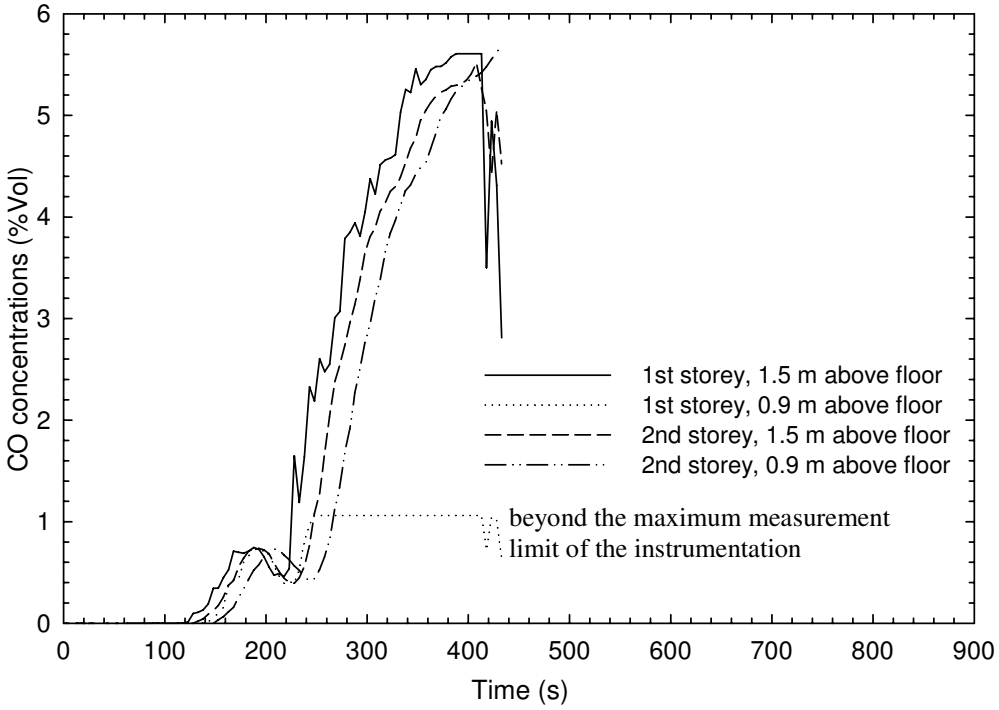


**Figure 36. CO measurements for Test UF-06R**

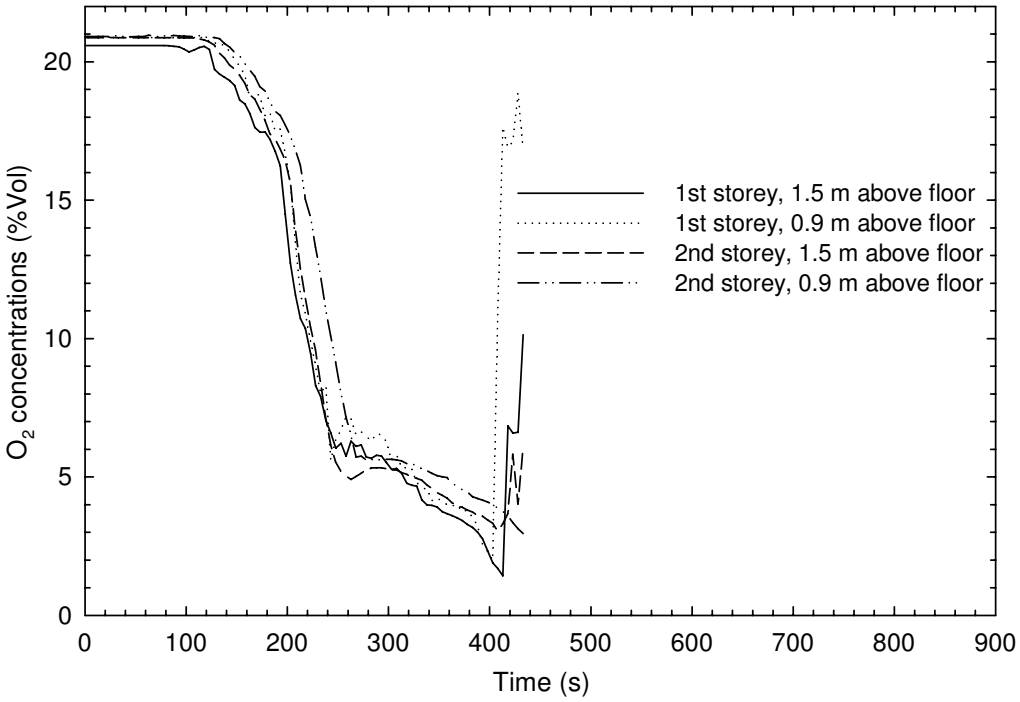


**Figure 37. $O_2$ measurements for Test UF-06R**

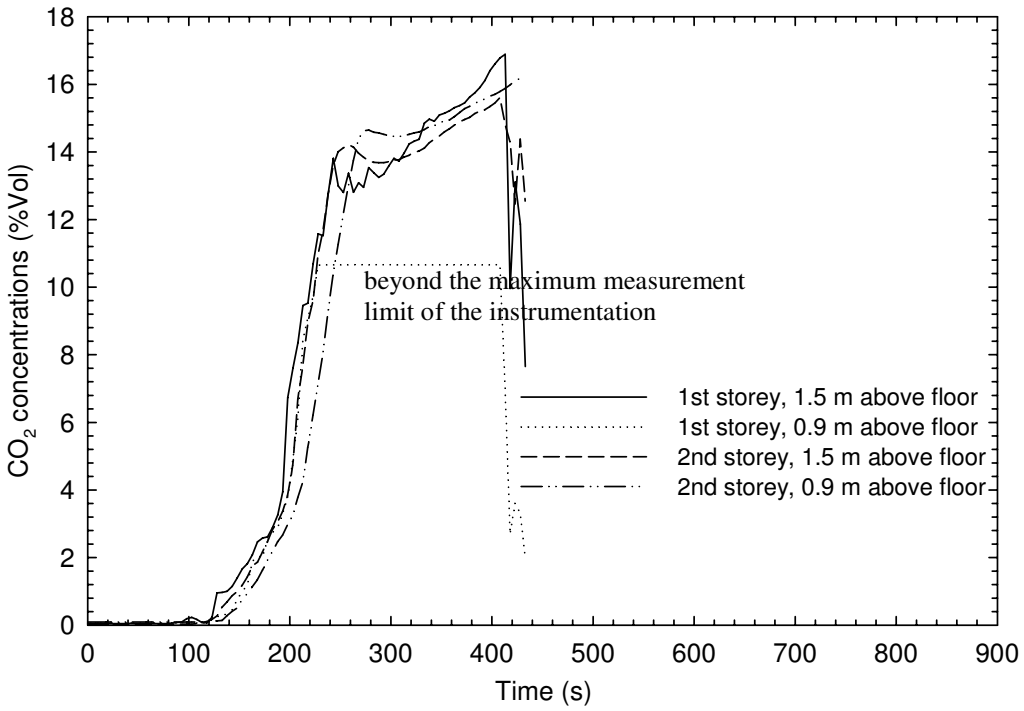


**Figure 38. $CO_2$ measurements for Test UF-06R**

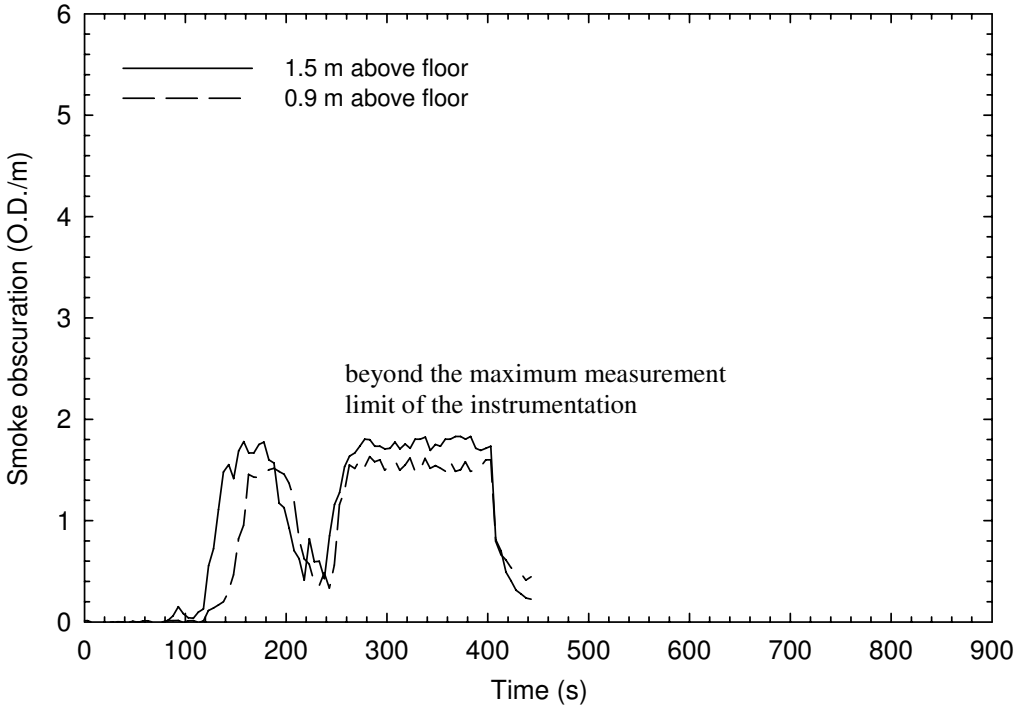


a) Smokemeters - 1st storey SW quadrant

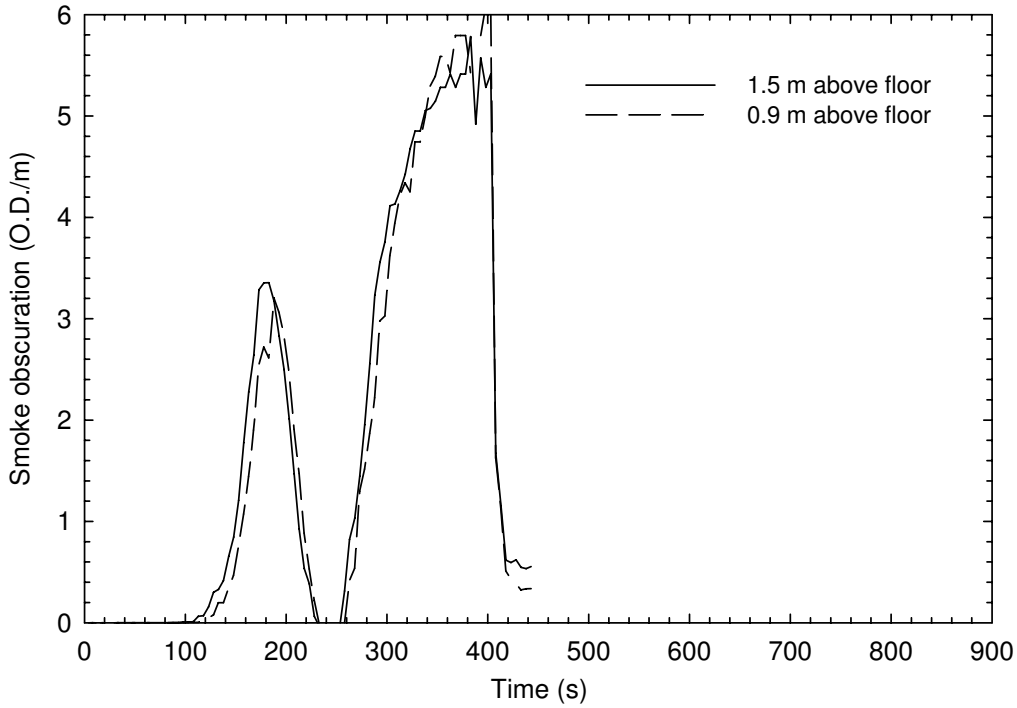


b) Smokemeters - 2nd storey corridor

**Figure 39. Optical density measurements for Test UF-06R**

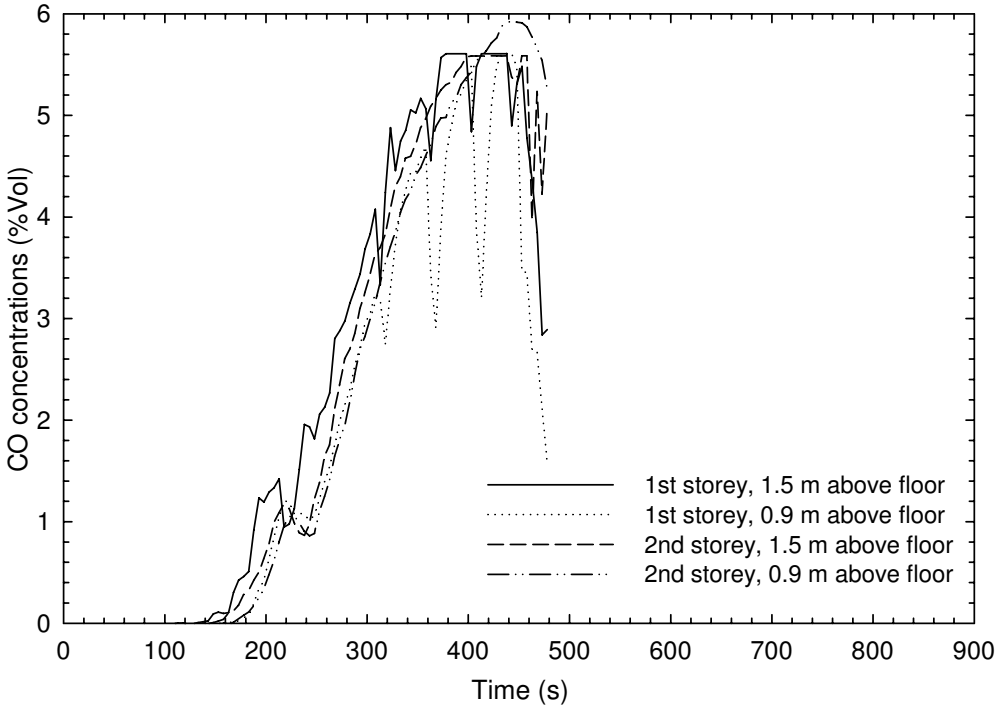


**Figure 40. CO measurements for Test UF-06RR**

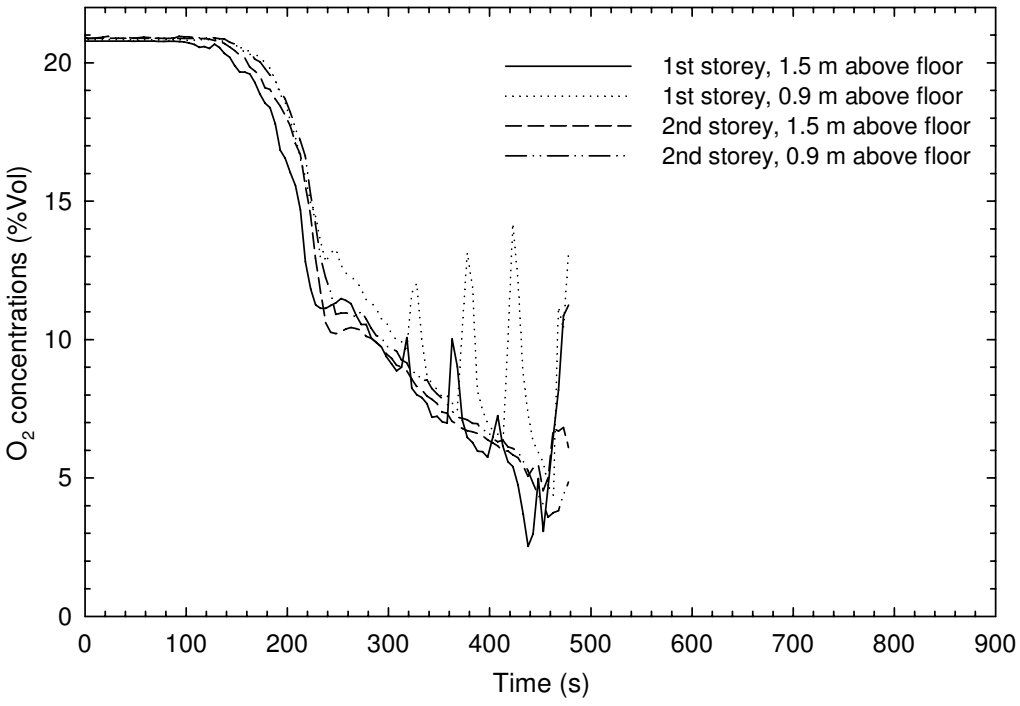


**Figure 41. $O_2$ measurements for Test UF-06RR**

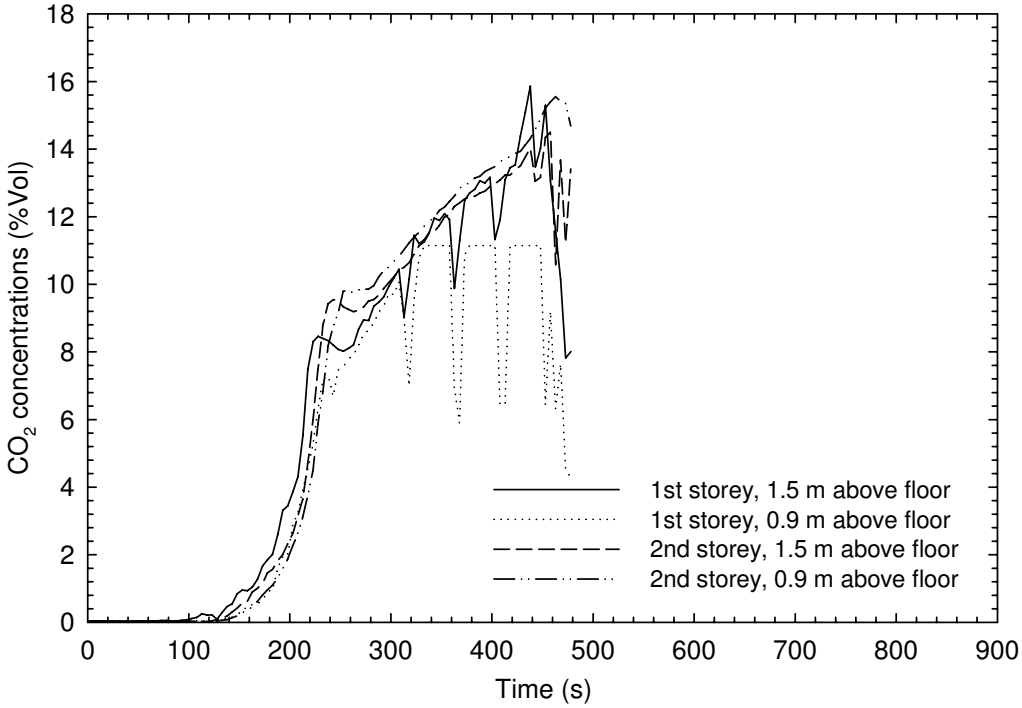


**Figure 42. $CO_2$ measurements for Test UF-06RR**

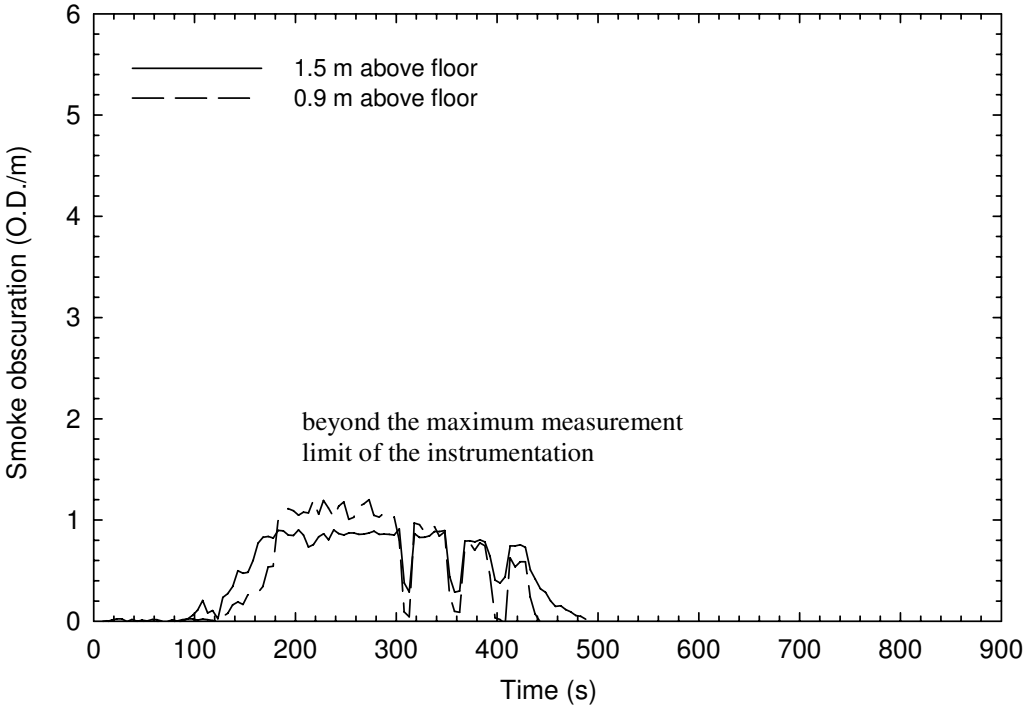


a) Smokemeters - 1st storey SW quadrant

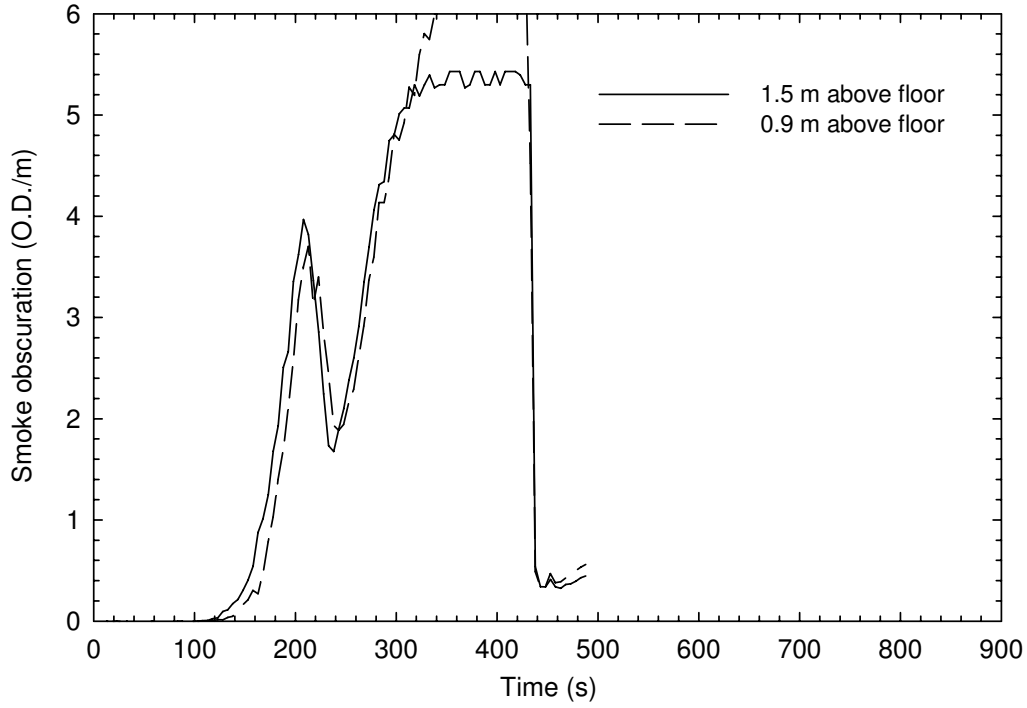


b) Smokemeters - 2nd storey corridor

**Figure 43. Optical density measurements for Test UF-06RR**

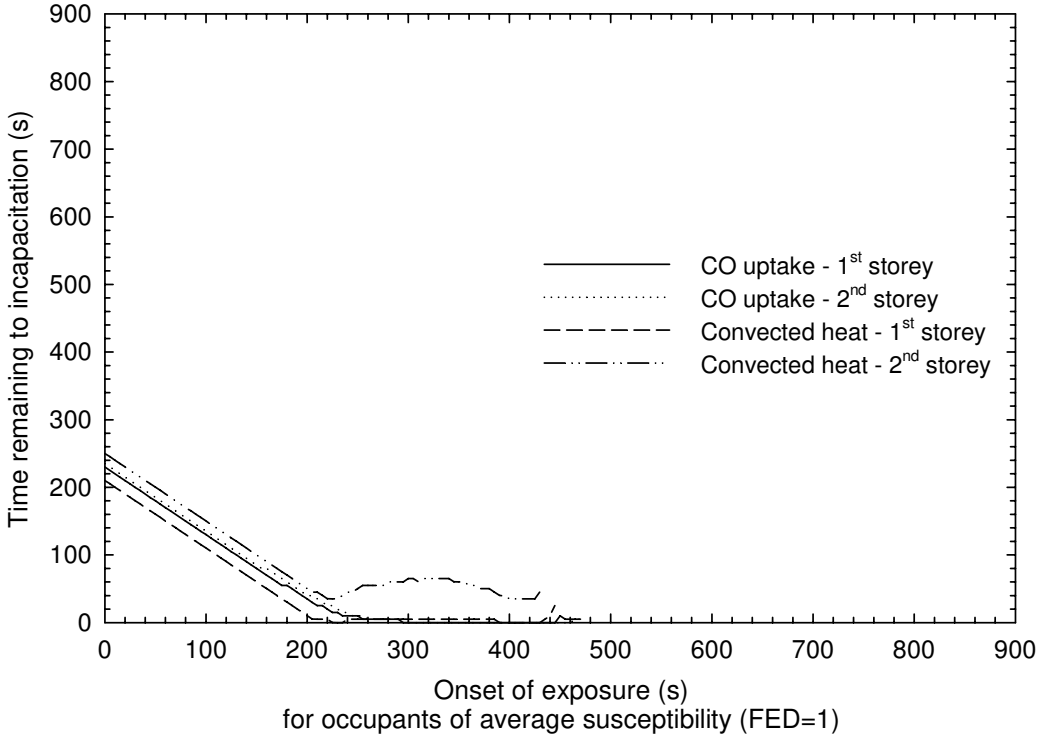


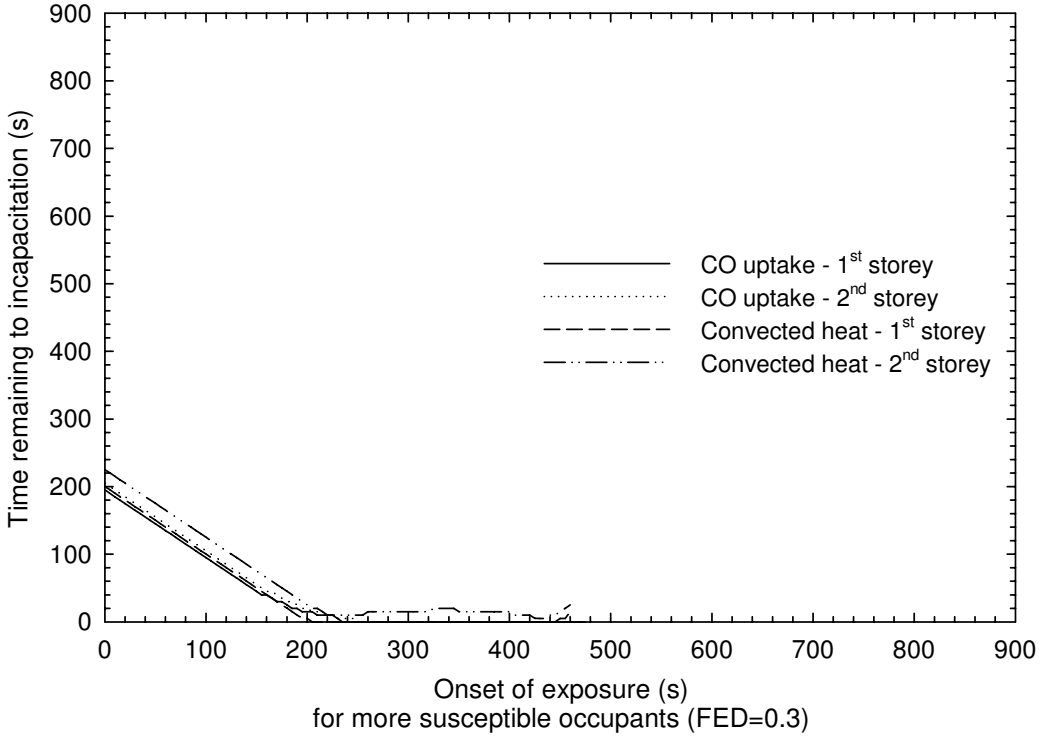


**Figure 44. Time remaining to incapacitation versus onset of exposure for Test UF-06 (ignition at time zero)**

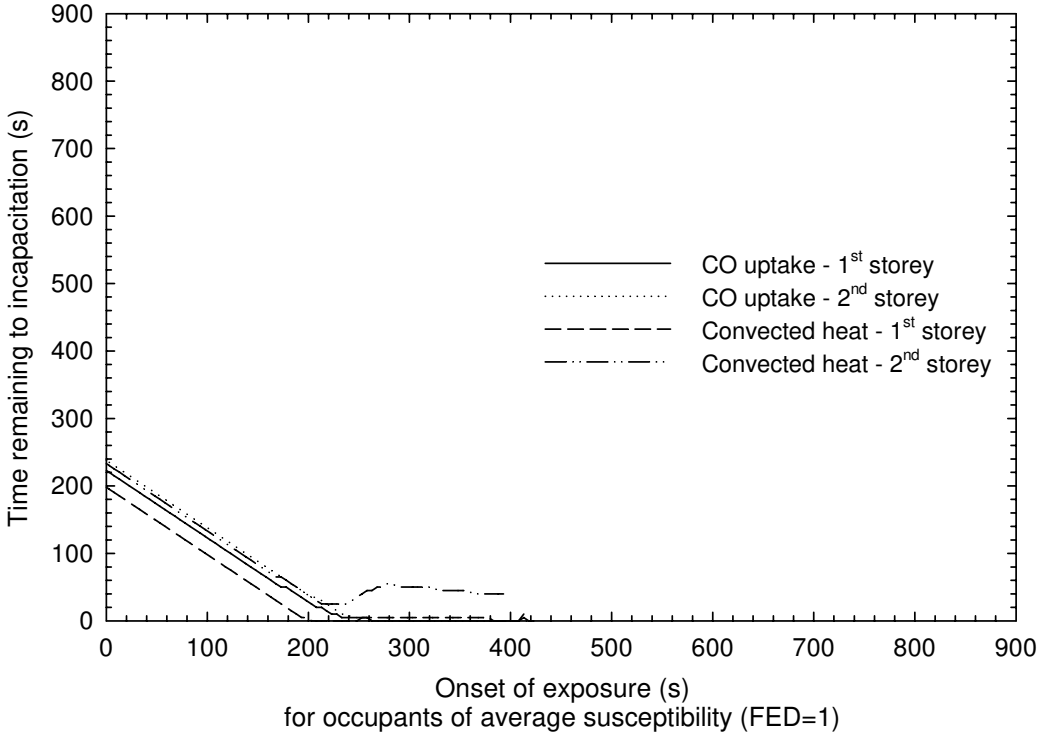


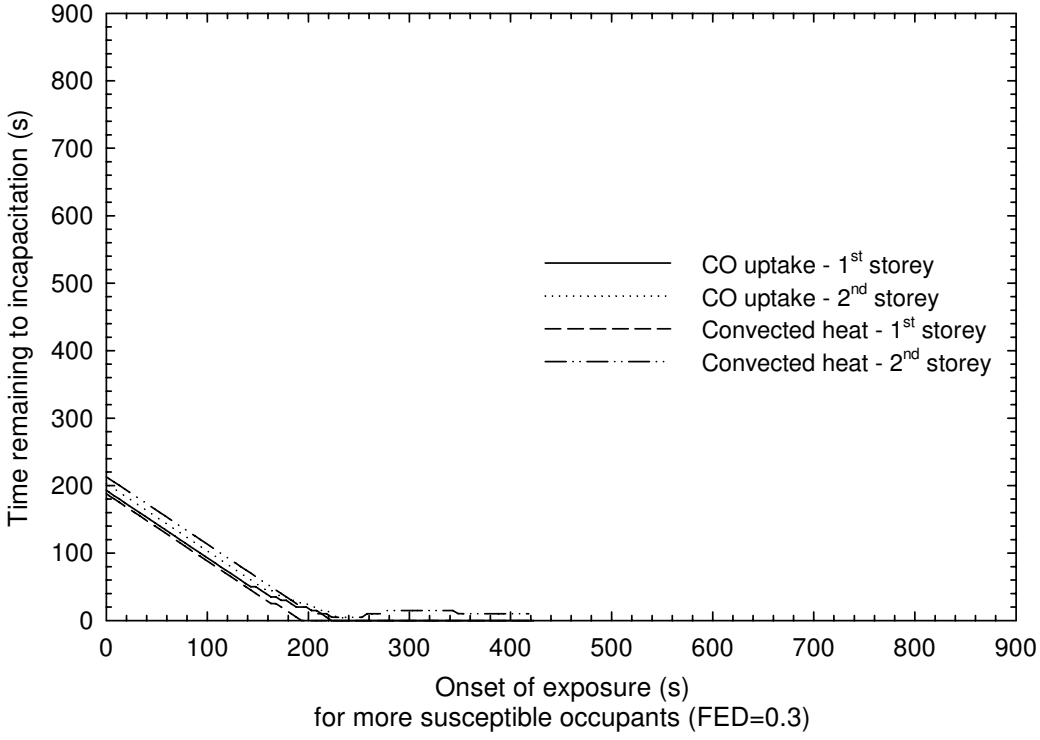


**Figure 45. Time remaining to incapacitation versus onset of exposure for Test UF-06R (ignition at time zero)**

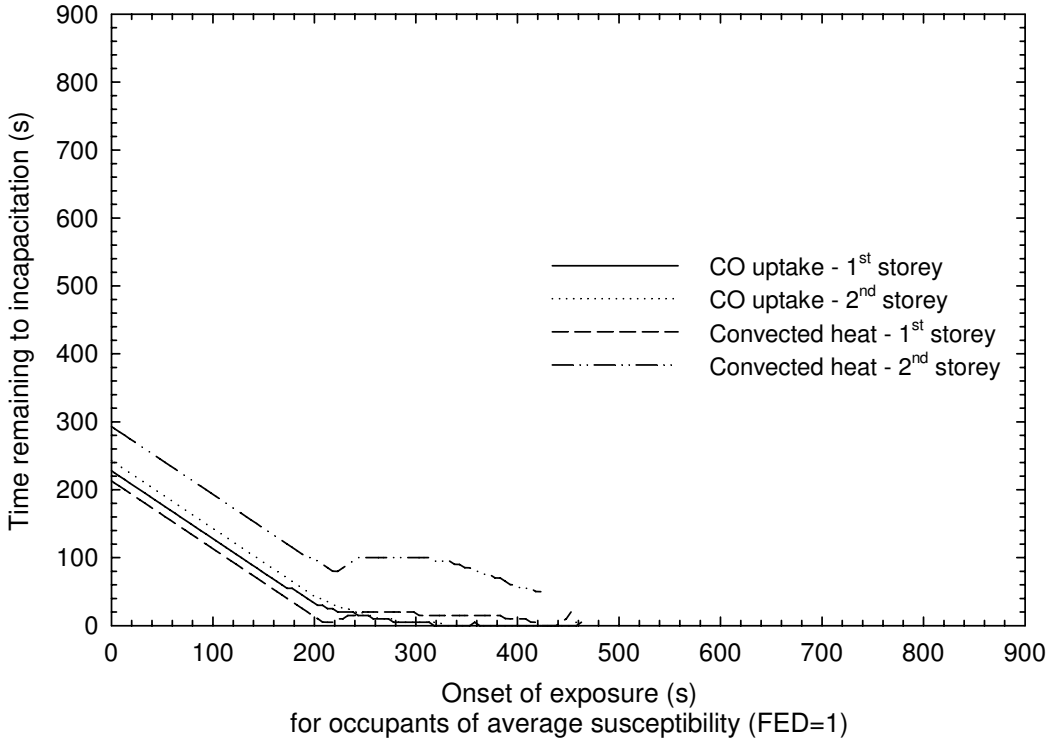


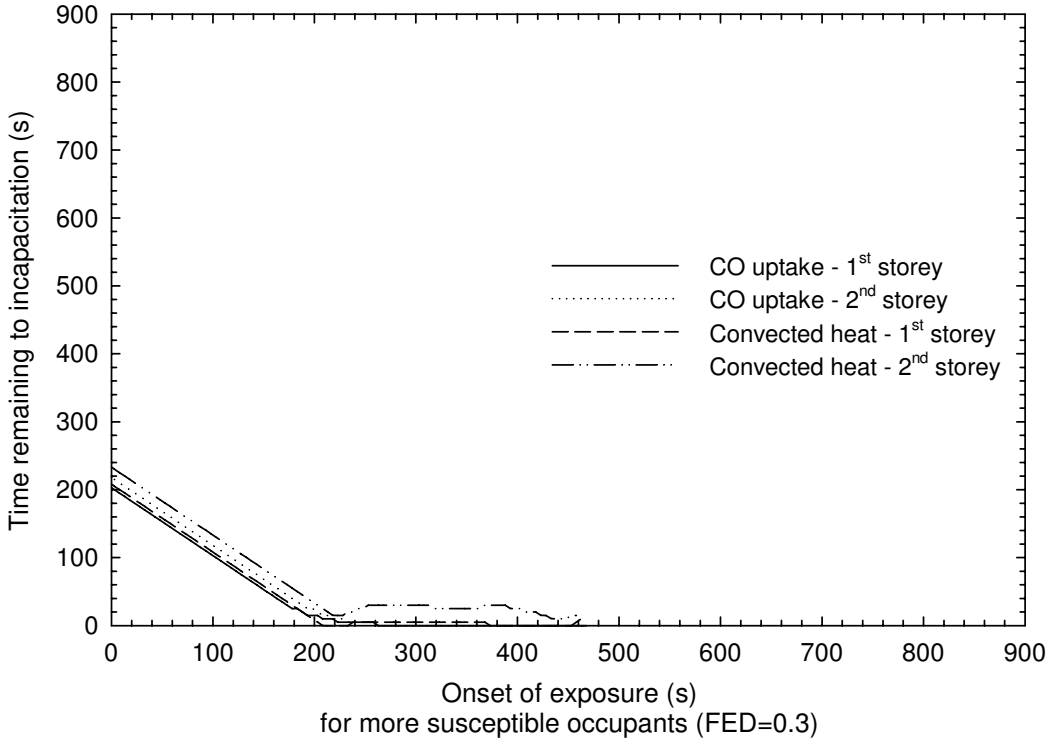


**Figure 46. Time remaining to incapacitation versus onset of exposure for Test UF-06RR (ignition at time zero)**

### 3.8 The Sequence of Events

Figure 47, Figure 48 and Figure 49 show the chronological sequence of the fire events in Tests UF-06, UF-06R and UF-06RR, respectively. There was good repeatability of the sequence of the fire events for the three tests.

The smoke alarms in the basement detected the fire quickly. The smoke alarm (photoelectric) located in the basement activated at 45 s in Test UF-06, 38 s in Test UF-06R and 43 s in Test UF-06RR. Interconnecting all of the smoke alarms in the house would help ensure an early fire alert.

The basement window was opened after it reached 300°C at 100 s in Test UF-06, 88 s in Test UF-06R and 109 s in Test UF-06RR. The exterior door on the first storey was opened at 180 s in the tests.

The timing for onset of potentially untenable conditions includes those for the complete smoke obscuration (OD $\geq$ 2 $m^{-1}$) and for exposure to heat and narcotic gases for susceptible (FED =0.3) and average (FED=1.0) occupants (see Section 3.7 for detailed discussions). The time after which the floor structure would be no longer usable for egress (382 s for UF-06, 380 s for UF-06R and 414 s for UF-06RR) was based on the shortest time to reach the maximum deflection.

In all three tests the untenable conditions were reached before the structural failure of the floor assembly. The tests were terminated after the floor failure.

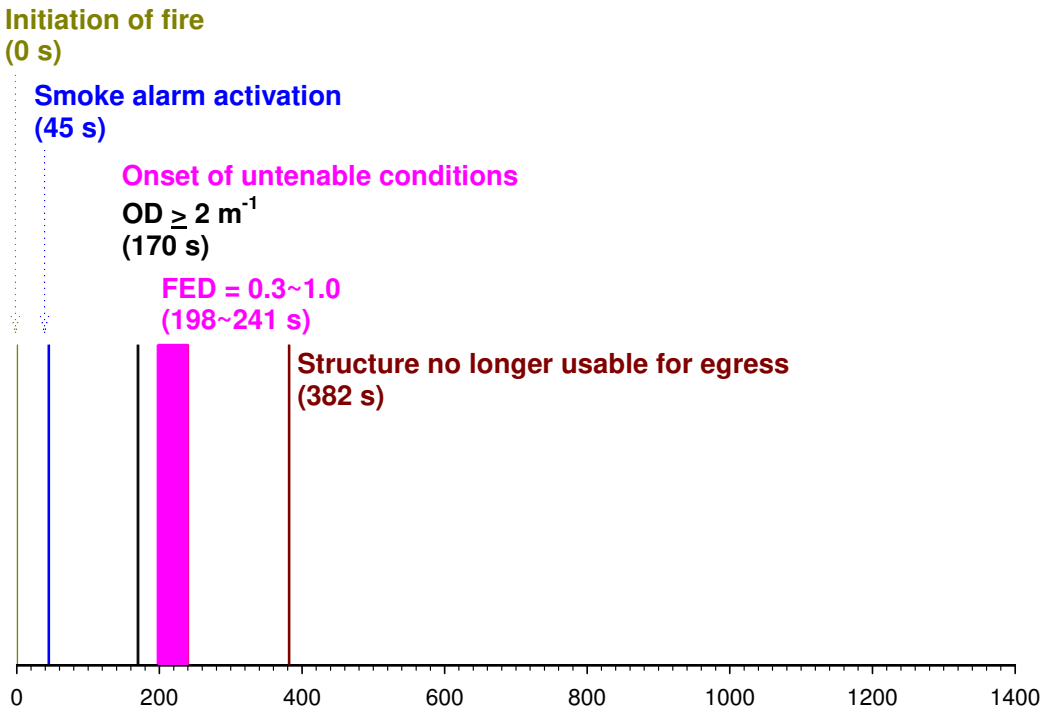


**Figure 47. Sequence of fire events in Test UF-06 (s)**

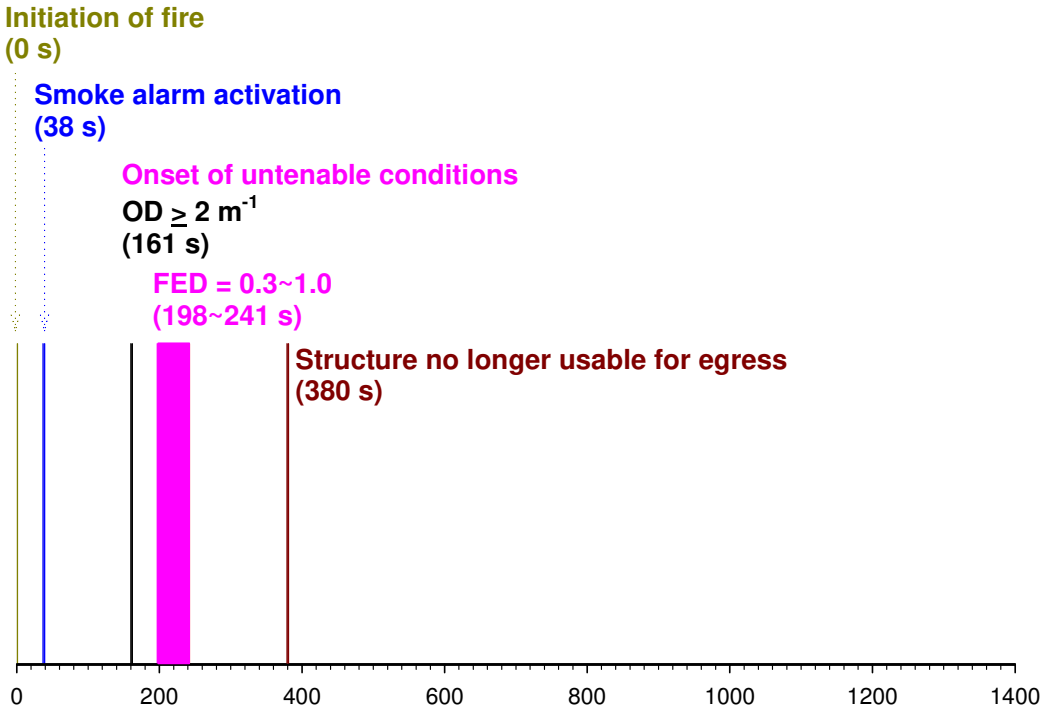


**Figure 48. Sequence of fire events in Test UF-06R (s)**

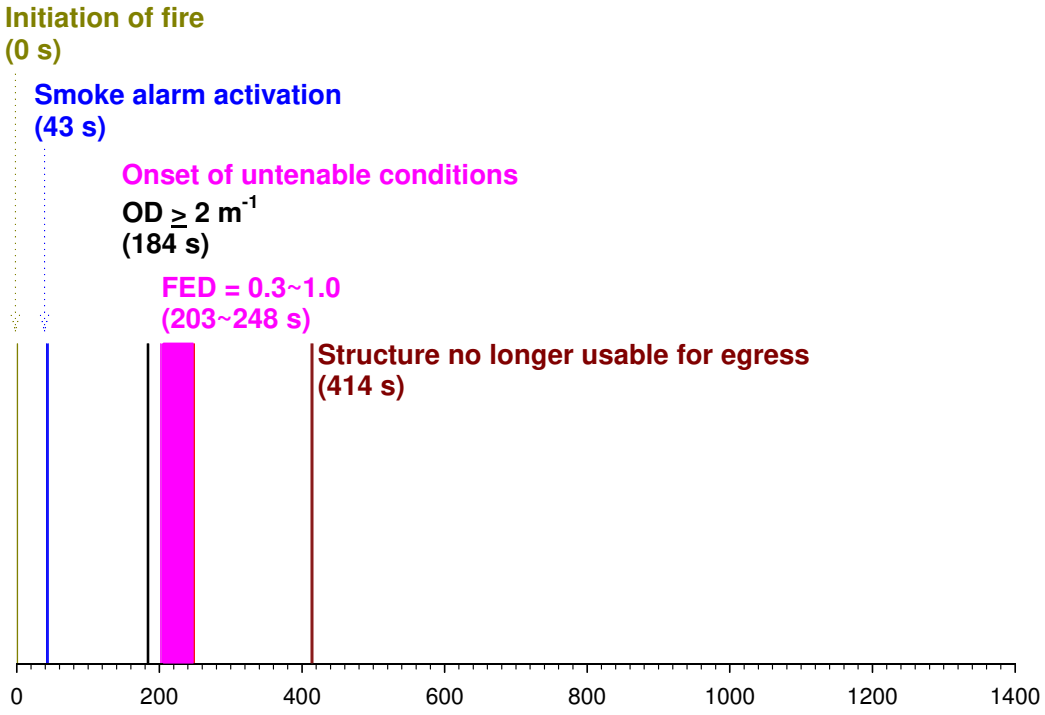


**Figure 49. Sequence of fire events in Test UF-06RR (s)**

## 4 SUMMARY

This report presents the results and analysis of Tests UF-06, UF-06R and UF-06RR as part of the research project on the fire performance of houses. The tests were conducted in the test facility that simulated a typical two-storey single-family house complying with the minimum code requirements in the NBCC.

Three loaded unprotected wood I-joist floor assemblies (also basement ceilings) were tested using a fire scenario that was characterized in a study documented in reference [6]. A number of measurements were conducted during the tests including temperatures at various locations (in the compartments and on the floor assemblies), fire detection times at various locations, gas measurements, smoke density measurements, flame penetration and deflection measurements for the floor assemblies.

The tests were conducted with the open basement doorway (no door in the basement doorway). Under this fire test scenario, structural failure occurred after the onset of untenable conditions (using incapacitation as an end point). These tests demonstrated good repeatability of the fire severity, smoke alarm responses, times to untenable conditions and to structural failure.

The test results must be interpreted within the context of the fire scenario used in the experiments. A relatively severe basement fire scenario was used in the full-scale fire experiments to establish the sequence of the events that would affect the ability of occupants to escape the house in the event of a basement fire.

## 5 ACKNOWLEDGMENTS

The National Research Council Canada gratefully acknowledges the financial and technical support of the following organizations that provided valuable input to the research as the project partners:

- Canada Mortgage and Housing Corporation
- Canadian Automatic Sprinkler Association
- Canadian Wood Council
- Cement Association of Canada
- City of Calgary
- FPInnovations - Forintek Division
- North American Insulation Manufacturers Association
- Ontario Ministry of Community Safety and Correctional Services/Office of the Fire Marshal
- Ontario Ministry of Municipal Affairs and Housing
- Wood I-Joist Manufacturers Association

The authors would like to acknowledge H. Cunningham (deceased), B. Di Lenardo, E. Gardin, J. Haysom (retired), I. Oleszkiewicz (retired), G. Proulx and M. Sultan who served on the IRC steering committee for the project. The authors also wish to acknowledge Don Carpenter, George Crampton, Eric Gibbs, Jocelyn Henrie, Malgosia Kanabus-Kaminska, Roch Monette, Richard Rombough, Michael Ryan and Michael Wright who contributed to the construction of the test facility, the setup of and conducting the fire tests.

## 6 REFERENCES


1. Canadian Commission on Building and Fire Codes; National Building Code of Canada; National Research Council of Canada, Ottawa, Canada, 2005.
2. Canadian Commission on Building and Fire Codes, User's Guide – NBC 2005, Application and Intent Statements, National Research Council of Canada, Ottawa, Canada, 2006.
3. Proulx, G., Cavan, N.R., Tonikian, R., Egress Times From Single Family Houses, Research Report 209, Institute for Research in Construction, National Research Council Canada, 2006.
4. Bwalya, A.C., An Extended Survey of Combustible Contents in Canadian Residential Living Rooms, Research Report 176, Institute for Research in Construction, National Research Council Canada, 2004
5. Leroux, P., Kanabus-Kaminska, J.M., Séguin, Y.P., Henrie, J.P., Lougheed, G.D., Bwalya, A.C., Su, J.Z., Bénichou, N., Thomas, J.R. Small-Scale and Intermediate-Scale Fire Tests of Flooring Materials and Floor Assemblies for the Fire Performance of Houses Project, Research Report 211, Institute for Research in Construction, National Research Council Canada, 2007.
6. Taber, B.C., Bwalya, A.C., McCartney, C., Bénichou, N., Bounagui, A., Carpenter, D.W., Crampton, G.P., Kanabus-Kaminska, J.M., Kashef, A., Leroux, P., Lougheed, G.D., Su, J.Z., Thomas, J.R., Fire Scenario Tests in Fire Performance of Houses Test Facility - Data Compilation, Research Report 208, Institute for Research in Construction, National Research Council Canada, 2006.
7. “ASTM E1537-02a: Standard Test Method for Fire Testing of Upholstered Furniture”, American Society for Testing and Materials, PA, USA, 2002.
8. Crampton, G.P. The Design and Construction of a Flame Conductivity Device to Measure Flame Penetration through Floor Systems, Research Report 223, Institute for Research in Construction, National Research Council Canada, 2006.
9. Forte, N. and Crampton, P., The Design and Construction of Electronic Deflection Gauges to Measure the Movement of Floor Assemblies in a Fire, Research Report 202, Institute for Research in Construction, National Research Council Canada, 2005.
10. EC1, Eurocode 1, “Basis of design and design actions on structures”, Part 2-2: Actions on Structures Exposed to Fire, ENV 1991-2-2, European Committee for Standardization, Brussels, Belgium, 1994.
11. SNZ, “Code of practice for the general structural design and design loadings for buildings”, SNZ 4203, Standards New Zealand, Wellington, New Zealand. 1992.
12. AS/NZS, “Structural design actions, Part 0: General principles”, AS/NZS 1170.0, Australia/New Zealand Standard, 2002.
13. ASCE 7-98, ASCE Standard, “Minimum design loads for buildings and other structures”, American Society of Civil Engineering, Reston, Virginia, 2000.
14. CAN/ULC-S101-04; Standard Methods of Fire Endurance Tests of Building Construction and Materials; Underwriters' Laboratories of Canada, Scarborough, Canada, 2004.
15. ISO Technical Specification 13571, “Life-threatening Components of Fire—Guidelines for the Estimation of Time Available for Escape Using Fire Data,” International Organization for Standardization, Geneva, 2002.
16. Purser, D.A., “Toxicity Assessment of Combustion Products,” in The SFPE Handbook of Fire Protection Engineering, ed. P.J. DiNenno, D. Drysdale, C.L. Beyler, W.D. Walton, R.L.P. Custer, J.R. Hall, Jr. and J.M. Watts, Jr., 3rd edition,

Society of Fire Protection Engineers /National Fire Protection Association, Quincy, Massachusetts, 2002, Section 2, Chapter 6.
17. Beyler, C., “Toxicity Assessment of Products of Combustion of Flexible Polyurethane Foam,” Fire Safety Science -- Proceedings of the Eighth International Symposium, International Association for Fire Safety Science, 2005, pp.1047-1058
18. Laursen, T., “Overview of Toxicity/Effectiveness Issues”, Proceedings of Halon Alternatives Technical Working Conference, Albuquerque, NM, 1993, pp. 357-367.
19. Sax, N.I. and Lewis, R.J., "Dangerous Properties of Industrial Materials" (7th ed.), Van Nostrand Reinhold, New York, 1989.
20. Peterson, J.E. and Stewart, R.D., “Predicting the carboxyhemoglobin levels resulting from carbon monoxide exposures,” Journal of Applied Physiology, Vol. 39, No. 4, pp. 633-638, 1975
21. Stewart, R.D., Peterson, J.E., Fisher, T.N., Hosko, M.J., Baretta, E.D., Dodd, H.C. and Herrmann, A.A., “Experimental Human Exposure to High Concentrations of Carbon Monoxide,” Archives of Environmental Health, Vol. 26, pp. 1-7, 1973
22. Babrauskas, V., “Combustion of Mattresses Exposed to Flaming Ignition Sources, Part I. Full-Scale Tests and Hazard Analysis,” NBSIR 77-1290, National Bureau of Standards, Washington, DC, September 1977.
23. Hauck, H. and Neuberger, M., “Carbon monoxide uptake and the resulting carboxyhemoglobin in man,” European Journal of Applied Physiology, Vol. 53, pp.186-190, 1984.
24. Gann, R.G., “Estimating Data for Incapacitation of People by Fire Smoke,” Fire Technology, Vol. 40, pp.201-207, 2004.
25. Christopher J. Wieczorek and Nicholas A. Dembsey, “Human Variability Correction Factors for Use with Simplified Engineering Tools for Predicting Pain and Second Degree Skin Burns”, Journal of Fire Protection Engineering, Vol. 11, No. 2, 88-111, 2001
26. Jin, T., “Visibility and Human Behavior in Fire Smoke,” in The SFPE Handbook of Fire Protection Engineering, ed. P.J. DiNenno, D. Drysdale, C.L. Beyler, W.D. Walton, R.L.P. Custer, J.R. Hall, Jr. and J.M. Watts, Jr., 3rd edition, Society of Fire Protection Engineers /National Fire Protection Association, Quincy, Massachusetts, 2002, Section 2, Chapter 4.
27. Babrauskas, V., “Full-Scale Burning Behavior of Upholstered Chairs,” NBS Technical Note 1103, National Bureau of Standards, Washington, DC, August 1979.
28. Bukowski, R.W., Peacock, R.D., Averill, J.D., Cleary, T.G., Bryner, N.P., Walton, W.D., Reneke, P.A., Kuligowski, E.D., “Performance of Home Smoke Alarms - Analysis of the Response of Several Available Technologies in Residential Fire Settings,” NIST Technical Note 1455, National Institute of Standards and Technology, December 2003.
29. Su, J., Bwalya, A., Lougheed, G., Bénichou, N., Taber, B., Kashef, A., Leroux, P. and Thomas, R., Fire Scenario Tests In Fire Performance Of Houses Test Facility – Data Analysis, Research Report 210, Institute for Research in Construction, National Research Council Canada, 2007.

**Table A 1. Test Summary for Test UF-06**

- Test ID: UF-06
- Test Date: Sept. 21, 2006
- Atmospheric Conditions: Temp: 17$^{O}$C RH: 87% Pres: 101.5 kPa↑
- Structure Tested:
  Wood I-joist 302, MSR 38x64 flange
  15.1 mm (5/8") OSB floor
  0.95 kPa load (144 concrete blocks, 2490 kg, 61 m pipe, 143 kg)

- Fire Load:
  Mock-up sofa at centre of basement (9.30 kg foam)
  Wood crib located 200 mm behind mock-up sofa (60.8 kg, 9 % MC)
  Wood crib located 200 mm from west side of mock-up sofa (61.1 kg, 9 % MC)
  Two wood cribs located under the mock-up sofa (31.5 kg, 31.4 kg, 9 % MC)
  80 s ignition with 19 kW burner (13 l/min)

- Ignition time after start of data: 1:05

- Doors: SE bedroom door closed / SW bedroom door open
  Door at top of basement stairs open
  First floor exterior door opened at 3:00 after ignition

- Window: Window opened at 1:40 after ignition (300 $^{O}$C)

- Floor collapse: 6:22 (382 s) after ignition

- Smoke Detector Activation Times:

| | Activation *(time from ignition)* |
|---|---|
| Smoke Detector #2, Photoelectric, Basement, bottom of stairs | 45 s |
| Smoke Detector #3, Ionization, 1$^{st}$ Floor, top of stairs | 75 s |
| Smoke Detector #4, Photoelectric, 1$^{st}$ Floor, top of stairs | 85 s |
| Smoke Detector #5, Ionization, 2$^{nd}$ Floor, top of stairs | 115 s |
| Smoke Detector #6, Photoelectric, 2$^{nd}$ Floor, top of stairs | 125 s |
| Smoke Detector #7, Ionization, SE bedroom, closed | 230 s |
| Smoke Detector #8, Photoelectric, SE bedroom, closed | 255 s |
| Smoke Detector #9, Ionization, SW bedroom, open | 130 s |
| Smoke Detector #10, Photoelectric, SW bedroom, open | 200 s |

**Table A 2. Test Summary for Test UF-06R**

- Test ID: UF-06R
- Test Date: March 15, 2007
- Atmospheric Conditions: Temp: -4$^{O}$C RH: 46% Pres: 102.3 kPa↑
- Structure Tested:
  Wood I-joist 302, MSR 38x64 flange
  15.1 mm (5/8") OSB floor
  0.95 kPa load (144 concrete blocks, 2490 kg, 61 m pipe, 143 kg)

- Fire Load:
  Mock-up sofa at centre of basement (9.33 kg foam)
  Wood crib located 200 mm behind mock-up sofa (64.4 kg, 7 % MC)
  Wood crib located 200 mm from west side of mock-up sofa (65.0 kg, 8 % MC)
  Two wood cribs located under the mock-up sofa (31.7 kg, 30.6 kg, 7 % MC)
  80 s ignition with 19 kW burner (13 l/min)

- Ignition time after start of data: 1:02

- Doors: SE bedroom door closed / SW bedroom door open
  Door at top of basement stairs open
  First floor exterior door opened at 3:00 after ignition

- Window: Window opened at 1:28 after ignition (300 $^{O}$C)

- Floor collapse: 6:20 (380 s) after ignition

- Smoke Detector Activation Times:

| | Activation *(time from ignition)* |
|---|---|
| Smoke Detector #2, Photoelectric, Basement, bottom of stairs | 38 s |
| Smoke Detector #3, Ionization, 1st Floor, top of stairs | 58 s |
| Smoke Detector #4, Photoelectric, 1st Floor, top of stairs | 78 s |
| Smoke Detector #5, Ionization, 2nd Floor, top of stairs | 113 s |
| Smoke Detector #6, Photoelectric, 2nd Floor, top of stairs | 123 s |
| Smoke Detector #7, Ionization., SE bedroom, closed | 198 s |
| Smoke Detector #8, Photoelectric, SE bedroom, closed | 223 s |
| Smoke Detector #9, Ionization, SW bedroom, open | 138 s |
| Smoke Detector #10, Photoelectric, SW bedroom, open | 163 s |

**Table A 3. Test Summary for Test UF-06RR**

- Test ID: UF-06RR
- Test Date: Oct. 11, 2007
- Atmospheric Conditions: Temp: 10$^{O}$C RH: 100% Pres: 100.8 kPa↓
- Structure Tested:
  Wood I-joist 302, MSR 38x64 flange
  15.1 mm (5/8") OSB floor
  0.95 kPa load (144 concrete blocks, 2490 kg, 61 m pipe, 143 kg)

- Fire Load:
  Mock-up sofa at centre of basement (9.38 kg foam)
  Wood crib located 200 mm behind mock-up sofa (63.6 kg, 9 % MC)
  Wood crib located 200 mm from west side of mock-up sofa (63.4 kg, 9 % MC)
  Two wood cribs located under the mock-up sofa (31.7 kg, 32.0 kg, 9 % MC)
  80 s ignition with 19 kW burner (13 l/min)

- Ignition time after start of data: 1:07

- Doors: SE bedroom door closed / SW bedroom door open
  Door at top of basement stairs open
  First floor exterior door opened at 3:00 after ignition

- Window: Window opened at 1:49 after ignition (300 $^{O}$C)

- Floor collapse: 6:54 (414 s) after ignition

- Smoke Detector Activation Times:

| | Activation *(time from ignition)* |
|---|---|
| Smoke Detector #2, Photoelectric, Basement, bottom of stairs | 43 s |
| Smoke Detector #3, Ionization, 1$^{st}$ Floor, top of stairs | 73 s |
| Smoke Detector #4, Photoelectric., 1$^{st}$ Floor, top of stairs | 78 s |
| Smoke Detector #5, Ionization, 2$^{nd}$ Floor, top of stairs | 128 s |
| Smoke Detector #6, Photoelectric., 2$^{nd}$ Floor, top of stairs | 138 s |
| Smoke Detector #7, Ionization, SE bedroom, closed | 223 s |
| Smoke Detector #8, Photoelectric., SE bedroom, closed | 248 s |
| Smoke Detector #9, Ionization, SW bedroom, open | 143 s |
| Smoke Detector #10, Photoelectric, SW bedroom, open | 153 s |